ธรณีวิทยาโครงสร้างของพื้นที่หินแปรขั้นต่ำบริเวณชายฝั่งทะเลจังหวัดชลบุรี
ภาคตะวันออก ประเทศไทย

นางสาว จุฑาทิพย์ บุษสาย

GEOLOGIC STRUCTURES OF THE LOW-GRADE METAMORPHIC TERRANE,

CHON BURI COASTAL AREA, EASTERN THAILAND

Miss Chuthathip Bussai

A Thesis Submitted in Partial Fulfillment of the Requirements

for the Degree of Master of Science Program in Geology

Department of Geology

Faculty of Science

Chulalongkorn University

Academic Year 2005

Thesis Title   Geologic structures of the low-grade metamorphic terrane, Chon

                      Buri coastal area, eastern Thailand
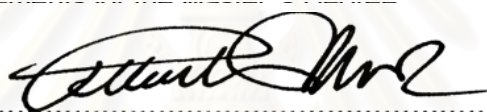
By   Miss Chuthathip Bussai

Field of study   Geology

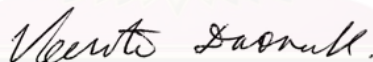Thesis Advisor   Assistant Professor Nopadon Muangnoicharoen, Ph.D.

Thesis Co-advisor   Assistant Professor Somchai Nakapadungrat, Ph.D.

Accepted by the Faculty of Science, Chulalongkorn University in Partial

Fulfillment of the Requirements for the Master 's Degree

.... Dean of Faculty of Science

(Professor Piamsak Menasveta, Ph.D.)

THESIS COMMITTEE
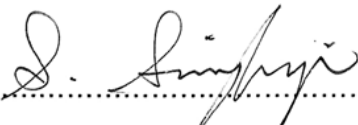
.... Chairman

(Assistant Professor Veerote Daorerk, M.Sc.)

.... Thesis Advisor

(Assistant Professor Nopadon Muangnoicharoen, Ph.D.)

.... Thesis Co-advisor

(Assistant Professor Somchai Nakapadungrat, Ph.D.)

.... Member

(Associate Professor Sampan Singharajwarapan, Ph.D.)

จุฑาทิพย์ บุษสาย : ธรณีวิทยาโครงสร้างของพื้นที่หินแปรขั้นต่ำบริเวณชายฝั่งทะเลจังหวัด
ชลบุรี ภาคตะวันออก ประเทศไทย. (GEOLOGIC STRUCTURES OF THE LOW-
GRADE METAMORPHIC TERRANE, CHON BURI COASTAL AREA, EASTERN
THAILAND) อ.ที่ปรึกษา : ผศ. ดร.นภดล ม่วงน้อยเจริญ, อ.ที่ปรึกษาร่วม : ผศ. ดร.สมชาย
นาคผดุงรัตน์, 135 หน้า. ISBN 974-53-1838-8.

การศึกษากระทำในพื้นที่หินแปรขั้นต่ำบริเวณชายฝั่งทะเลจังหวัดชลบุรีจากบริเวณตำบลบางพระ
อำเภอศรีราชาถึงอำเภอสัตหีบ ซึ่งเป็นพื้นที่ประกอบด้วยหินตะกอนเม็ดละเอียดและหินคาร์บอเนตอายุ
คาร์บอนิเฟอรัสถึงเพอร์เมียน และถูกแทรกดันโดยมวลหินแกรนิตอายุไทรแอสซิกซึ่งปรากฏโผล่บริเวณ
ทางด้านตะวันออกนอกแนวเขตพื้นที่ศึกษา การศึกษาใช้การวิเคราะห์ข้อมูลทางโครงสร้างธรณีวิทยาเพื่อ
กำหนดลักษณะทางธรณีวิทยาโครงสร้างและขั้นตอนของการเปลี่ยนแปลงรูปร่างที่เกิดขึ้น

จากข้อมูลการศึกษาทางธรณีวิทยาโครงสร้าง พบว่าหินแปรขั้นต่ำในพื้นที่ศึกษาแสดงการเปลี่ยน
แปลงรูปร่าง 3 ครั้ง และมีการแปรสภาพ 2 ครั้ง การเปลี่ยนรูปร่างครั้งเก่าแก่ที่สุด (D_1) เกิดขึ้นพร้อมๆกับ
การแปรสภาพด้วยอุณหภูมิและความดัน (M_1) ดังปรากฏหลักฐานของการคดโค้งของหินเป็นแบบที่มีมุม
ระหว่างแขนแคบจนถึงแบบบานพับโดยมีระนาบแกนเอียงเทด้วยมุมปานกลางไปทางทิศตะวันตก มีแกน
การคดโค้งวางตัวในแนวเหนือ – ใต้จนถึงแนวตะวันออกเฉียงเหนือ – ตะวันตกเฉียงใต้ และมีรอยแตก
และรอยเลื่อนปกติวางตัวเกิดร่วมด้วย จากการศึกษาธรณีวิทยาโครงสร้างขนาดจุลภาคพบว่าแกน
แสงของแร่ควอรตซ์มีการวางตัวอย่างมีทิศทางที่เฉพาะเจาะจง และสอดคล้องกับทิศทางของแกนการคด
โค้งนี้ การเปลี่ยนรูปร่างครั้งที่สอง (D_2) แสดงโดยการเกิดการคดโค้งแบบตัวขวางซ้อนทับลงไปบนรอย
การคดโค้งเดิมและทำให้เกิดการคดโค้งรบกวนแบบที่หนึ่งของ Ramsay (1967) ในขณะที่ได้มีการแทรก
ดันตัวขึ้นมาของหินแกรนิตพร้อมกันหรือติดตามมากับการคดโค้งนี้ ซึ่งทำให้เกิดการแปรสภาพด้วยความ
ร้อน (M_2) การเปลี่ยนแปลงรูปร่างครั้งสุดท้าย (D_3) ทำให้เกิดรอยเลื่อนย้อนมุมต่ำซึ่งดึงเอาชั้นของหินที่ถูก
แปรสภาพไปแล้วมาวางตัวอยู่บนหินอัคนีที่ไม่ถูกแปรสภาพ สำหรับอายุของการเกิดรอยเลื่อนย้อนมุม
ต่ำนี้ยังไม่สามารถสรุปแน่นอนได้ แต่น่าจะอยู่ในช่วงมหายุคมีโซโซอิกตอนกลางถึงตอนบนหรือยุคเทอร์
เชียรีตอนต้น โดยสังเกตจากชั้นหินตะกอนรูปพัดทางด้านตะวันออกของพื้นที่ศึกษาซึ่งน่าจะมีอายุอยู่
ในช่วงเทอร์เชียรีและไม่ได้แสดงหลักฐานว่าได้รับผลกระทบใดๆจากรอยเลื่อนย้อนมุมต่ำนี้

ภาควิชา............ธรณีวิทยา............ ลายมือชื่อนิสิต........จุฑาทิพย์ บุษสาย..............
สาขาวิชา............ธรณีวิทยา........... ลายมือชื่ออาจารย์ที่ปรึกษา..................................
ปีการศึกษา...........2548................ ลายมือชื่ออาจารย์ที่ปรึกษาร่วม.........................

A low-grade metamorphic terrane along Chon Buri coastal area from Sri Racha to Sattahip, regionally consisting of fine-grained clastic sediments and carbonate rocks of Carboniferous-Permian age, was studied. These rocks were intruded by a Triassic granitic pluton that exposes and marks the eastern limit of the study area. The purpose of this study is to clarify the geologic structure and deformation phases using a structural analysis.

The detail study here reveals three deformation episodes and two metamorphism events. The oldest deformation (D_1) which accompanies a dynamothermal metamorphism (M_1) is recognized by the elongate tight-to-isoclinal folds with fold axial planes being inclined moderately to the west and the axes trended somewhat north-south to northeast-southwest with crossed extensional joints and mormal faults. The microscopic study of c-axis of quartz grains in four orientated thinsections of quartz tectonite also shows a preferred orientation with a point maximum that conform these fold axes. The second deformation (D_2) formed the NW-SE cross folds superimposing on the previous folds thus resulted as type-1 interference pattern of Ramsay (1967). This interference folding episode may occur together with, or being shortly followed by a granitic intrusion in Triassic and caused a thermal metamorphism (M_2). The last deformation (D_3) caused a low-angle reverse faulting which brought the metamorphosed stratified units to overlie the non-metamorphosed younger igneous body. The age of this faulting is inconclusive, though thought to be Middle-to Late Mesozoic or very early Tertiary judging from the unaffected Tertiary alluvial-fan unit lying further to the east.

Department ....Geology..........   Student's signature........ *C. Bussai*
Field of study ....Geology...........   Advisor's signature....... *N. dim*
Academic year............2005...............   Co-advisor's signature........ *S. Nakpadst*

ACKNOWLEDGEMENTS

CONTENTS

LIST OF FIGURES

Figure   Page

Figure   Page

Figure   Page

Figure   Page

Figure   Page

Figure   Page

GLOSSARY

Khao   =   Hill

Ko   =   Island

Ban   =   Village

Amphoe   =   District

Changwat   =   Province (administrative)

CHAPTER I

INTRODUCTION

1.1 Preface

The low-grade metamorphic rocks are noted to widely distribute in Thailand. Their ages of original rocks and metamorphism are still dubious by several different previous stratigraphic interpretations. The usual classification of the low-grade metamorphic rocks in Thailand to be inferred as Lower Paleozoic age is possibly premature summary (Campbell, 1975). As metamorphism is not necessarily to follow the stratigraphic boundaries, to equate the rocks of a particular metamorphic facies to chronostatigraphic unit is probably not correct.

The Medium to high grade foliated metamorphic rocks of eastern Thailand had been generally accepted as a Lower Paleozoic sequence of progressive regional metamorphic rocks. These rocks associate the low-grade regional metasedimentary sequence of late Paleozoic age (Salyapongse, 1992). There were two important metamorphic events influencing on these rock units. The cleaved rocks were ascribed as regional metamorphic rocks by an effect of Carboniferous orogeny and later enhanced-graded metamorphism by Triassic granitic intrusion. The metasedimentary rocks formed a dominant part of the mainland margin of the eastern gulf while scattered exposures of granitic intrusion occurred further to the east. Sattahip Shale (Bunopas, 1981), mostly deformed and metamorphosed, was thought to be Silurian-Devonian in age. However there were some parts of the rock units found to be overlain by the Permian rocks with the presence of fusulinid (Nakinbodee and others, 1976) and believed to be of the Carboniferous age (Salyapongse and Jungyusuk, 1980). Lithologically some of these rock units were similar to the Ordovician argillaceous limestone and its association occurred elsewhere in the country.

1.2 Purpose and Scope of Study

As of no systematic structural study has ever been done in this area before this study was thus designed to emphasize the geologic structure by using a classical

structural analysis and to construct a structural model. Later the mechanism causing these structures would be contemplated. The study is to correlate the geologic structure in mesoscopic and microscopic scales in order to construct a macroscopic structural model. Hopefully this attempt may explain the mechanism that creates these structures. The systematic structural study may be helpful to elucidate and clarify doubtful chronostratigraphy in this area. In this study, the rock units to be focused are the low grad-metamorphic rocks on the mainland with an exclusion of all other cropped out on the islands while the granitic intrusion would mark the eastern limit of the study area.

1.3 Location and Accessibility

The study area is located along the coastal area of Changwat Chon Buri, eastern Thailand from Ban Bang Phra to Amphoe Satahip while the contact zone of a granitic pluton marks the eastern limit. This area is encompassed in the 1:50,000 topographic maps Sheets 5135 II (Amphoe Sri Racha), 5134 I (Amphoe Bang Lumung), and 5134 II (Amphoe Sattahip), covering an area of approximately 286 squarekilometers. It is in between Latitudes 13°13''00' N to 13°35''00' N and Longitudes 100°50''00' E to 101°00''00' E.

The area is only approximately 90 kilometers from Bangkok and is easily reached via Highway 3 (Sukhumvit Highway), Highway 36, Highway 331 and Highway 332. There are also several asphaltic roads branching out from these main highways. Unfortunately parts of the study area are unaccessible as the restricted military zone especially the naval base in Sattahip.

1.4 Physiography

The physiography of the study area is characterized by low hills, undulating terrain, and beach area. The topography is mostly flat to gentle undulating with moderate gradients. The low hills are in Sattahip and Sri Racha areas covering approximately half of the total area. They form hill chains N-S to NNE-SSW directions. The highest elevation is on Khao Chalak in Sri Racha area with an elevation of 322 meters above the mean sea level. Most undulating and flat area is in Bang Lamung area

located in the central part of the study area.

There is no main river in the study area. There are only small streams and gullies which drain from the hills down to the lower agricultural area then out to the sea. The drainage systems are sub-dendritic pattern.

According to the meteorological records from the Meteorological Department from 2000 to 2004, the average annual rainfall recorded in Sattahip is about 1211.8 mm annually. The maximum annual rainfall is 1392.6 mm in 2001, and the minimum 928.5 mm in 2004. The period of rainy season is from June to October with monthly rainfall approximately 99 mm. to 186.2 mm. The recorded maximum temperature is 33.4°C, and the minimum 25.3°C.

1.5 Previous Geologic Studies

The rock units in this part of eastern Thailand were thought to be resultants of a low-graded metamorphism which flanked to the west of the high-graded metamorphosed Pre-Cambrian rocks which exposed extensively in Phanatnikhom-Nong Yai and Chon Buri-Rayong granite. The age of these low-graded rock units are still debated as Silurian-Devonian or up to Carboniferous sequences. Unfortunately this is unclear due to the insufficient evidences of geochronologic study and unclear stratigraphic correlation as compared to those in the other regions of Thailand.

The metamorphic rocks which include those in the Chon Buri-Sri Racha area were reported and outlined of their extent in several regions in Thailand. Around here rock description starts from the youngest Phanom Sarakarm schist, Kanchanaburi quartzite, gneiss and schist, Si Chang metamorphosed limestone, to the oldest Sri Racha quartzite. Those rocks were thought to be Precambrian in age by Buravas (1959). Some of these rocks were subsequently remapped (Javanaphet, 1969) and indicated to be the Paleozoic rocks. However the work did not include most of the gneissic rocks and some of the crystalline schists. Workman (1972) described Chon Buri massif as consisting of quartz-feldspathic gneisses, migmatites, and granites of various ages. The margin of granitic gneisses was mentioned as bands of low-grade metamorphic rocks in the Lower Paleozoic sequence.

Bunopas (1981) studied a shale unit in Sattahip area and called the unit Sattahip shale. The lithology was composed of shale and argillaceous sandstone with limestone lens. The rocks obviously developed well cleavage and noted to be mesoscopic folds. These rocks are deformed and metamorphosed as the low-grade metamorphic rocks which some parts was contact metamorphic rocks due to granite intrusion. The age of this rock formation is still uncertain because no fossils have been found in this rock formation. It is possible to be Silurian-Devonian or up to Carboniferous-Permian.

Dheeradilok and Lumjuan (1983) summarized the study of the metamorphic belt and "Precambrian" rocks of Thailand. They established two main metamorphic facies series. The first one was a low-pressured Amphibolite facies series of Precambrian to Carboniferous rocks which occupied the axial part of the belt. The another one was a low-pressured Greenschist facies series of Lower Paleozoic ages occurred along both flank of the belt extending from northern to the southern Peninsula. The high-grade metamorphic rock of amphibolite facies in northern Thailand was essentially considered to be Precambrian in age.

Taiyaqupt and others (1986) reported the geology and stratigraphy of the Sri Racha area in southwestern Changwat Chon Buri. The stratigraphic units are late Paleozoic sedimentary-metasedimentary rocks believed to be of Permian and Carboniferous age and could possibly be as old as Devonian, The Triassic granites and Quaternary sediments were also recorded The Carboniferous rocks were divided into 3 units, in order of descending age, namely interbedded schist and quartzite, quartzite, and metacarbonate. These dynamothermal metamorphic rocks were found mainly in the western part of the area. The Permian clastic and non-clastic sedimentary rocks were restricted to the area adjacent to the Bang Phra reservoir. The regional structure had a general trend of NE-SW and a general dip to the west. A large overturned anticlinal fold with a NNE-plunging axis was traced for more than 35 km from the south to the north of the area. The south to the middle portions of the anticline was a homoclinal structure with interbedded schists/quartzites distinctively characterized the core. At the central part, the structure became a small overturned syncline whose axis was located at the valley between Khao Chalak and Khao Yai Li. The rocks exposed in the northern part of

the area were the carbonates and quartzites of the western normal limb.

The rocks croping out along the coastal area of Sri Racha and Sattahip area were compared with previous works and subsequently mapped as Carboniferous age following Salyapongse and Jungyusuk (1980). The rocks consisting of quartz schist, marble, feldspathic phyllite, quartzite, red siltstone and sandstone were believed to have experienced at least two deformation events. The obvious development of cleavage and foliation bands was noted. The non-foliated Late Triassic granite found in the same area of foliated phyllite and quartz schist indicated that the age of deformation should be before Late Triassic.

Salyapongse (1992) reported the foliated contact metamorphic rocks of the eastern gulf, from Amphoe Muang to Amphoe Sattahip of Changwat Chon Buri. The rocks had been generally mapped as Lower Paleozoic sequence of progressive regional metamorphism. These rocks associated the Lower-graded regional metasedimentary sequence of Late Paleozoic age. Extensive mapping of the area indicated that the metamorphic rocks were occurred in a contact zone between the metasedimentary sequence and a granitic batholith. The country rocks formerly experienced at least a cleavage-forming metamorphism, and the foliated contact metamorphic rocks will be clearly recognized only in the upgrading zone. The mineral assemblages of the calc-silicate rocks indicated albite-epidote-hornfels up to hornblende-hornfels facies. The grade of metamorphism increased rapidly, within a short distance (a kilometer) towards the granitic body irrespective of the direction of the planar structure originally developed in the country rocks.

Putthapiban and Salyapongse (1993) studied and described the geology of Changwat Chon Buri. The rocks found along the coastal area from Amphoe Muang to Amphoe Sattahip were identified as the metamorphosed sedimentary rock which is caused by low-grade metamorphism. This rock unit was composed of metasandy shale, metalimestone, metachert and metaquartz sandstone. Sericite and recrystallined calcite could be observed in metaargillaceous rocks and metalimestone repectively. As a result of mild metamorphism, the trace of fossils was still noticeable. Coral and fusulinid were

found in metalimestone and Bryozoa in matasandy shale. Radiolaria found in metachert was a clue to be Carboniferous to Permian in age.

Geology of Khao Phlu Ta Luang and Khao Chi Chan in Amphoe Sattahip was described by Chaodumrong and others (2002). The rocks of Khao Phu Ta Luang consisting of the laminated to thin bedded, gray to light gray chert and thinly-interbedded shale were faulted and folded with axial plane dipping westward nearly parallel to bedding plane. The structural styles were observed as the tight-overturned and recumbent folds. The evidence of recrystallized radiolarian was noted in the chert. However its Carboniferous - Permian age was obtained from stratigraphic correlation. There were three main rock types cropping out at Khao Chi Chan, namely marble, calc silicate hornfels and granite. Marble, originally Carboniferous – Permian limestone, is mainly calcium carbonate in composition with a few fine grained, light gray dolomite bands and alternating brown to dark gray bands that was formed as a result of the granite intrusion. Foliation lying parallel to the bedding dipped to the SE direction. The contact metamorphism causing a mimetic recrystallization generated the mineral assemblages oriented parallel to the original cleavages. White wollastonite was observed and was an important evidence to indicate the verification of the contact metamorphism.

1.6 Methodology

There are 4 procedures, showing in a flowchart in Figure 1.1, to achieve this study.

1.6.1 Literature reviews and field investigation plan

The previous works done in or being related to the present study area were reviewed of the general geology, stratigraphy and structural geology. The geologic maps and aerial photographs were used to gain background knowledge of rock types and geologic structures. Topographic maps were also used for determining the accessibility of the study area and subsequently field investigation was properly planed. Aerial photos were also interpreted for general geomorphology and geology, to be checked in the field later. Unfortunately, some areas, especially within Sattahip Naval

```
        ┌─────────────────────────────────┐
        │   LITERATURE REVIEW AND         │
        │   FIELD INVESTIGATION PLAN      │
        └─────────────────────────────────┘
```

Previous Work Study	Geology Review	Aerial Photographic Interpretation

FIELD INVESTIGATION

Mesoscopic Structural Data Collection	Roughly Lithologic Description	Orientated Specimens Collection

DATA ANALYSIS

Mesoscopic Analysis
- Stereographic Plot
- Rose Diagram

Microscopic Analysis
- Petrography and Microstructure Observation
- Lattice Prefer Orientation study

Macroscopic Structure and Structural Geology Map	Structural Geology Model and Mechanism

INTEPRETATION AND CONCLUSION

Figure 1.1 Methodology flowchart of the study

Base could not be accessed due to a reason of maximum security.

1.6.2 Field investigation

The study area is divided into two main separtated parts. The first part covers the area in Amphoe Sattahip and Amphoe Bang Lamung while, another part is in map Amphoe Sri Racha. The reason is that there is no metamorphic exposure in between, only the highly weathered granitic rock. The roughly lithologic and mesoscopic structural data had been first described and collected, then more on the mesoscopic structures in the outcrops of interest. Orientated four specimens were carefully collected for more detail of mesoscopic structural data back in the office and microscopic study. The size of specimens is about 15 x 15 x 15 centimeters or larger.

1.6.3 Data analysis

The mesoscopic field structural data were systematically analyzed by the classical lower-hemispheric equal-area stereographic projection and rose diagrams. The StereoNett version 2.6 program written by Johanness Duyster, University Rurh-university-Bochum, Germany is a selected for this study. A few orientated samples were collected for a further in office study of the detailed fabrics and their orientation. These hand specimens were also meant for microscopic study, including petrography and microstructure observation, using a polarized-light microscope. Four orientated thinsections of the quartz schist were selected for a quartz optic axis orientation observation by using a Universal Stage-equipped petrographic microscope following the method of Emmons (1959). Unfortunately, these thinsections could only be obtained from the Sri Racha area.

1.6.4 Interpretation and conclusion

The macroscopic structures of the study area would later be summed up by the analysis of mesoscopic and microscopic structures. The mechanism causing these structures was also determined. In term of petrological study, the metamorphic event could be determined by the detail of metamorphic index minerals and their textures. And later, the tectonic history of the area was explained.

CHAPTER II

REGIONAL GEOLOGY

This chapter is to review the general distribution of metamorphic rocks in Thailand, and the geology of eastern Thailand, especially in Changwat Chon Buri in terms of the stratigraphic units and igneous activities, metamorphism and concerned age determination, and historical geology.

2.1 The review of metamorphic rocks in Thailand

The regional dynamothermal metamorphic rocks in Thailand are considerably limited or restricted both in spatial distribution and in stratigraphic units. A major zone or belt of metamorphism concentrates along the western mountain range of the country starting from Changwat Chiang Rai and Changwat Mae Hong Son in the north, and extending down south through the western part of Changwat Chiang Mai, Lampang, Lamphun, Tak, Kamphangphet, Nakhon Sawan, Uthai Thani, and Kanchanaburi, then pinching out in Changwat Prachuab Khirikhan. The metamorphic rocks crop out again in the Peninsula just south of Changwat Surat Thani and then extend to the Thai-Malaysian border. Two minor separated belts of metamorphic rocks are located in Uttaradit area and in the eastern portion of the country (Pongsapich and others, 1983).

The metamorphic rocks are tentatively divided into two portions. The first group, the inferred Precambrian one, is characterized by high grade metamorphic rocks and anatexites. The other group is of the inferred Lower Paleozoic (Cambrian-Devonian) age and is characterized by the low grade metamorphic rocks (Figure 2.1). However, it should be noted that not all rocks of the Lower Paleozoic age were subjected to the metamorphism.

The low grade metamorphic rocks expose extensively in Thailand and their age of deposition and metamorphism are questionable. The general practice of the classification of all gneisses and schists as Precambrian rocks and the low grade metamorphic rocks as Lower Paleozoic rocks could probably be hasty in conclusion because the metamorphic isograds do not necessarily follow the stratigraphic
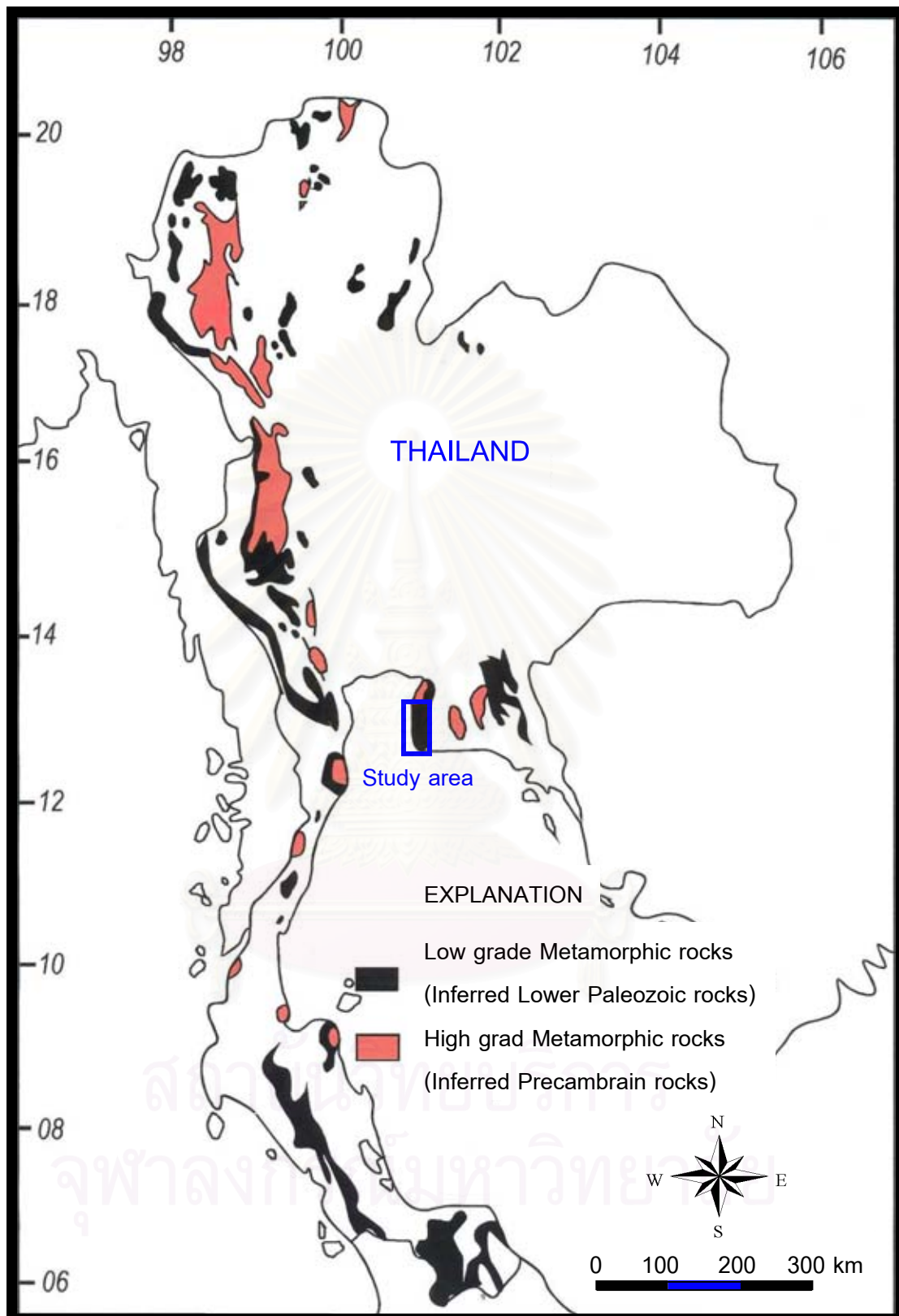
Figure 2.1 Distribution of metamorphic rocks in Thailand (after Pongsapich and others, 1983). The location of the present study is included.

boundaries. Thus to equate the rocks of a particular metamorphic facies to the chronostratigraphic units is not necessarily applicable. These Lower Paleozoic rocks affected by the regional dynamothermal metamorphism are said to be of Cambrian, Ordovician, and Silurian-Devonian ages. However not all the rocks of these ages were transformed by the metamorphic process. Parts of them still retain their sedimentary characteristic origins, particularly in the Southern Thailand (Bunjitradulya, 1978).

Baum and others (1970) reported the Lower Paleozoic strata in northern Thailand which had been affected by low grade dynamo-metamorphism. These rocks consisted of the Cambrian clastic rocks and Ordovician limestones. The age of the Ordovician strata was based on conodont faunas, whilst the age of unmetamorphosed Cambrian rocks was based on the fact that, in places, they underlied the Ordovician strata. These Lower Paleozoic rocks had locally been transformed into phyllites and schists with gradational contacts with their equivalent unmetamorphosed sedimentary rocks. The differences between the underlying Precambrian rocks of higher metamorphic grade and Lower Paleozoic metamorphic rocks of low metamorphic grade on their exhibition in the style of deformation under this dynamo-metamorphism were pointed out by Baum and others (1970).

The occurrence of Lower Paleozoic rocks in the Uttaradit area in northern Thailand was outlined to have been metamorphosed to the greenschist facies by Piyasin (1972). The rocks herein were reported to be Cambro-Ordovician quartzites, Ordovician limestones, and Silurian-Devonian clastics (including tuffs) and cherts. These resultant metamorphic rocks were phyllites, chlorite phyllites, and schists. The metamorphism was considered to have taken place during a Lower Carboniferous Oregeny. Sripatanawat (1972) described the rock units in the Nakhon Sawan area, central Thailand, and reported the Lower Paleozoic metamorphic rocks as Cambrian schists, quartz-mica schist, muscovite schist, and massive recrystallized limestone lenses, the Ordovician limestone with the interbeds of phyllite and the undifferentiated Silurian-Devonian quartzite, phyllite, slate and phyllitic tuff were also reported.

The report on the geology of the Lampang area was summarized by Piyasin

(1972). The Silurian-Devonian Donchai Group was believed to be a geosynclinal facies of low grade metamorphic rocks (greenschist facies) which consists of phyllite, quartzo-feldspathic schist, chloritic phyllite, lime silicate phyllite, black slate, bedded chert, and tuff. No fossil had been found in these rocks, but the given age was based on the degree of metamorphism and stratigraphical position. Piyasin (1972) suggested that the low grade metamorphism occurred during a Carboniferous orogeny.

Koch (1973) reported that the dynamothermal metamorphism affected the Lower Paleozoic strata of northern Changwat Kanchanaburi, western Thailand, to only those parts of the sequence that had been downfolded enough to attain sufficient temperature and pressure. Products of the metamorphism were sericitic slate, biotite-muscovite schist, biotite schist and calc-silicate rocks, all considered to be Cambrian in age. The age of this metamorphism was ascribed to be Post-Jurassic.

The Phitsanulok area was compiled by Bunopas (1978). The report on the Lower Paleozoic metamorphic rocks was described as three rock units. The first unit was Cambrian quartzite, quartz mica schist, and phyllite which were found in a group of isolated hills east of Changwat Tak and along the Tak-Mae Sot highway. The second one was Ordovician agillaceous limestone interbedded with greenish gray slate and dark gray massive limestone which was found at Pong Nam Ron area, southeast of Changwat Tak, and mica bearing limestone found along the Tak-Mae Sot highway. The other unit was Silurian-Devonian phyllitic tuff, phyllitic greywackes, argillite, cherts and marble. The metamorphism event was considered to have taken place during a Carboniferous orogeny.

2.2 General geology of the Eastern Thailand

According to the concept of the tectonostratigraphic terrane (Bunopas and Vella, 1978, and Barr and Macdonald, 1991), Eastern Thailand was developed from the welding of two main allochthonous continental terranes (Figure 2.2), namely Shan-Thai terrane in the west and Indochina terrane in the east, along the Nan-Sa Kaeo Suture Zone in late Triassic (Bunopas, 1983). Both terranes had their origins on the northwestern margin of Gondwana in the southern Hemisphere during Lower Paleozoic
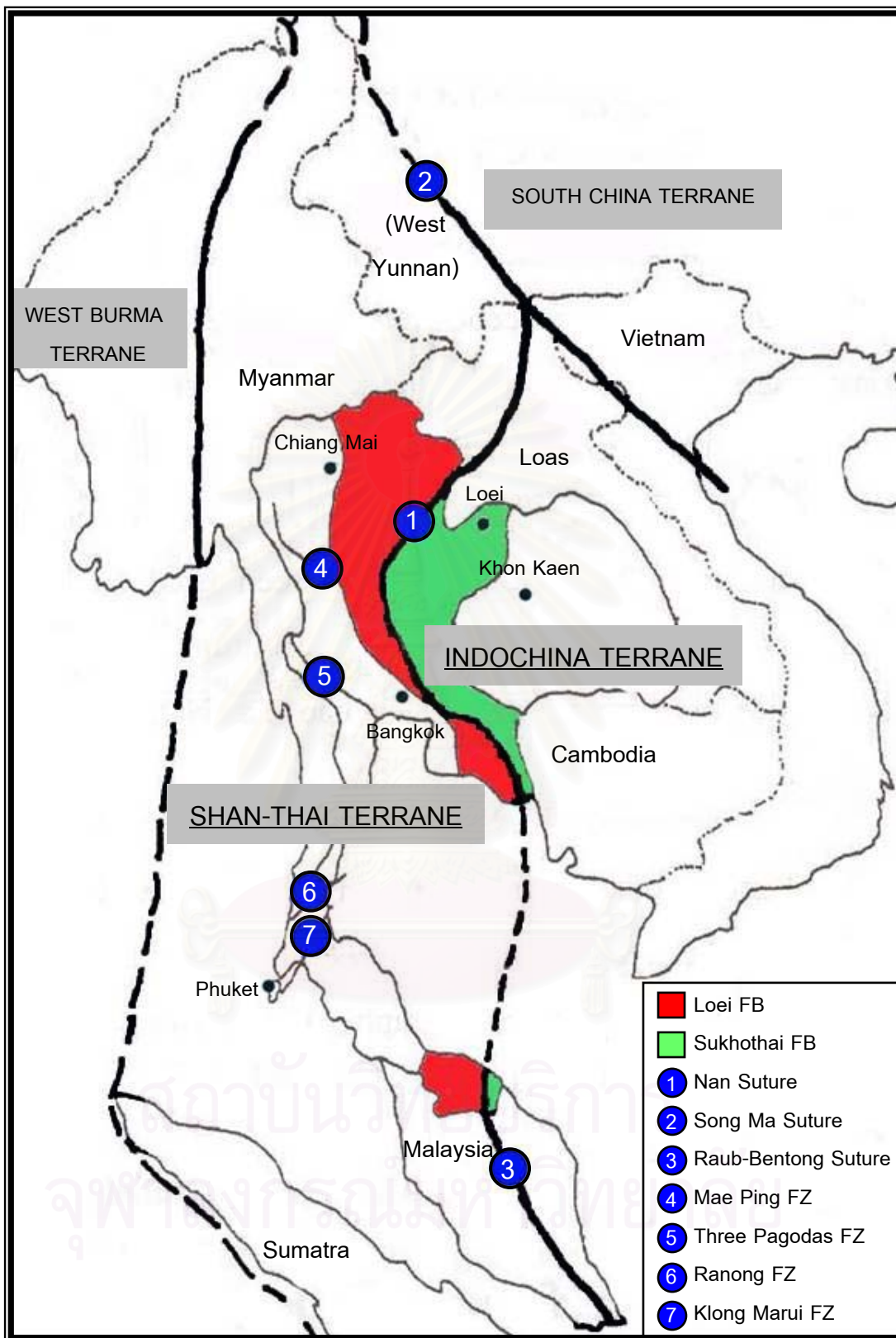
Figure 2.2 Principal tectonic structures in Thailand (From Department of Mineral Resource 1999).

(Burrett and others, 1990). Geology of two terranes in Eastern Thailand is distinctively contrast and described in details by Salyapongse and others (1997). The geologic units and the schematic cross section are shown in Figure 2.3 while a detail descripcion of the lithologic units is as below.

2.2.1 Shan-Thai Terrane

The Precambrian amphibolite facies of the Shan-Thai Terrane were formed as the oldest crystalline basement rocks. The rock assemblages described by Areesiri (1983) generally include migmatite, segregation banding gneiss, calc-silicate rock, marble, frequent bands of amphibolite or hornblende schist and quartz-mica schist. The Mesozoic S-type granites together with concordant and discordant pegmatites are commonly associated. The association between the Cambrian-Ordovician siliciclastic-carbonate rocks and the Precambrian rocks is regularly observed in the western mountain range of Thailand (Bunopas, 1983, and Salyapongse, 1992). The following younger rock sequence is possibly Silurian-Devonian age and it might have been inferred as Precambrian. The Silurian-Devonian rocks consisting of phyllitic quartz conglomerate, quartzitic phyllite, carbonaceous phyllite, metasandstone, metatuffaceous sandstone, metasiltstone, and slate appear to be transitional to the Carboniferous sandstone-shale-chert-limestone and the Permian sandstone-shale-chert-limestone (Bunopas, 1983).

The Permian-Triassic volcanic rocks appear when approaching the Sukhothai fold belt. These volcanic rocks appear ascended through the Precambrian rocks and their associated Middle- to Upper Paleozoic rocks mentioned earlier. Within the Sukhothai fold belt, the Permian metatuffs are particularly different from the Permian nonvolcanogenic unit occurred to the west, while the Carboniferous rocks of both areas are compatible. The oncolitic limestone of the Lower Triassic age clearly indicates very shallow marine environment whereas further to the east the Middle Triassic bedded chert and intraformational basaltic rocks are definitely very deep marine facies (Salyapongse and other, 1997).   By these facts, the tuff, tuffaceous rocks and terrigeneous sediments occurring only to the west of the chert and basaltic rocks unit
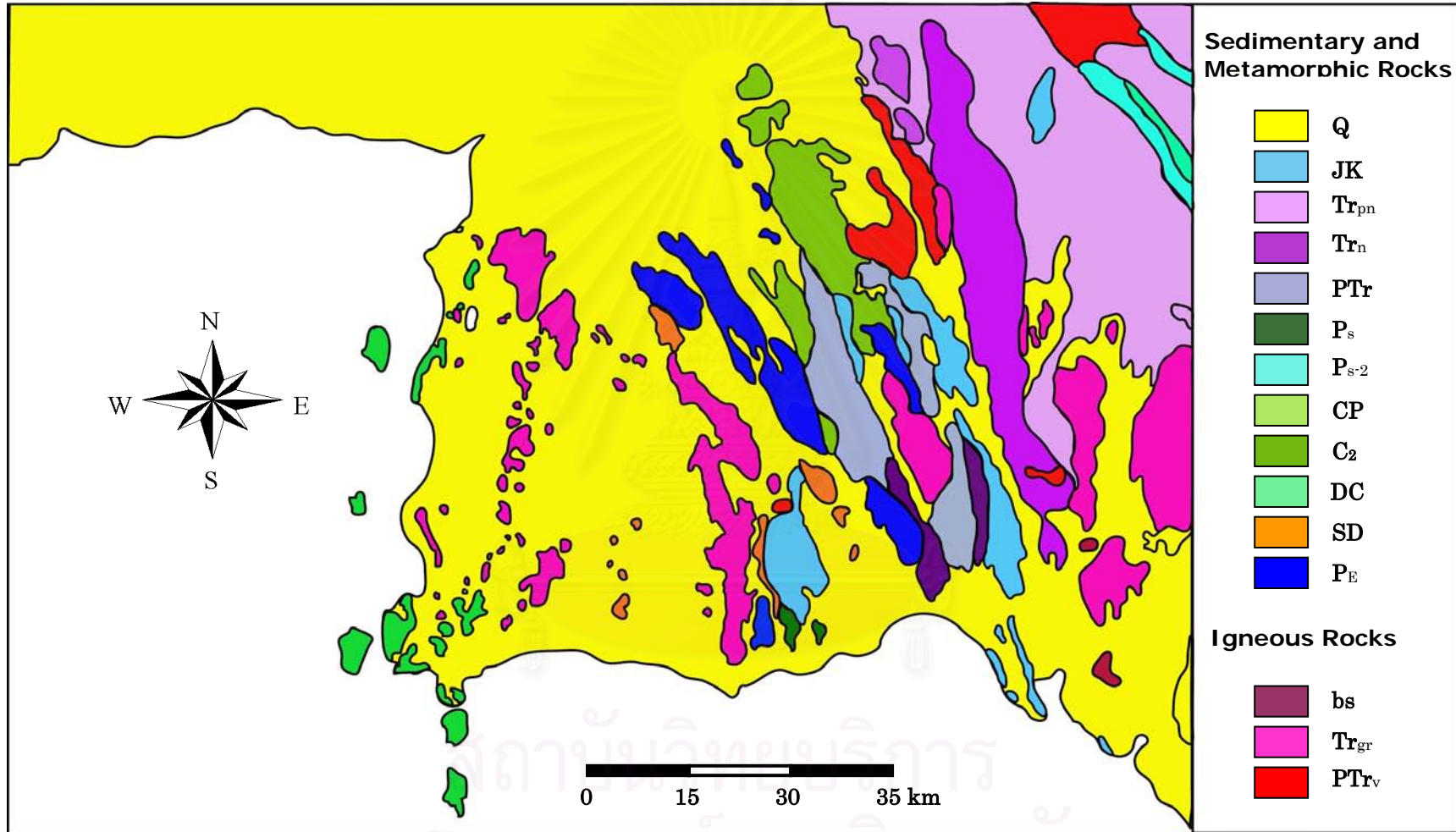
Figure 2.3 Geologic map of Eastern Thailand (Modified after Department of Mineral Resources, 1999).

must represent the intermediate facies between the shallow and the deep marine facies during the Triassic time. These successions are considered as the end of the Shan-Thai terrane. The Jurassic-Cretaceous red beds and the Tertiary sediments within the Shan-Thai terrane are related to the events after collision between the Shan-Thai and the Indochina terranes.

2.2.2 Contiguous Area

The actual contact between the Shan-Thai and the Indochina terranes are believed to be completely covered by the Upper Triassic greywacke unit. This unit is considered to represent an infill sediment along the remnant basin between the two plates (Salyapongse, 1992). The area occupied by the greywacke and the overlapping area on both margins of the two continents hence was called the contiguous area. After the collision of the two terranes, the younger Jurassic-Cretaceous red beds, the Jurassic I-type granites and the Cenozoic basalts completed the geologic succession.

2.2.3 Indochina Terrane

Within Indochina terrane, the remnant exposures are mostly elongated in the NNW direction in the southern part while change to the EW direction to the north. The oldest rocks of this terrane consist of greenschist to amphibolite metachert, metatuff, recrystalline limestone, metavolanics and metasubvolcanics of Devonian-Carboniferous deformed sequence of the older island arc volcanics. These rocks were formed as a large scale fault slab inserted between two groups of the Permian chert-basalt-ultramafic limestone assemblages. Shallow water Permian limestone appears exotic, tectonically transported from the shelf environment located to the east. Permian to Triassic igneous rocks in the area comprise of mafic-ultramafic plutonic rocks, basaltic breccia and hyaloclastite, and rhyolitic to andesitic volcanics. The Jurassic-Cretaceous red beds of the Khorat Group become extensive and limit themselves to the southeastward and northward (Salyapongse, 1997).

2.3 The Stratigraphic Rock Units and Granite Intrusion found in Changwat Chon Buri

2.3.1 Precambrian

In general, the medium- to high grade metamorphic rocks such as orthogneiss, paragneiss, schist, calc-silicate and marble of amphibolite facies have long been regarded as Precambrian rocks in Thailand. These rocks crop out in Shan-Thai terrane (northern, western and southern Thailand), commonly as cores of the N-S and NW-SE trending anticlinoria and fault belts but no exposure in the northeastern Thailand (Indochina terrane). Their foliations also follow the following trends, i.e. parallel the NW-SE Mae Ping fault zone at the Lan Sang of Changwat Tak, the NW-SE Three Pagoda fault zone at Khao Chon Khai of Changwat Kanchanaburi and Nong Yai of Changwat Chon Buri, and the N-S trending at Khanom of Changwat Nakhon Si Thammarat. An age determination of these rocks was based on the stratigraphic position as they underlie the Lower Paleozoic rocks. However, there is no radiometric dating for the Precambrian age.

The inferred Precambrian Khao Chao gneisses at Ban Nong Yai were mapped and studied in details by Areesiri (1983). These gneisses consist of quartzofeldspathic biotite gneiss, biotite hornblende gneiss, biotite gneiss, hornblende diopside gneiss, biotite sillimanite gneiss and biotite diopside gneiss with common associations as calc silicate, marble and amphibolite. The essential mineral assemblages are quartz, plagioclase, K-feldspar, biotite, sillimanite, diopside, garnet and hornblende. Cordierite is locally presented in conjunction with quartz, garnet, biotite and sillimanite assemblage. Areesiri (1983) also reported the occurrence of amphibolites which found intercalated with the gneissic rocks in the most units. These amphibolites are composed of normal amphibolite, biotite amphibolite, diopside amphbolite, garnet amphibolite and hornblende amphibolite.

2.3.2 Silurian – Devonian – Carboniferous

Two Silurian-Devonian-Carboniferous stratigraphic units were identified by the Department of Mineral Resources (1999). Unfortunately, the poorly preserved fossils which had been found in two localities, i.e. Ko Si Chang and Laem Thong Lang on the mainland made an age determination uncertain. The first unit of Silurian-Devonian-Carboniferous rocks exposes in Pattaya - Sattahip area, consisting of greenish gray to

grayish brown slaty shale and sandstone with intercalated thin-bedded limestone. The weathering color of shale and sandstone is reddish brown to white. The second unit generally crops out in low land area, adjacent to the Inferred Precambrian gneiss, in eastern Amphoe Klaeng. It composes of schist, quartzitic schist, phyllite and metaschist with well developed cleavage. In many localities, it exists as roof pendants on the granite batholith (Salyapongse and others, 1997).

2.3.3 Carboniferous – Permian

The Carboniferous-Permian sequences generally start from siliciclastic-carbonaceous, sandstone-mudstone rich, with minor chert and argillaceous limestone lenses in the lower part. This lower part graded into bedded chert, well-bedded siliceous shale, carbonaceous shale, sandy shale and more argillaceous limestone in the upper part (Salyapongse and others, 1997). At Khao Rewadi near Bang Pra reservoir, the known Middle Permian section includes a sequence of sandstone, sandy shale, chert and small lenicular limestone where Middle Permian fusulinids, calcisphere, small foraminifers and algae were found (Bunopas, 1981).

2.3.4 Granite Intrusion

Nakapadungrat and Putthapiban (1992) divided the granite of Thailand into three granite belts, based on the different petrographic, geochemical, and isotopic characteristics, mineralization and geographic location, namely the eastern, central and western belts. In the eastern belt, granites occur as small batholiths of zoned and unzoned plutons of a compositionally expanded characteristic from tonalite, granodiorite to dominantly granite. They are of Triassic age, having I-type affinity and carry base metals, gold and molypdenum. Contrarily, the western belt granites, being of Cretaceous age, are mixed population of S-type and I-type rocks. S-type granites occur as large batholiths where as I-type granites occur as small plutons. Mineralization is dominated as argillic dissemination, pegmatites and endogenous greisen-bordered vein swarms of cassiterite and wolframite. The central belt granites, on the other hand, occur as major batholiths and large complex plutons of restricted compositional range and

commonly associated with gneissic granite and migmatites. They are S-type granites, mainly of Triassic age, with tin-tungsten mineralization.

The granitic exposures found in Changwat Chon Buri belong to the central granite belt and are a part of Rayong-Bang Lamung Granite formed as elongate N-S trending batholiths in land on the eastern flank of the Gulf of Thailand. The igneous rocks intruded the westerly-located Carboniferous-Permian sedimentary sequence and the easterly-exposed Precambrian sequence of amphibolite facies, while the Silurian-Devonian rocks are mostly occurred as roof pendants.

In a granite quarry in Changwat Chon Buri, Suriyachai and Salyapongse (1995) had recognized three granite phases, namely Granite I, Granite II and Granite III. Granite I is the main phase of the Rayong-Bang Lamung Granite which is distinctively uniformed both in the mineral composition and the general features throughout. It is holocrystalline, and has a coarse to very coarse-grained (>3 cm.), equigranular to porphyritic texture. Frequent inclusion of mafic mineral clots (chiefly biotite) and gneissic rocks are encountered. The porphyritic granite has sericitized K-feldspar phenocrysts with continuous and wide ranges of grain sizes. Phenocrysts and clusters of the larger mineral phases comprise more than 50% of the rock. The euhedral feldspar phenocrysts range in grain dimensions from 1 up to 8 cm long. Quartz phenocrysts are from 3 to 10 mm across. Books or aggregates of biotite crystals, as large as 1 cm, is widely scattered. These larger mineral phases and phenocrysts are, in turn, embedded in a finer grained groundmass of the same mineral assemblage and the fine-grained muscovite (Suriyachai and Sulyapongse, 1995).

2.4 Review of some Carbonate rocks in Changwat Chon Buri

The carbonate rock deposits are widely distributed over the entire north-south Chon Buri-Sattahip coastal terrain, as well as on Ko Si Chang off Sri Racha coast. With an exception of the deposit on Ko Si Chang, all depostis are confined along two hill chains, the Khao Choeng Thian-Khao Leam Chabang chain and the Sattahip chain (Hinthong and Sarapirome, 1983).

Nakinbodee and others (1976) suggested a small fossiliferous limestone lens interbedded in black shale at Khao Rewadi in Sri Racha area as of Late Carboniferous-Early Permian age. Here, *Pseudofusulina* was firstly mentioned. Later on, a Kubergandian-Murgabian age (Lower Permain) has been amended by Bunopas and other (1983). The fossil assemblage has been identified, namely calcispheres (*Diplosphaerina*), pseudoalgae (*Tubiphytes*), algae (*Solenopora*), smaller foraminifers (*Globivalvulina*, *Climacammina*, *Endothyra*, *Tetrataxis*) and fusulinids (*Neofusulinella* of *phairayensis* Colani, *Toriyamaia* sp).

A nautiloid in massive limestone specimens from Ko Si Chang collected by the geologists of the Department of Mineral Resources was identified by R. Ingavat as probably *Multicameroceras*, an Ellesmeroceroida which indicate an Early-Middle Ordovician age (Nakinbodee and others, 1976). However, the age of this rock sequence is controversial, as argued to be in the range of Silurian to Middle Carboniferous or Silurian-Devonian (Suwanasing, 1973). Later, Salyapongse and others (1981) stressed that the age should be Carboniferous.

Hinthong and Sarapirome (1983) studied some of the distributed carbonate rocks in Chon Buri area which include the carbonate rock deposits on Ko Si Chang, Khao Chi On, Khao Bandai Krit and Khao Rai-Khao Bai Si. The carbonate rocks on Ko Si Chang are predominantly gray laminated recrystalline limestone and medium gray banded marble. The significant features are the presence of chert nodules and calcite pockets. From the western part to the eastern part of this island, laminae in limestone generally vary in color and composition. Those found at the western part are of the alternation of light to medium gray and dark gray, whereas those at the eastern part of the island are of medium gray and yellowish-brown materials.

There are three rock types being recognizable to occupy three different portions of Khao Chi On (Hinthong and Sarapirome, 1983). The rock exposed at the northern part is coarse-grained biotite-granite, whereas banded limesilicate rock is exposed at the southern end of the mountain. At the central part recrystalline limestone (or banded marble) is exposed with contacts to the northerly biotite-granite and southerly

limesilicate rock. Normally, the limesilicate rock is light gray to medium gray in color, with alternation of light and dark gray bands and laminae of siliceous and argillaceous materials. Trains of thin chert lenses are common and usually associated with the siliceous bands. The argillaceous wavy bands, medium gray in color, each approximately 1.50 cm thick, are also common in the banded recrystalline limestone.

At Khao Bandai Krit, most rocks consist of predominantly alternating banded limesilicate rocks of light- and dark-gray colors. Occasionally light gray banded interbedded marble is found. The carbonate rock deposites at Khao Rai-Khao Bai Si comprise dominantly of light- to medium gray banded and laminated argillaceous-arenaceous with dolomitic limestones. Recrystalline limestones of similar color are also occasionally observed. These limestones are believed to be lenses in the alternative sequence of slaty shale and well-bedded chert (Hinthong and Sarapirome, 1983).

In Amphoe Sattahip, marble and calcsilicate hornfels at Khao Chi Chan were described by Salyaphongse and others (1997) as originally Carboniferous-Permian cleaved limestone. The rocks have mainly calcium carbonate composition with some dolomite. They are fine grained, light gray banded (1-5 cm thick) with alternating brown- to dark gray bands or streaks, about 1-2 cm thick (Salyaphongse and others, 1997, and Chaodumrong and others, 2002). The contact metamorphic resultants could be from the intrusion of the 211±11 Ma granite (Nakapadungrat and others, 1984). The mineral assemblage generated by mimetic recrystallization due to contact metamorphism is oriented parallel to the original cleavages. Elongated patches of white, purplish brown and green colors in the rocks represent varieties of the calcsilicate minerals.

2.5 Metamorphism and Age Determination

The gneisses of Khao Chao at Ban Nong Yai as studied by Darbyshire (1988) were believed to have been subjected to at least 3 episodes of deformation and 2 episodes of metamorphism. The first deformation and the first metamorphism were closely related to have taken place during the Late Carboniferous orogeny. The second and the third deformations occurred in related to the second metamorphism which is concurrent to the Permo-Triassic orogeny. These interpretation and conclusion was

made purely from the field observations and structural analyses. The evidences include the cross-cutting axial plane cleavages over the original foliation being accompanied with crystallization of minerals of the amphibolite grade. The injection of veined pegmatite-aplite parallel to these cleavages was also thought to represent the second period of metamorphism and its related events. As a consequence, these later tectonic related events were claimed to be responsible for the processes of partial melting, pegmatite-aplite formation and migmatization. Radiometric dating using Rb-Sr isochron approach had been carried out on samples of foliated equigranular granite found within the gneisses of Nong Yai (Khao Chao). It indicates an age of 75±22 Ma with an initial $^{87}Sr/^{86}Sr$ ratio of 0.7054±0.0002.

Medium to high grade foliated metamorphic rocks of the eastern Gulf of Thailand coastal areas, from Amphoe Muang Chon Buri to Amphoe Sattahip, had been generally mapped as lower Paleozoic sequence of progressive regional metamorphic rocks associated with lower grade regional metasedimentary sequence of late Paleozoic age. Petrographic study of these metamorphic rocks was done and compared to the field evidence by Salyapongse (1992). Extensive mapping of the area indicated that the metamorphic rocks were occurred in a contact zone between the metasedimentary sequence and a granitic batholith. The mineral assemblages commonly observed from the calc-silicate rocks indicate albite–epidote-hornfels up to hornblend-hornfels facies. The metamorphic grade as characterized by index minerals increases very rapidly within a short distance (up to one kilometer) towards the granitic contact irrespective of the direction of cleavage or schistosity pre-existed in the rocks.

Nakapadungrat and others (1984) had chemically analyzed twenty-five samples of the major phase granite from the Rayong-Bang Lamung batholith. Their study results were summarized as SiO_2, 66 to 72%, Al_2O_3, 13 to 15%, Fe_2O_3, 0.05 to 0.5%, FeO, 2.5 to 4 %, CaO, less than MgO, <1%, Na_2O, generally about 3%, K_2O, about 4 to 5%, and H_2O, about 0.05 to 0.7%. The Rb-Sr whole rock isochron suggested that the major phase granite emplaced at about 211±11 Ma with an initial $^{87}Sr/^{86}Sr$ ratio of 0.7263±0.0006.

CHAPTER III

LITHOLOGY IN THE STUDY AREA

This chapter describes the rock units observed in the present study as exposed in Sattahip and Sri Racha areas. There are only two rock units, the CP unit of Carboniferous-Permain age and granite body which is believed to be of Triassic age. The emphasis of this study is laid on the CP unit whose age of Carboniferous-Permian is derived from a stratigraphic correlation by which the rock unit is overlain by the rocks at Khao Rewadi which includes a limestone lens being interbedded in a black shale, and that the limestone contains Permain fossil assemblage (Bunopas and others, 1983) where Nakinbodee and others (1976) otherwise mentioned a Late Carboniferous-Early Permain age. Base on the evidence of these fossils the Carboniferous-Permian age of CP unit is used for this study though the exact age confirmation of this rock unit is still controversial.

The study area in Sattahip, Bang Lamung and Sri Racha map sheets (Figure 3.1) is divided into 2 main parts due to the groups of exposures (Figure 3.2). The southern part is Sattahip area and the northern part, Sri Racha area. Both areas are of essentially metamorphosed sedimentary sequence exposures believed to be of the CP unit. The middle Bang Lamung area receives less interest as it is a low land area which is underlain by the highly weathered Triassic granite. In each sedimentary-rock area, the study was done on all reachable rock exposures. However, in Sattahip area, due to the restriction of maximum security in some military zones, the field investigation has not been accomplished in few locations.

3.1 CP Unite

The sedimentary rocks and their metamorphic resultants totally found in the study area are believed to be of Carboniferous-Permian age. The CP unit consists of black, white and pink shales, chert, carbonaceous mudstone, micaceous sandstone, micaceous shale and blue-gray to brown quartz sandstones with gray argillaceous limestone lenses. The metamorphic resultants are hornfelses and quartz schist and
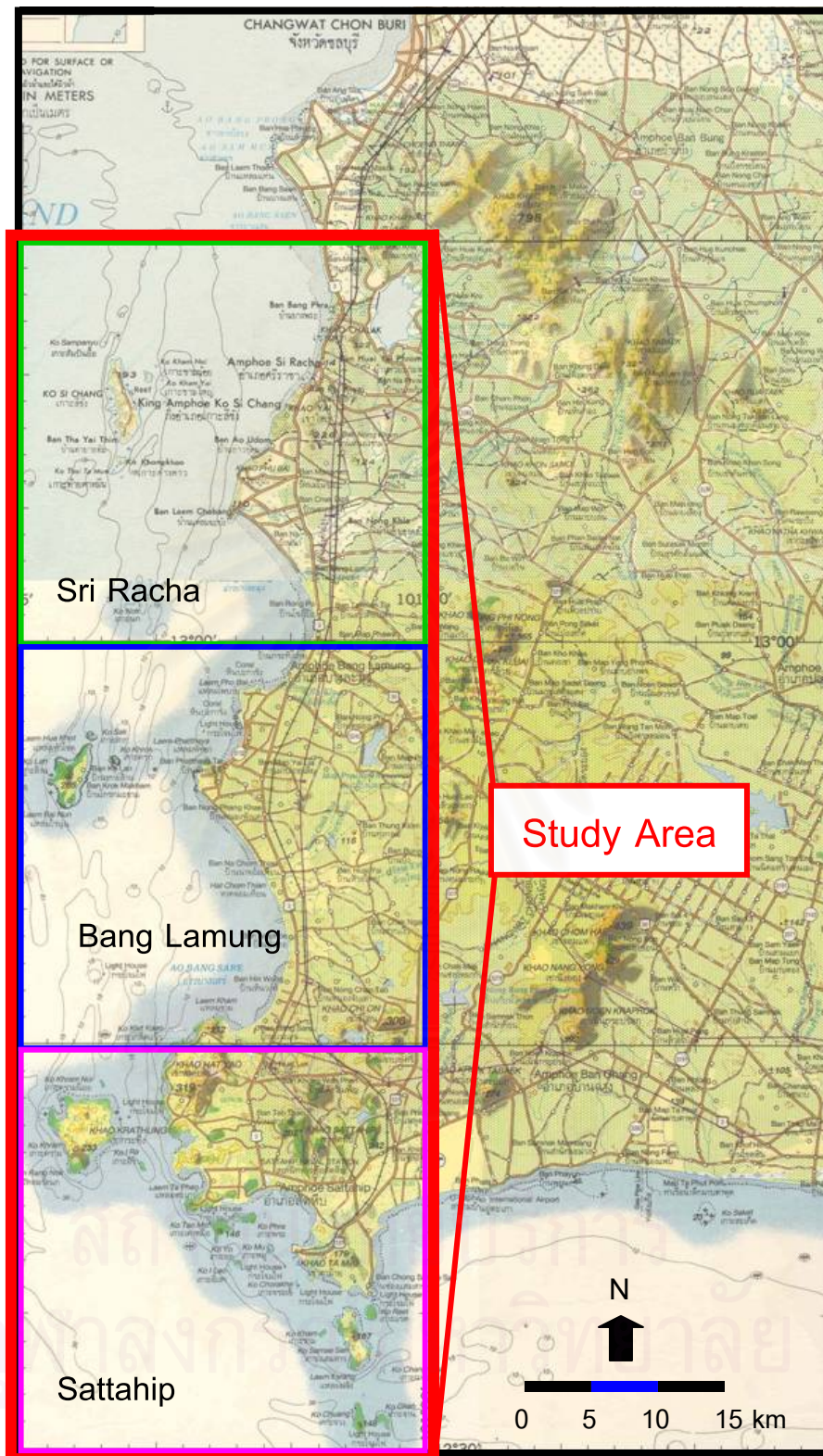
Figure 3.1 Study area as devided into Satthip, Bang Lamung and Sri Racha areas.
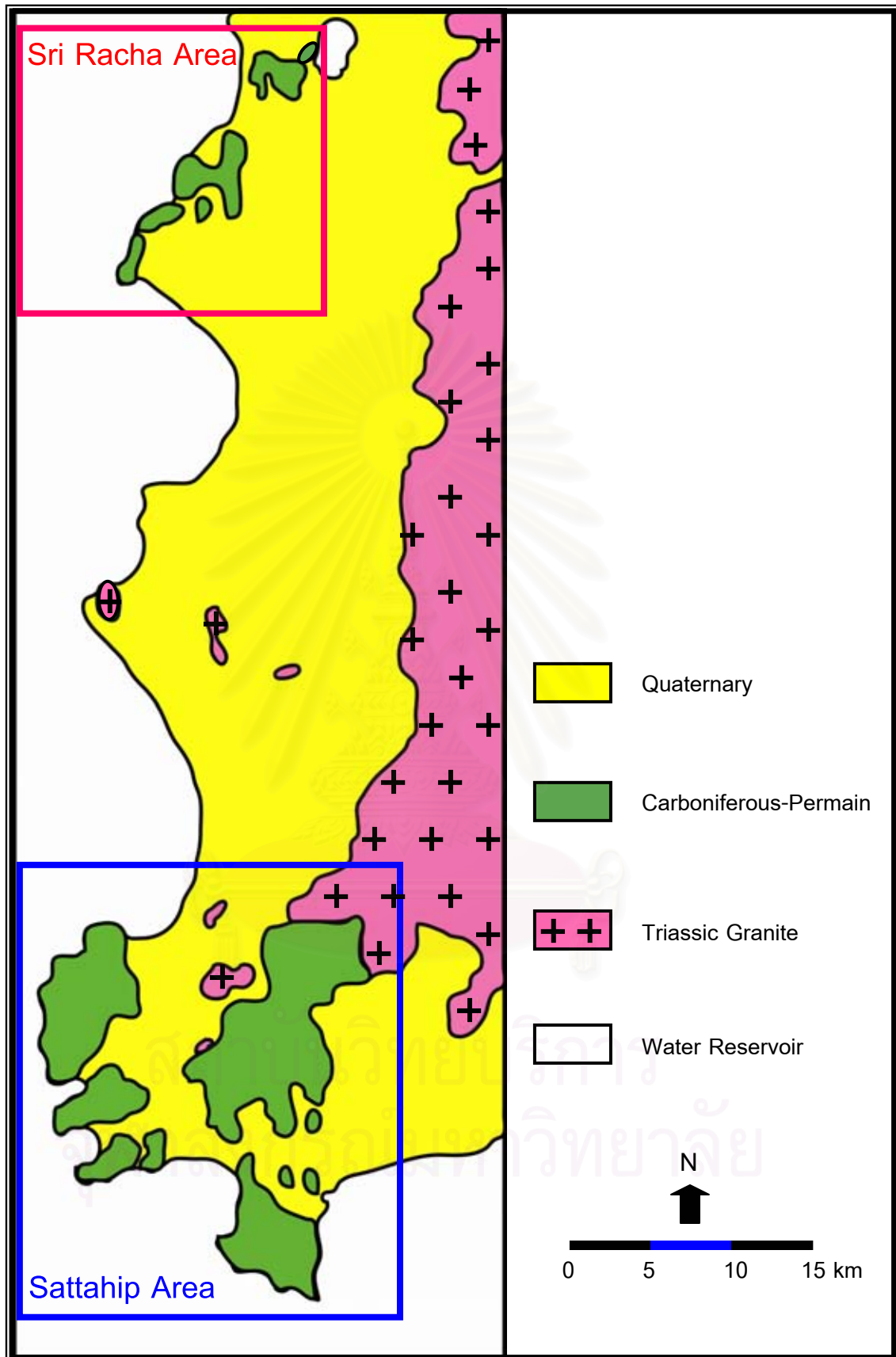
Figure 3.2 Geologic map of the study area with framed Sattahip and Sri Racha areas

(Modified after Department of Mineral Resources, 1999).

locally andalusite spotted slate.

3.1.1 Sattahip area

The Sattahip area is further divided into 5 subareas (Figure 3.3) as following, Sattahip I, Sattahip II, Sattahip III, Sattahip IV and Sattahip V, based on the accessibility of the geologic structures in the areas, to be analyzed in the later chapters. The division of 5 subareas is merely for convenience when rocks from each location are mentioned in the text. Rocks found in these areas consist mainly of shale interbedded with medium to coarse-grained sandstone. Lenses of carbonate rock are locally found in Sattahip V area. The detail lithology shows black, reddish brown, to white shales, slaty shale, laminated mudstone, micaceous shale, micaceous sandstone, hornfelses, chert, argillaceous limestone, marble and calcsilicate hornfels. All rocks here are believed to of the CP unit. The shale and mudstone sequence interbedded with sandstone had experienced several events of metamorphism and deformation explained in details below.

Because of the restriction in Sattahip Naval Base, some specific areas are not permitted for entrance. The possible outcrop for field investigation is thus generally along the road sides and on the beaches. Sattahip I subarea covers the hill chain of Khao Laem Kham, Khao Hat Yao, and Khao Hat So. The rocks found at Khao Laem Kham are obviously hornfels (Figure 3.4), partly spotted hornfels, spotted slate (Figure 3.5), and locally andalusite hornfels (Figure 3.6) with greenish gray shale intercalated with grayish black medium-grained sandstone (Figure 3.7). The andalusite hornfels, locally exposed only in this Sattahip I subarea, can possibly be used as indicator of contact metamorphism. These rocks exposing along the shore line show their bedding planes gently to moderately dipping to the east. The spotted slate is also found dominantly at Khao Mon and Khao Sattahip in the subarea of Sattahip IV locating in the east-central part of Sattahip area.

The hill to the south of Khao Laem Kham is Khao Hat Yao which makes the main central and almost all southern parts of this Sattahip I area. Because of the security restriction, only the western part of this hill is allowed for a geologic observation.
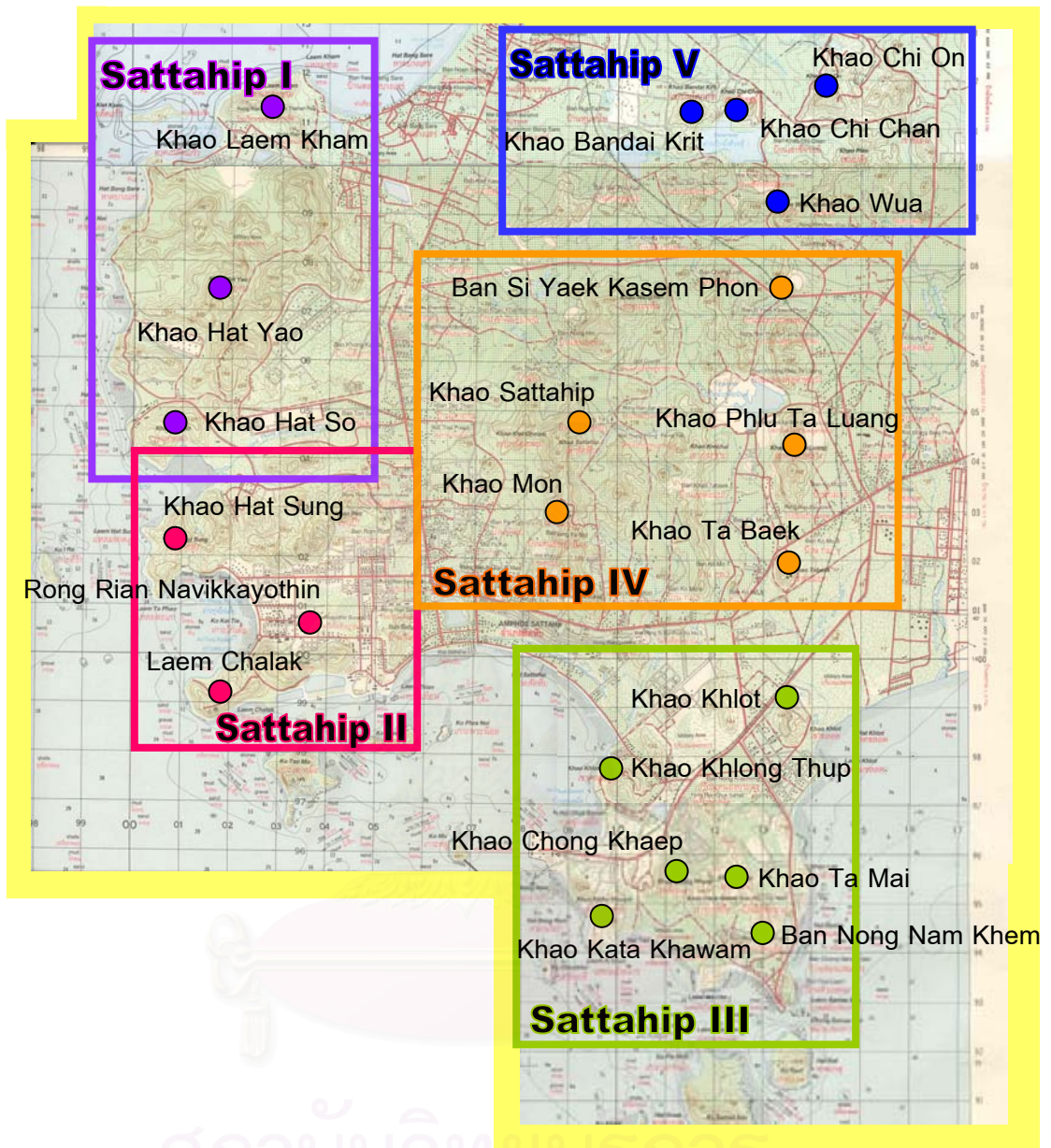
Figure 3.3 Topographic map of Sattahip area being subdivided into 5 subareas. The subareas are Sattahip I, Sattahip II, Sattahip III, Sattahip IV and Sattahip V.

Figure 3.4 Hornfels at Khao Laem Kham (Sattahip I). Attitude of bedding (parallel to cleavage planes) is (strike/dip) 338/32 NE. Grid reference 0701785 E 1411151 N.

Figure 3.5 Andalusite hornfels showing square to longitudinal euhedral andalusite crystals, and spotted hornfels (lower right corner) at Khao Laem Kham (Sattahip I). Grid reference 0701842 E 1411327 N.

Figure 3.6 Spotted slate at Khao Laem Kham (Sattahip I). Attitude of bedding (parallel to cleavage planes) is (strike/dip) 329/31 NE. Grid reference 0701831 E 1411303 N.

Figure 3.7 Shale intercalated with grayish black sandstone with joints and irregular fractures directions (Sattahip I). Bedding attitude is 348/31 NE. Grid reference 0701951 E 1411488 N.

The majority of rocks here are composed of laminated mudstone interbeded with shale (Figure 3.8).

The well exposed shale-mudstone sequence (Sattahip Shale of Bunopas, 1983) locally interbedded with sandstone is mainly found in Sattahip I subarea as described above. The rocks also exposue in Sattahip II subarea, along the coast of Laem Chalak (Figure 3.9) and Khao Hat Sung (Figure 3.10), and in Sattahip III at Khao Chong Khaep, Khao Ta Mai, in the northwestern part to Khao Kata Kawam, and at Ban Nong Nam Khem. Petrographically the rocks from these subareas are quite the same in term of mineral composition (Figures 3.11, 3.12 and 3.13). Sandstones interbedded with these shales and mudstones are bluish gray, yellowish brown, reddish brown, fine to medium grained and subangular to subrounded (Figure 3.14). The mesoscopic folds are commonly found in these rocks in Sattahip II subarea (Figure 3.15) and are also obviously noticeable in light gray thin bedded chert and thin-interbedded shale of Khao Phlu Ta Luang (Figure3.16) and Khao Tabaek (Figure 3.17), and northern part of Ban Si Yaek Kasem Phon (Figure 3.18) in Sattahip IV and Khao Khlot in northeastern part of Sattahip III (Figure 3.19).

The main carbonate rocks crop out in area of Sattahip V covering Khao Chi Chan, Khao Chi On, Khao Bandai Krit and Khao Bai Si. Rocks compose of marble (Figure 3.20), calcsilicate hornfels (Figures 3.21 and 3.22) and recrystallized argillaceous limestone (Figure 3.23). The argillaceous limestone is also found at southwestern Khao Phlu Ta Luang in Sattahip IV area and at Khao Wua in Sattahip V area (Figure 3.24). Banding is obviously shown by interlayering of calsilicate at Khao Chi Chan and Khao Chi On. The bedding planes are approximately conformable to the foliation, dipping to SE, thus suggest the tight to isoclinal folds. The contact zone between granite and carbonate sequence country rocks is observed at Khao Chi Chan whereas a very clear banding in calcsilicate is observed when approaching the granite intrusive body (Figure 3.25).

3.1.2 Sri Racha area

Similar to Sattahip area, Sri Racha area is subdivided into 3 subareas, by the

Figure 3.8 White to reddish brown shale at shore line of Khao Hat Yao (Sattahip I). The
attitude of bedding, 1-4.5 cm thick, is 28/22 SE. Grid refernce 0700108 E
1405379 N.

Figure 3.9 Black shale at Laem Chalak (Sattahip II) showing a limb of angular fold. The
attitude of bedding is 280/53 N. Grid reference 0702553 E 1400277 N.

Figure 3.10 Medium to coarse grained sandstone underlying bedded mudstone at Khao
Hat Sung (Sattahip II). Attitude of bedding is (strike/dip) 351/9 E. Grid
reference 0700860 E 1401436 N.
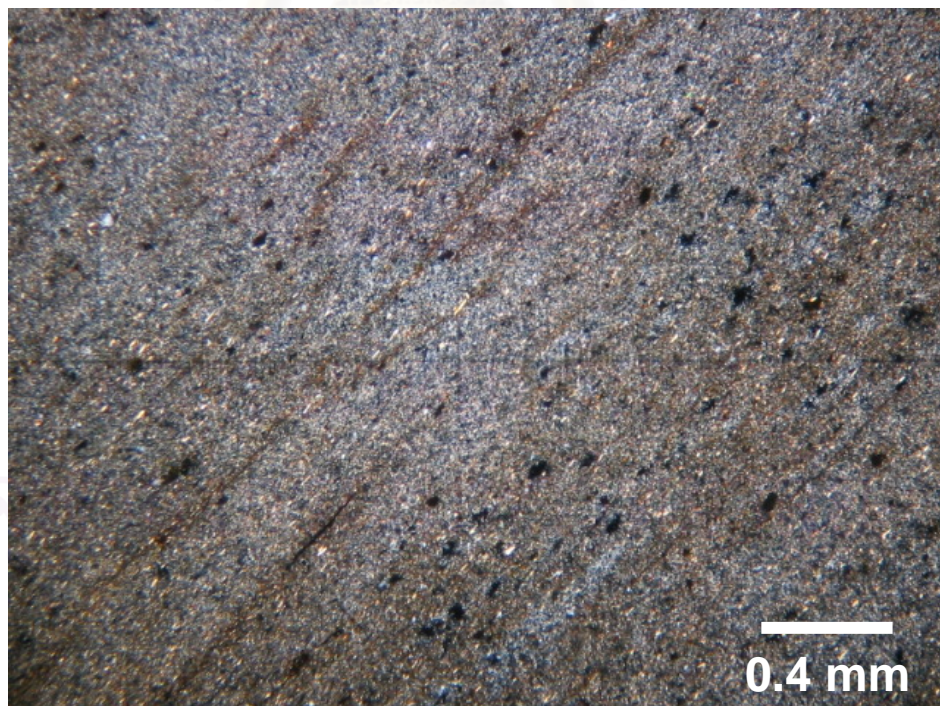
Figure 3.11 Photomicrograph of siliceous shale at Laem Chalak (Sattahip II). Crossed
nicols. Grid reference 0702553 E 1400277 N.
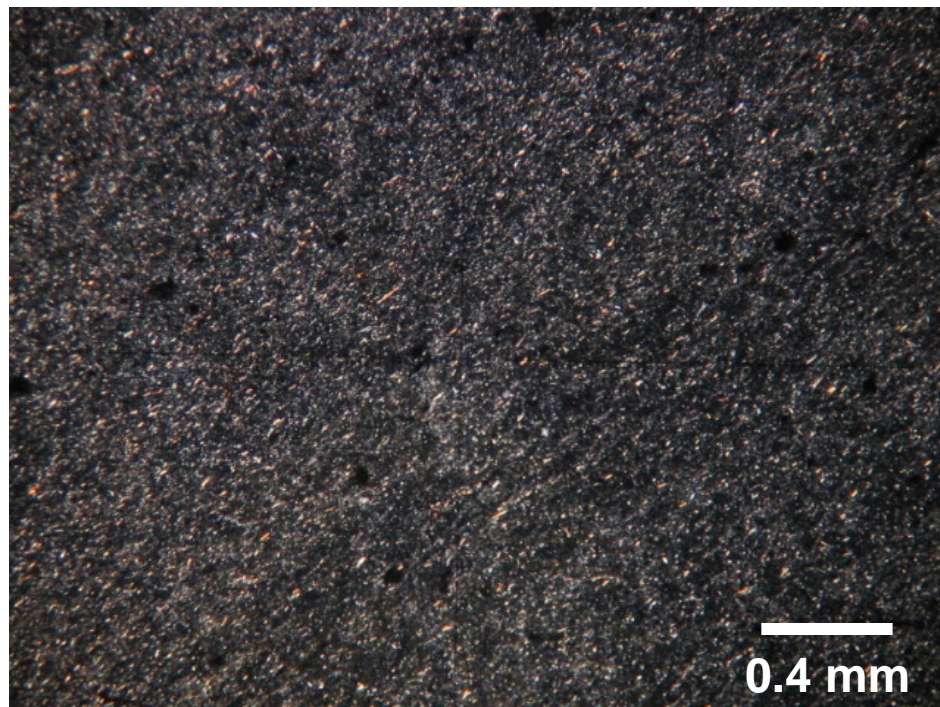
Figure 3.12 Photomicrograph of mudstone with minor sericite at Laem Samae San
(Sattahip III), Crossed nicols. Grid reference 0713425 E 1393321 N.
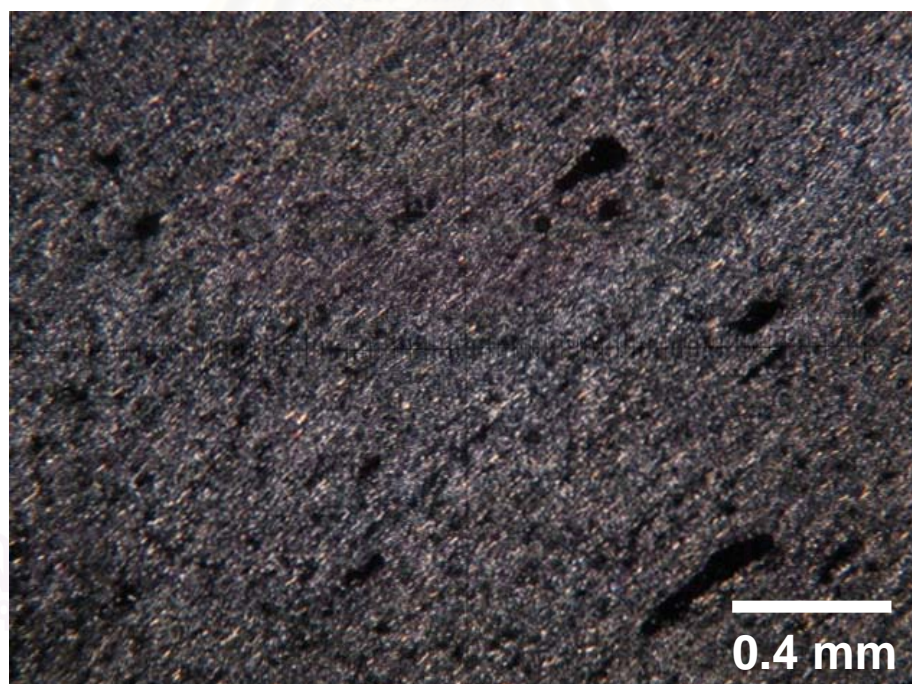
Figure 3.13 Photomicrograph of siliceous shale with minor sericite from northwestern
part to Khao Kata Kawam (Sattahip III). Crossed nicols. Grid reference
0708974 E 1395837 N.
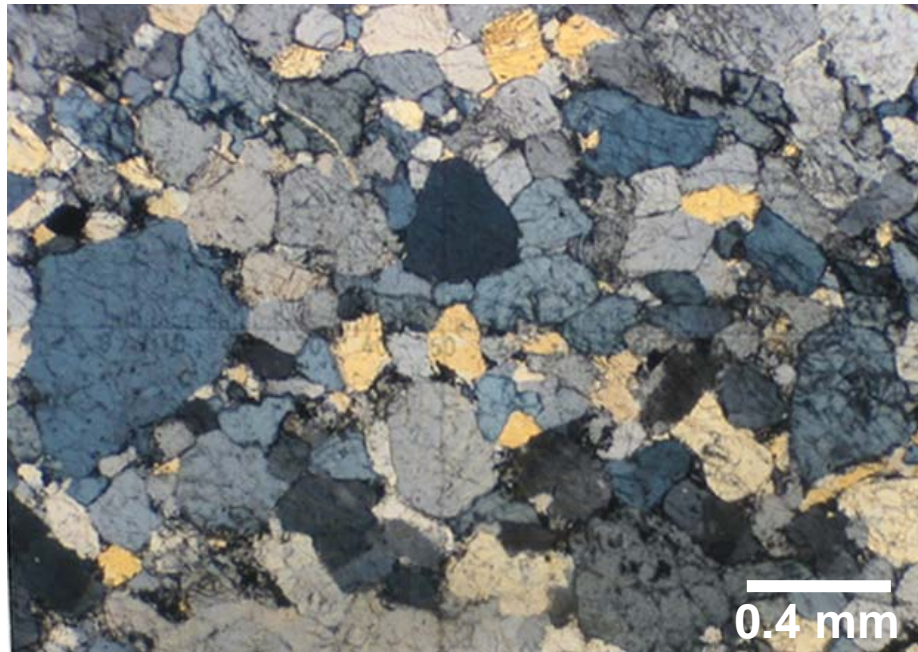
Figure 3.14 Photomicrograph of medium-grained, poorly-sorted, subangular to subround quart sandstone at Rong Rian Navikkayothin Burana (Sattahip II). Crossed nicols. Grid reference 0703371 E 1400865 N.

Figure 3.15 Angular folds in white- and reddish brown-weathered colored of black shale interbedded with reddish mudstone at Laem Chalak (Sattahip II). Grid reference 0702553 E 1400277 N.

Figure 3.16 Complex angular folds of bedded chert interbeded with siliceous shale in a
quarry in northern part of Khao Plu Ta Luang (Sattahip IV). Grid reference
0713947 E 1404780 N.

Figure 3.17 Concentric open fold of bedded chert in a Quarry of Khao Tabaek (Sattahip
IV). Grid reference 0713629 E 1401847 N.

Figure 3.18 Complex neutral angular fold in a quarry to the north to Ban Si Yaek Kasem

Phon (Satthip IV). Grid reference 0713367 E 1407565 N.

Figure 3.19 Upright plunging open fold at Khao Khlot (Sattahip III), with axial plane

351/82 E (strike/dip) and fold axis 353/21 (trend/plunge). Grid reference

0713594 E 1399138 N.

Figure 3.20 Buddha Image engraved in marble and recrystallized limestone at Khao Chi Chan (Satthip V). Grid reference 0712772 E 1411619 N.

Figure 3.21 Exposure of calcsilicate rock at Khao Chi On (Sattahip V). Grid reference 0714361 E 1411248 N.

Figure 3.22 Foliated calcsilicate rock at Kho Chi On at the same location as in Figure
3.21. Grid reference 0714361 E 1411248 N.

Figure 3.23 Gently NNE dipping bedded argillceous limestone exposed at the
southwestern part of Khao Plu Ta Luang. Brittle fractures are commonly
observed. Grid reference 0713296 E 1403793 N.

Figure 3.24 Argillaceous limestone at Khao Wua (Sattahip V). Attitude of bedding is (strike/dip) 102/32 S. Grid reference 0713099 E 1409310 N.
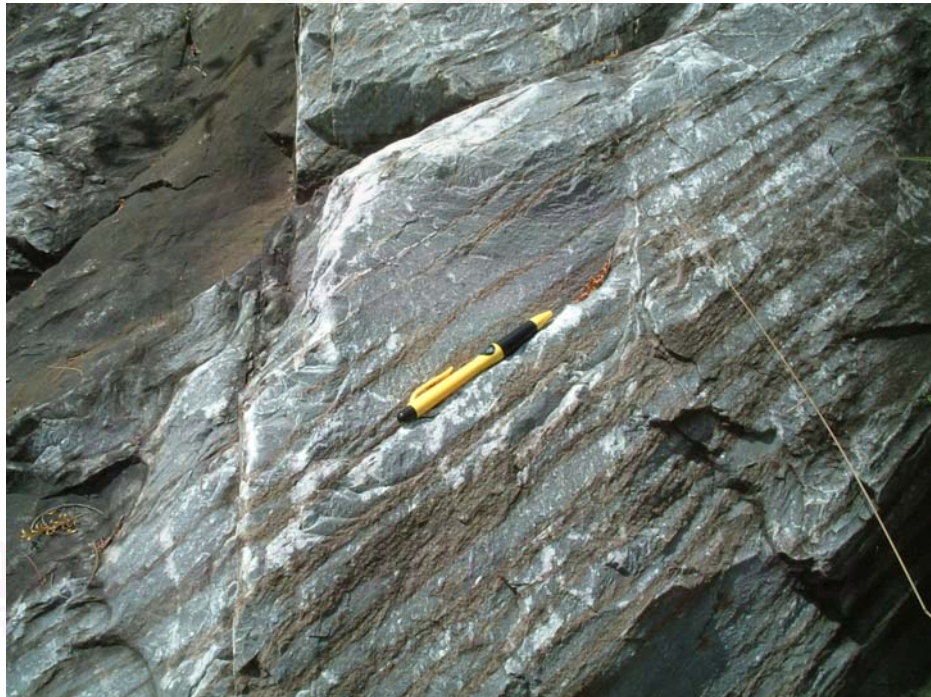
Figure 3.25 Foliation in calsilicate at Khao Chi Chan near the contact zone of granite. Attitude of foliation is 35/43 SE, 42/46 SE. Grid reference 0712772 E 1411619 N).

same purpose that mentioned for that of Sattahip area, The subareas are Sri Racha I, Sri Rach II and Sri Racha III (Figure 3.26). The general structural trend of rocks in the whole Sri Racha area is in the NE-SW direction as exposed mostly at Khao Laem Chabang, Khao Bo Ya, Khao Nong Ang and Khao Phunai in Sri Racha III subarea (Figure 3.27 and 3.28). The trend changes to east-west at Khao Khwang in Sri Racha II subarea. The rocks found on these hills are quartzites, and then gradually change to sericite-quartz schist. The lithology of these rocks is well defined by the petrographic study. Quartzitic rocks at Khao Laem Chabang, Khao Bo Ya, Khao Phu Bai, Khao Ban Uttaphong and in the western part of Khao Khwang are massive quartzite with minor amount of small flakes of sericite (Figure 3.29, 3.30, 3.31 and 3.32) whereas quartz mica schist (Figure 3.33) or phyllite and sericite quartz schist are found at Khao Phu, in the eastern part of Khao Khwang (Figure 3.34) and in the northeastern part of Laem Hin Khao (Figure 3.35).

The carbonate rocks are less commonly found in Sri Racha area. They mainly expose in Sri Racha I subarea at Khao Yai Si and Khao Rewadi, and sporadically crop out at Laem Hin Khao in Sri Racha II subarea. The rocks cropping out at the western part of Khao Yai Si are greenish gray limesilicate rocks with ptygmatic bands (Figure 3.36).

3.2 Granites

The granites in the study area expose mainly in Amphoe Bang Lamung in the middle between Sattahip area to the south and Sri Racha area to the north. This batholithic body is believed to be of S-type granites and belong to the Rayong-Bang Lamung Granite by which the age of intrusion is Upper Triassic (Nakapadungrat and others, 1984). However Suriyachai and Sulyapongse (1995) mentioned that there are three granitic phases of this intrusion.

As it is highly weathered, a good exposure of granite is hardly found. However there are few fairly good outcrops in Bang Lamung area that could be studied. It was noted that the granite is generally coarse-grained with porphyritic texture of quartz and feldspar phenocrysts (Figures 3.37, 3.38, 3.39 and 3.40). The mineral assemblases are majorly quartz, feldspar, muscovite, and biotite with minor accessory minerals.
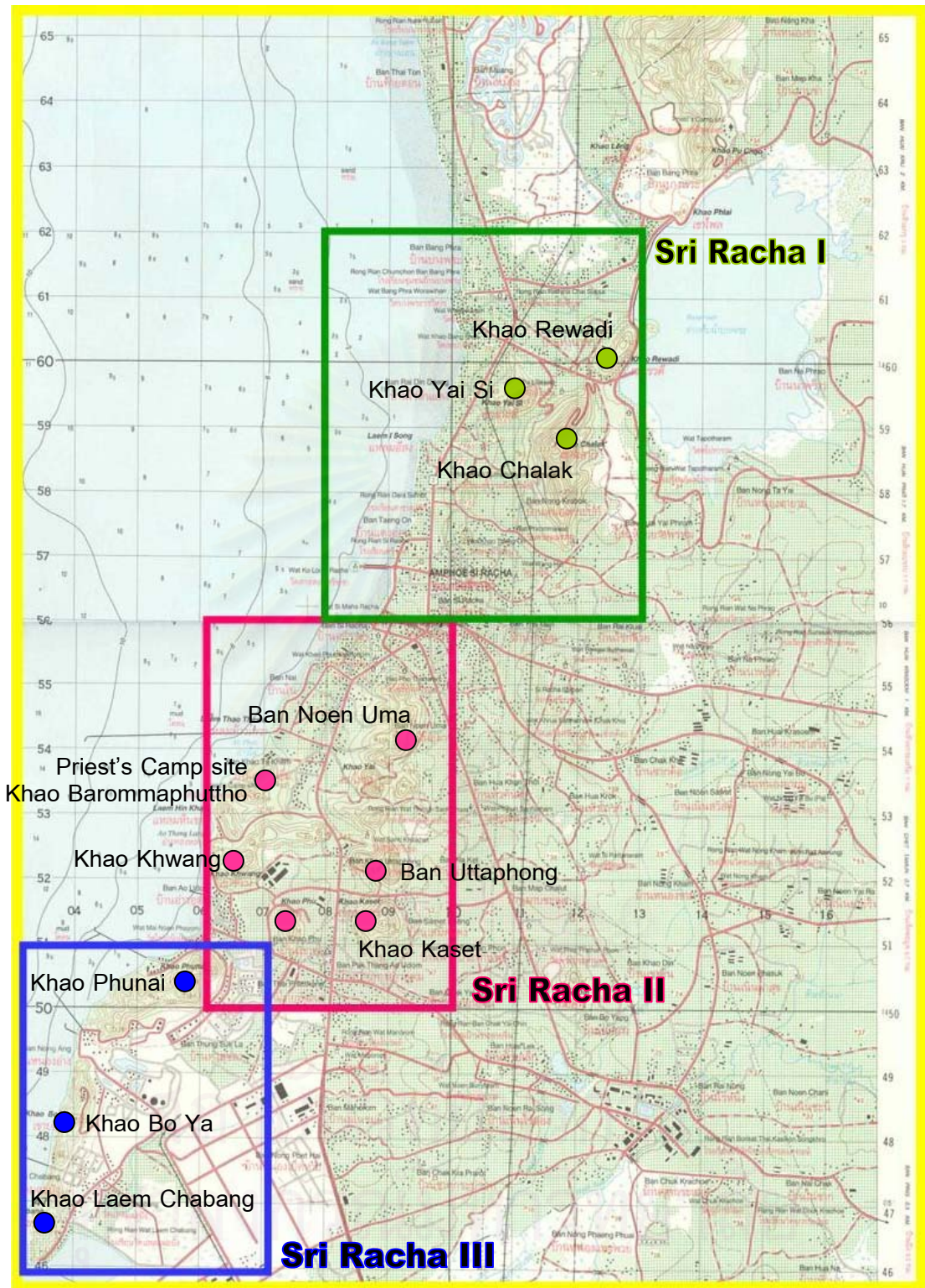
Figure 3.26 Topographic map of Sri Racha area beinh subdivided into 3 subareas. The
subareas are Sri Racha I, Sri Racha II and Sri Racah III.

Figure 3.27 Bedding of quartzite at Khao Laem Chabang (Sri Racha III). The attitude of
bedding is (strike/dip) 212/40 NW. Grid reference 0703520 E 1446150 N.

Figure 3.28 Bedding of quartzite at Khao Phunai (Sri Racha III). The attitude of bedding
is (strike/dip) 237/42 NW. Grid reference 0704778 E 1450448 N.
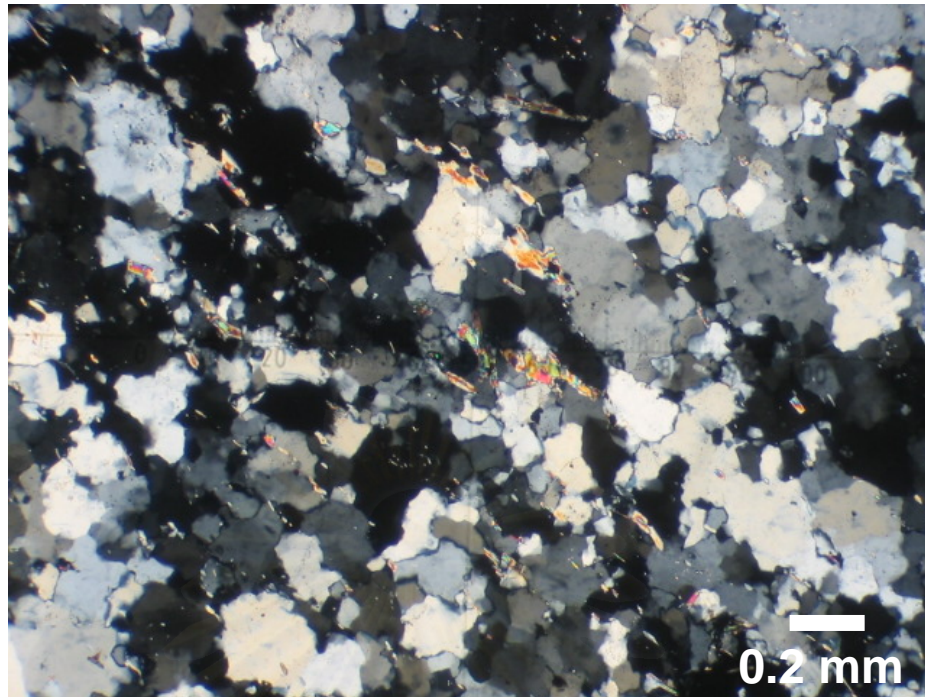
Figure 3.29 Photomicrograph of micaceous quartzite at Laem Chabang (Sri Racha I).

Crossed nicols. Grid reference 0703565 E 1446204 N.
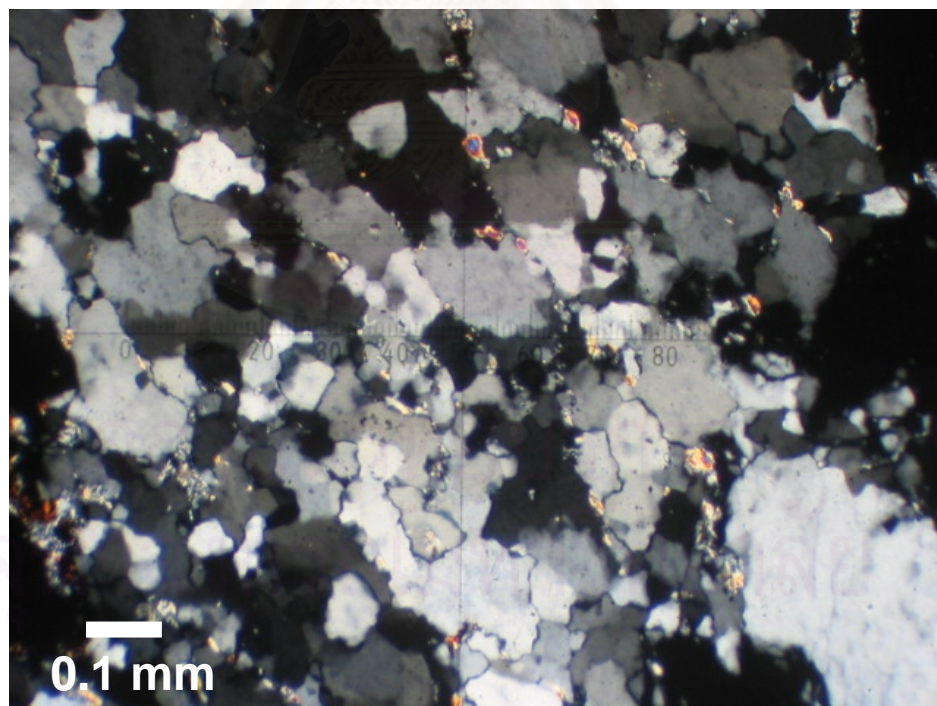
Figure 3.30 Photomicrograph of micaceous quartzite at Khao Bo Ya (Sri Racha I).

Crossed nicols. Grid reference 0704193 E 1448324 N.
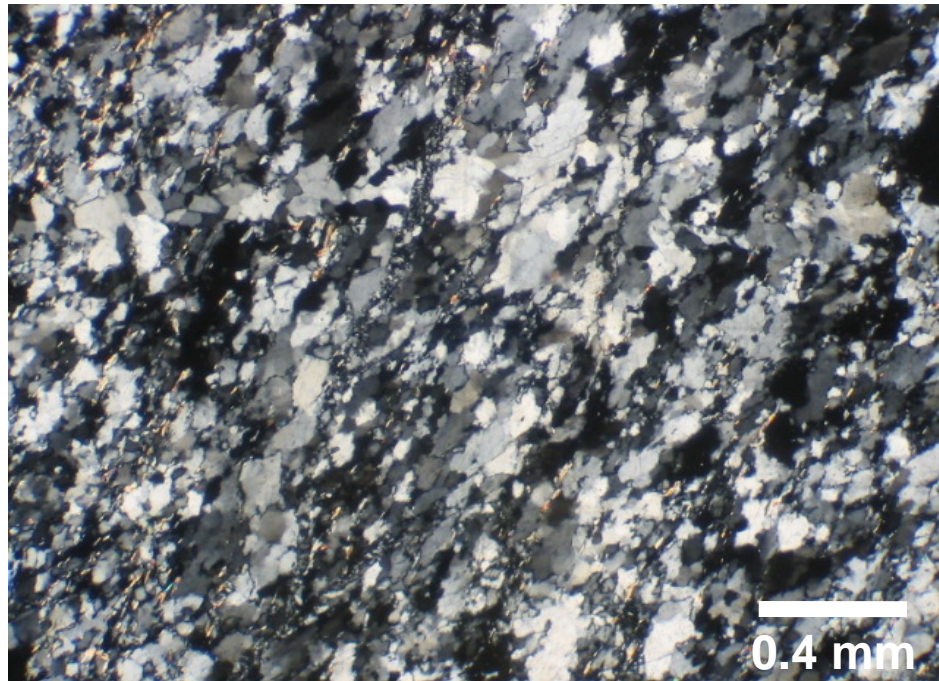
Figure 3.31 Photomicrograph of micaceous quartzite in western Khao Khwang (Sri Racha II). Crossed nicols. Grid reference 0706164 E 1452192 N.
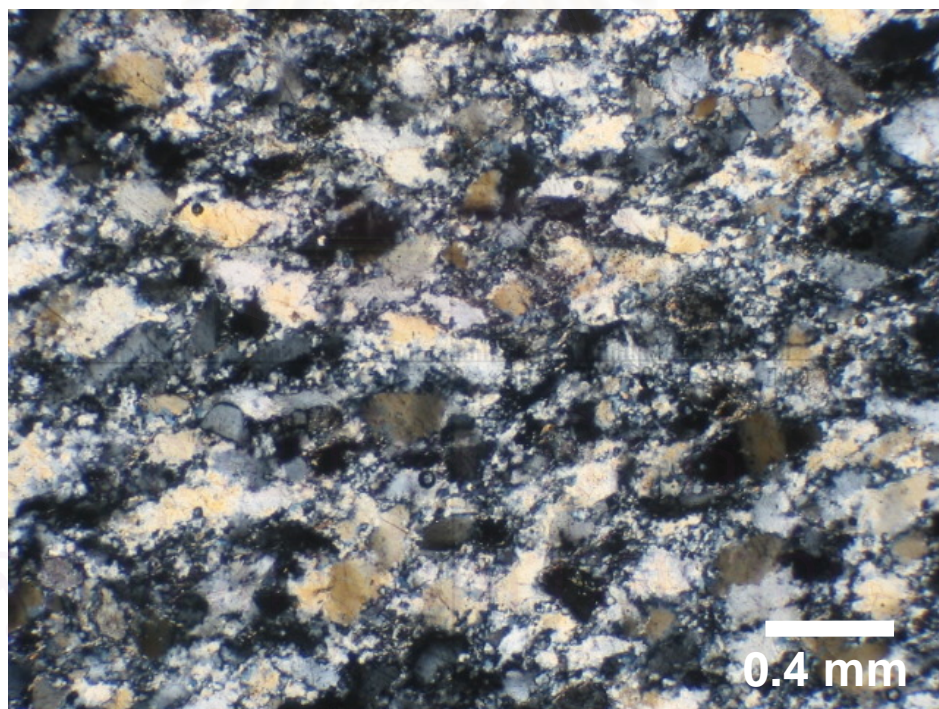
Figure 3.32 Photomicrograph of quartzite at Khao Phunai (Sri Racha I) illustrating dynamic recrystallized quartz porphyloclasts. The porphyroclasts are augen-like among finer grained quartz matrix. Crossed nicols. Grid reference 0704656 E 1450361 N.
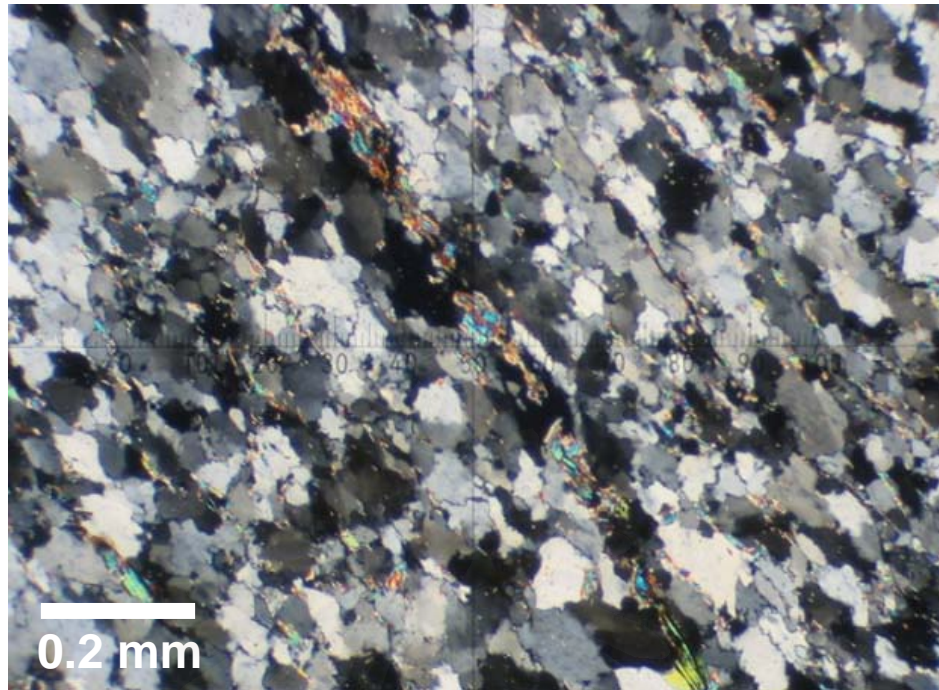
Figure 3.33 Photomicrograph of micaceous quartzite at Khao Ban Uttaphong (Sri Racha II). Crossed nicols. Grid reference 0708407 E 1452507 N.
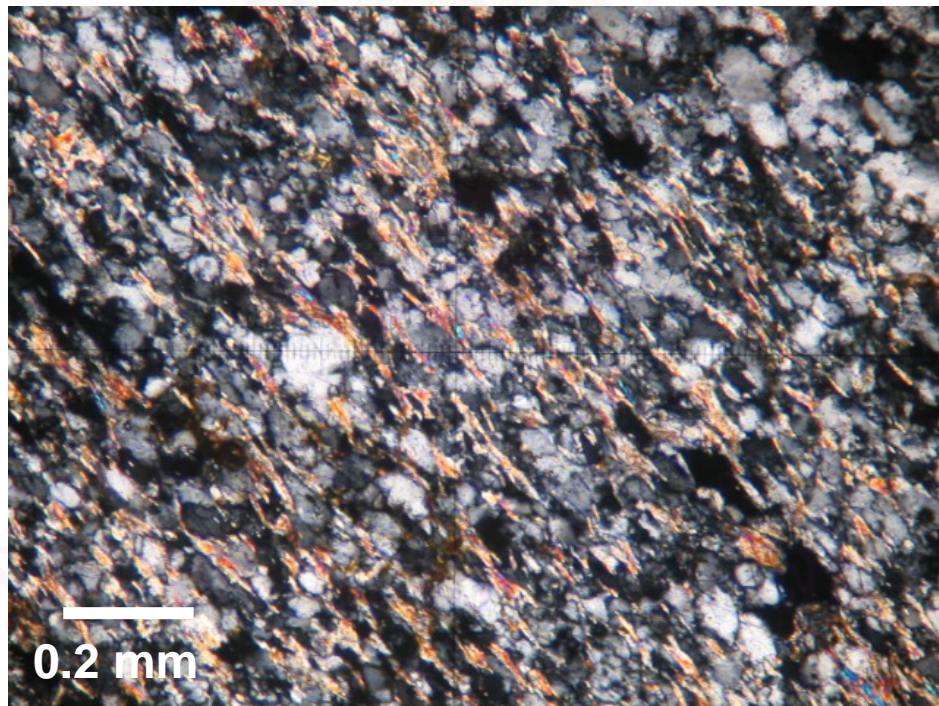
Figure 3.34 Photomicrograph of quart mica schist in eastern Khao Khwang (Sri Racha II). Crossed nicols. Grid reference 47707996 E 1452597 N.
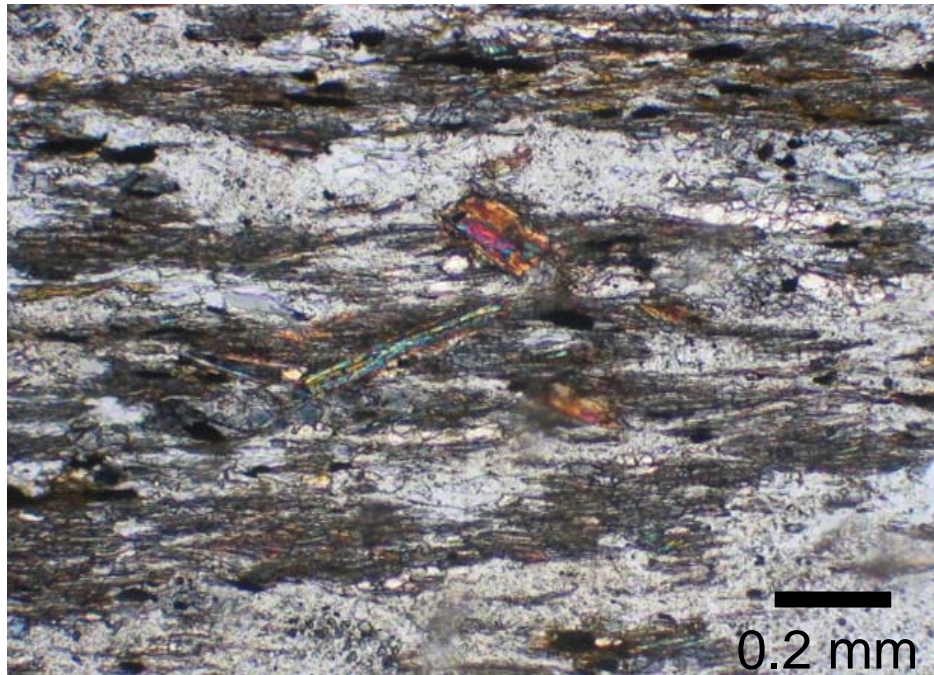
Figure 3.35 Photomicrograph of quartz mica phyllite at the Priest's Camp Site Khao

Barommaphuttho (Sri Racha II), showing the subhorizontal mica-rich layers

and quartz microlithons. Crossed nicols.Grid reference 0706972 E 1453426 N.

Figure 3.36 Ptygmatic banding in calcsilicate rocks at Khao Yai Si (Sri Racha I). Grid

reference 0710931 E 1460272 N.

This granite could be of the major phase Granite I of Suriyachai and Sulyapongse (1995). In Sattahip and Sri Racha area, on the other hand, the granite is mostly weathered and the exposures are found scattering at the ground level all over the place. The lithology is commonly found as the remains or residuals of weathered granites. In Sattahip area it is noticed that the rock at Ban Klet Kaeo is highly weathered foliated granite (Figures 3.41 and 3.42). The fine- to medium grained, porphyritic biotite-muscovite granite is also found in the study area. These granites are believed to be of the minor phases namely Granite II and Granite III as mentioned by Suriyachai and Sulyapongse (1995) by which one of these granite phases has a close relationship with pegmatite-aplite composite veins and is commonly concentrated near the roof or around the periphery of the batholith. Moreover many large and small quartz veins significantly associate Rayong-Bang Lamung Granites.

Figure 3.37 Exfoliated porphyritic granite at Khao Din in Bang Lamung area. Grid
reference 0713747 E 1413877 N.

Figure 3.38 Porphyritic granite at Khao Din (same locality as in Figure 3.37). The
feldspar phenocryst is about 1.5x3 cm^2 and is surrounded by coarse-
grained equigranular matrix.

Figure 3.39 Porphyritic granite exposure at shore line of Hat Bang Sare, Bang Lamung area. Grid Reference………..

Figure 3.40 A close up view of porphyritic granite illustrating the feldspar phenocrysts at Bang Lamung area (Same locality as that in Figure 3.39).

Figure 3.41 Exposure of highly weathered granite at Ban Klet Kaeo (Sattahip V). Grid reference 0707566 E 1408481 N.

Figure 3.42 Highly weathered foliated granite at the same locality as in Figure 3.4.

CHAPTER IV

STRUCTURAL GEOLOGY IN THE STUDY AREA

This chapter describes the finding and the analysis of the geologic structures using the equal-area lower-hemisphere sterographic projection and rose diagram. The statistical significance of the stereonet plots and rose diagram were obtained from a graphical depiction of the computer program, StereoNett Version 2.46, written by Duyster (2000) of Ruhr-Universität Bochum, Germany.

4.1 Descriptive Mesoscopic Structures

The procedure in structural study usually begins with a field-based investigation of the mesoscopic structures, then supplemented by laboratory study of hand specimens. In this study area, the bedding planes as well as the fold elements were observed and measured for the orientations in order to analyze the mesoscopic structural data and then extrapolate to form a macroscopic structure. There are several places where mesoscopic folds were noticed and sedimentary bedding still observable and reflected the initial gross stratigraphic sequence prior to deformation. These structural data are described as following.

4.1.1 Folds

Mesoscopic folds could be seen in several places both in Sattahip and Sri Racha areas. The fold elements were observed and measured in order to determine the orientation of fold axes and axial planes. Two main directions of fold axes were noted in the study area. The first trending is in NE-SW direction with gentle plunging to NE direction (Figures 4.1, 4.2 and 4.3) and the other trends in the NW-SE to NNW-SSE direction with gentle to moderate plunging to NW-NNW direction (Figures 4.4, 4.5 and 4.6). The axial plane orientation varies from subhorizontal (Figures 4.7 and 4.8) at Khao Hat Sung to steeply dipping to ENE direction at Khao Plu Ta Luang (Figures 4.9 and 4.10).
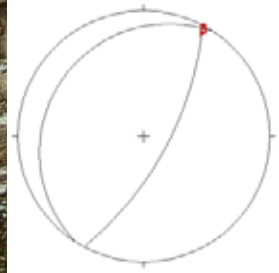
Figure 4.1 Angular fold at Ban Khao Tabaek. Fold axis is 29/2 (trend/plunge). Grid
reference 0713629 E 1401847 N.
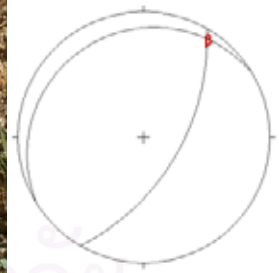
Figure 4.2 Folds at Ban Khao Tabaek. Fold axis is 33/7 (trend/plunge). Grid reference
0713629 E 1401847 N.

Figure 4.3 Kink folds at Khao Wua illustrating axial plane dipping to SE. Fold axis is 40/7 (trend/plunge). Grid reference 0713055 E 1409002 N.
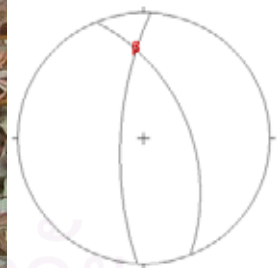
Figure 4.4 Upright plunging fold at Khao Khlod. Fold axis is 355/27 (trend/plunge). Grid reference 0713594 E 1399138 N.
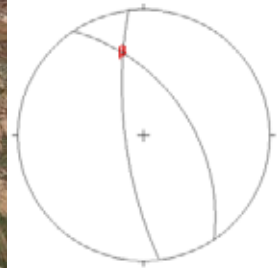
Figure 4.5 Upright plunging fold at Khao Khlod. Fold axis is 346/30 (trend/plunge). Grid reference 0713594 E 1399138 N.
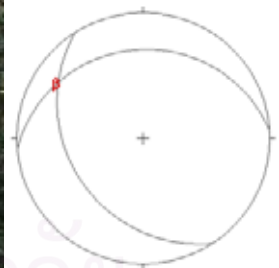
Figure 4.6 Neutral fold in Sri Racha area. Fold axis is 303/19 (trend/plunge). Grid reference 0707912 E 1453121 N.

Figure 4.7 Overfold at Khao Hat Sung with gently dipping axial plane 264/18 N. Grid

reference 0700942 E 1401640 N.

Figure 4.8 Concentric neutral fold at Khao Hat Sung with sub-horizon axial plane 234/25 N.

Grid reference 0700762 E 1401537 N.

Figure 4.9 Upright chevron fold at northern part of Khao Plu Ta Luang illustrating axial
plane orientation 25/72 SE. Grid reference 0713935 E 1404803 N.

Figure 4.10 Rounded-closure similar fold at northern part of Khao Plu Ta Luang
illustrating axial plane trending 20/80 SE. Grid reference 0713935 E
1404803 N.

In the study area the folds morphology could be classified into two main categories. The first category is isoclinal to tight neutral fold, found at Khao Hat Sung (Sattahip II) and Khao Wua (Sattahip V), in addition to the layer thickness that maintain constantly and known as parallel folds. Folds at Khao Tabaek (Satthip IV) are gently plunging, concentric folds. According to their fold shapes and orientation of fold axes, they are able to gather in the same category. The second group is characterized by gently plunging, upright angular folds at Khao Plu Ta Luang and Khao Khlod

4.1.2 Joints

Systematic joint sets are commonly distributed throughout the study area. The rose diagram of 178 fractures in Sattahip area shows a statistic significance that most joints trend in the WNW-ESW direction (Figure 4.11a). In contrast to those in Sattahip area, the major trend of joints in Sri Racha area is NNW-SSE direction (Figure 4.11b). Plumose structures found on mainly joint surfaces in siliceous shale at Khao Plu Ta Luang indicate an evidence of tensile cracks, not shear displacement surfaces. Generally these joints are thus believed to be extensional fractures. They could orientate perpendicularly to the σ_3 dirction, or in the otherwords be parallel to σ_1/σ_2 plane. These stress-field configurations $\sigma_1/\sigma_2/\sigma_3$ have not yet been considered in related to those originate other structures in the study area.

4.1.3 Faults

In the study area, a very large-scale fault is found locally in Sattahip area at Khao Mon (Figure 4.12). It is a very low angle fault but without proof of displacement direction. Here the fault was found to cut the aplite dykes which perhaps associating the deep-seated intrusive bodies. Thus the igneous activity is noted to be older than faulting based on the cross-cut relationship. In the other word, the faulting was occurred in later episode after the igneous intrusion.

Also to the west of Khao Mon, another outcrop was observed with a fault plane forming a clear plane of separation of two contrasting strata of rock (Figure 4.13). Moreover there is a difference of the nature of metamorphism between the underlying
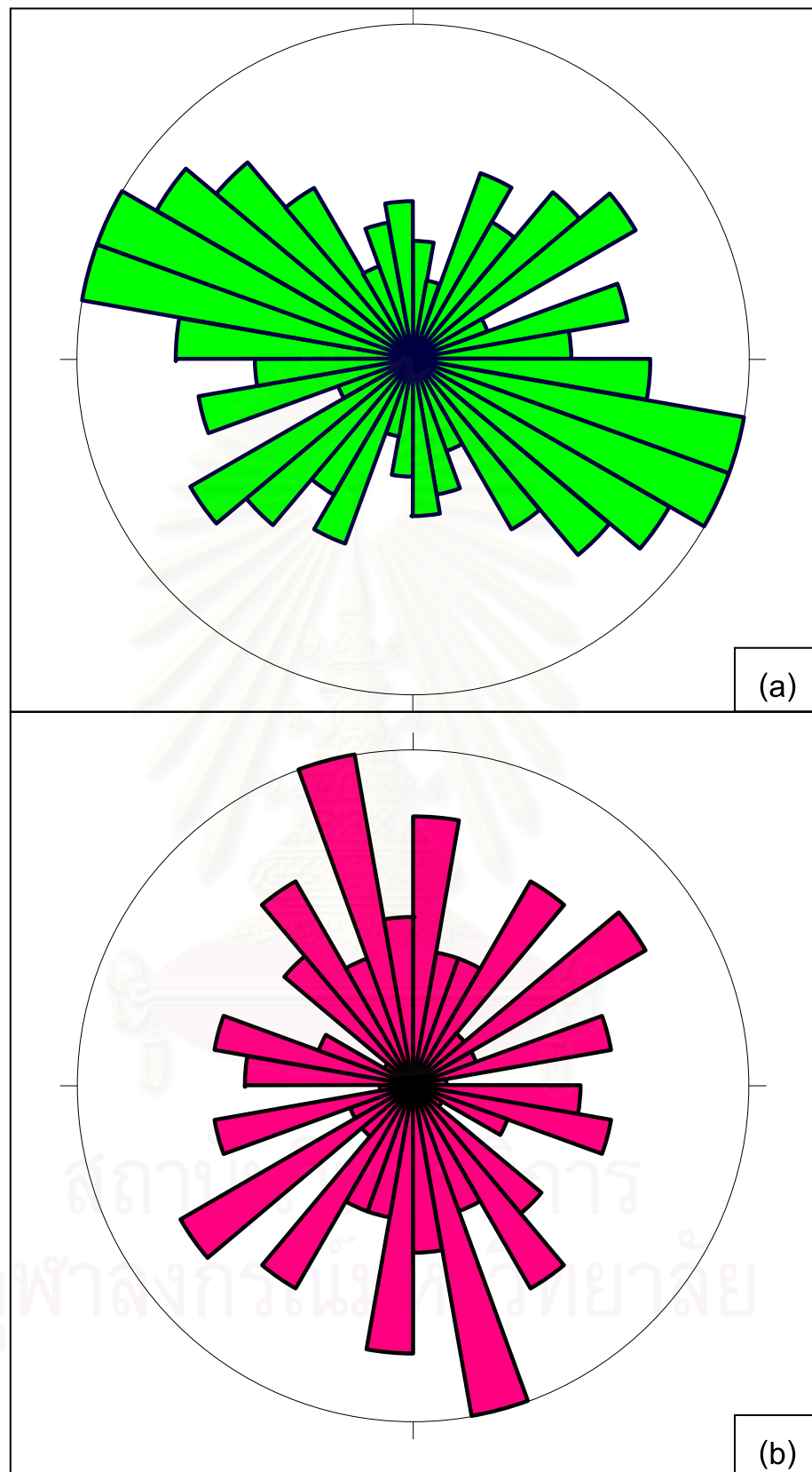
Figure 4.11 Rose diagrams of 178 strike values of fractures in Sattahip area (a) and of

88 of fractures in Sri Racha area (b). Major trending is in WNW-ESE direction

and NNW-SSE direction respectively.

Figure 4.12 Low-angle SW dipping fault at Khao Mon (Grid reference 0709186 E 1401189 N). The whole fault (a) is approximately 40 m long and cross-cutting the aplite dykes shown in the close-up pictures (b and c). Based on the cross-cut relation, the fault is younger than igneous activity of aplite dykes.

Figure 4.13 Fault in a quarry to the west of Khao Mon (Grid reference 0710308 E

1403994 N). Spotted slate overlies unmetamorphosed black shale.
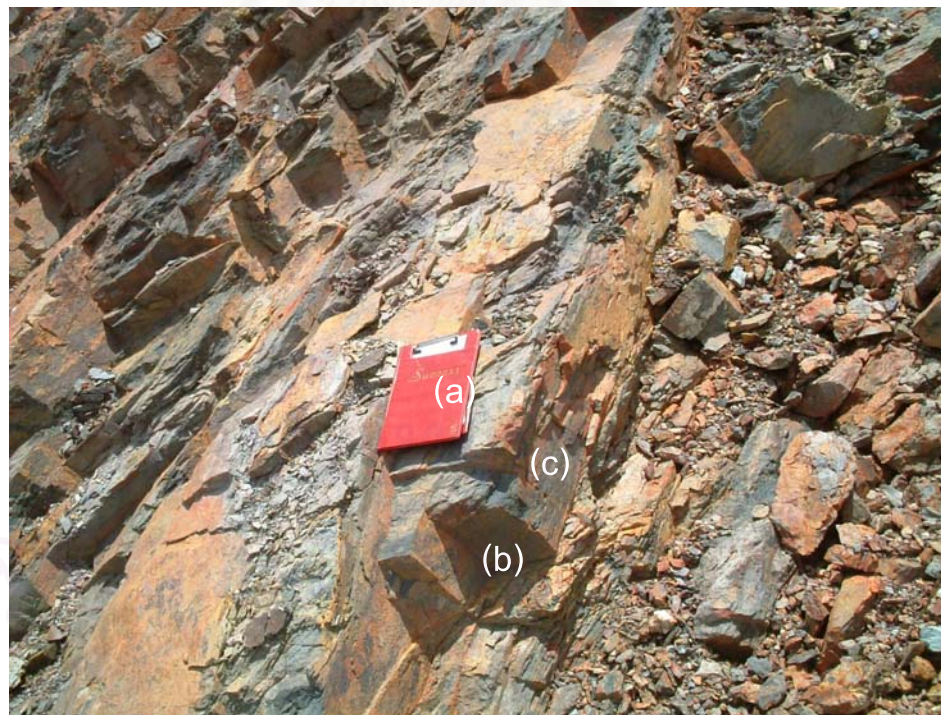
Figure 4.14 Overlying spotted slate (Figure 4.13) with blocky characteristics. The

fractures are a) 3/45 E (beds?), b) 136/57 SW (joints), and c) 255/72 NE

(joints).

and overlying strata.   Descriptive lithology of the underlying rock is of a weathered, black argillaceous rock, while the overlying rock is spotted slate with obviously three fracture sets (Figure 4.14). The contact between these unique rock types which is interpreted to be fault contact brought the older (metamorphosed) rocks to overlie the younger (unmetamorphosed) rocks, thus characterizing a reverse fault. However the determination of the relative age of faulting is solely based ona fact that the overlying spotted slate experienced the metamorphism while there is no evidence of metamorphism in underlying argillaceous sediment. This puts the age of faulting to be post-metamorphism or younger than the age of the unmetamorphosed sediments.

Analogy to a low-angle fault at Khao Chalak in Amphoe Sri Racha (near Bang Phra water reservoir) where fault plane was noted between the underlying calc-silicate rock and overlying quartzite unit (Figure 4.15), the fault here was thought to be simultaneously developed with those seen in Sattahip area.

Other than the sharp contrast between the rock units, no brecciated rock fragments, either large- or small scale, has ever been found in the field. However there is another evidence of a low-angle fault at Khao Hat Yao (Figure 4.16). The fault plane illustrates the explicit polished surface of slickenside that result from friction along the fault plane. The slip direction of fault could be implied to be parallel to the gigantic slickenside striae, 60-70 cm across, that are about 20° counterclockwise to the dip direction of fault plane. This fault is possibly developed in the same event with other low angle faults mentioned above, those which are supposed to be originated contemporaneously by an ENE-WSW horizontal shortening. If all reverse faults are thought to be in the same system, the fault observed at Khao Hat Yao, with the slip direction trends nearly ENE-WSW and dips 32° with reverse sense of movement to WSW direction, may be a good representative of fault movement among these reverse faults.

Some sheared foliatons and dynamic crystal growth observed in the thinsections of rock specimens collected from several locations close to the fault planes (See Chapter V) might also indicate the dynamic metamorphism associating this large reverse faults.

Figure 4.15 Low angle fault (at arrow tips) at Khao Yai Si in Sri Racha area. Fault plane is between the underlying calc-silicate rocks and overlying quartzite. Grid reference 0710931 E 1460272 N.
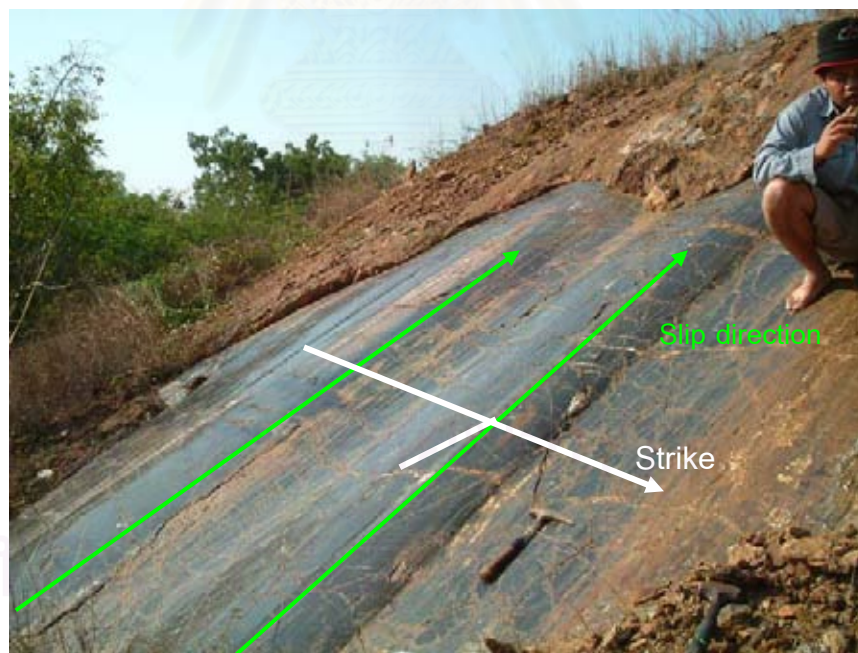
Figure 4.16 A glassy-slickenside on fault plane at Khao Hat Yao striking near N-S direction with moderate dipping to the east (356/35 E). The fault steps on slickenside striae found on this fault plane seems to be a clue of reversed movement with slip direction to WSW (green arrows). Grid reference 0702932 E 1406132 N.

No other large-scale fault had been further observed in the study area, while the insignificant small-scale faults with small normal displacement are grouped with the extensional joints in the previous topic.

4.2 Regional Geologic Structural Interpretation

The general trend of stratigraphic layers in Sattahip area is in NE-SW direction with dipping to the northwest and southeast. In term of structural analysis, the bedding planes are plotted in stereonet using a computer program StereoNett Version 2.46 written by Dr. Johannes Duyster of Ruhr-Universität Bochum, Germany. The lower-hemisphere equal-area stereonet plots of bedding planes are shown in ¶-diagrams as below. Contouring poles of bedding planes from the whole study area display the pattern of a small circle indicating the conical fold style rather than the cylindrical one which is the effect of refolded folding (Figure 4.17). Notable that bedding planes from Sattahip III is distributed incompatibly from the others, however the pattern of contouring still be preserved as a small circle. When contouring the poles by excluding poles of bedding planes from Sattahip III, the pattern is enhanced to be strongly small circle (Figure 4.18). The pole diagram shows the small circle pattern representing that the fold figure has elongation in NE-SW direction. This type of folds could be considered to be refolded folds as dome-basin, Type-1 refolded folds of Ramsay's (1967), which is a characteristic of conical kind.

4.3 Unconformity

In Sri Racha area, there is the evidence of alluvial fan sequence at Khao Din (Figure 4.19). The rock exposure is well exposed at the southern part of Khao Din (Figure 4.20) and illustrates that the strata of rocks strike nearly N-S direction and gently dip to the west. This rock sequence has shown effect from metamorphism, granitic intrusion, or even large-scale fracturing. The age of this deposition has not been defined yet, however it is certainly younger than the low-graded metamorphic rocks and possibly younger than the age of granite intrusion of the study area, which is not older than Late Triassic. This fan-unit is speculated to be the Tertiary deposits. Unfortunately, no outcrop of actual contact between this alluvial fan unit and the underlying basement
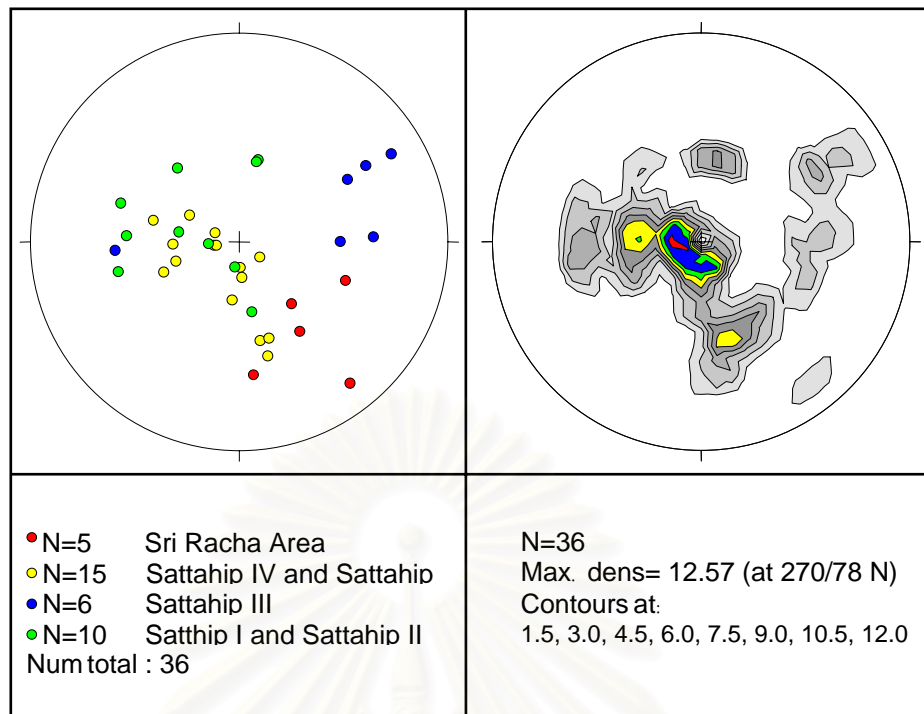
Figure 4.17 Stereonet plot of 36 poles of bedding planes from the whole study area
showing the small circle pattern with major elongated fold in northeast-
southwest direction.
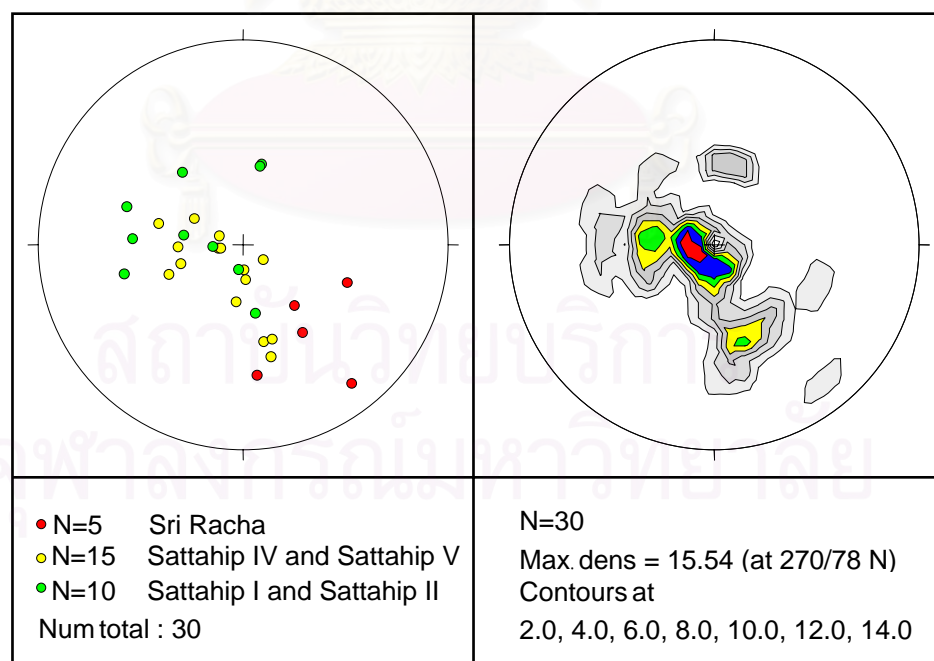
Figure 4.18 Stereonet plot of 30 poles of bedding planes from the whole study area
excluding Sattahip III area, showing the obvious small circle pattern with

Figure 4.19 Alluvial fan deposit at Khao Din (Sri Racha area) with westerly dipping. Grid reference 0711687 E 1450842 N.

Figure 4.20 Alluvial fan sequence at the southern part of Khao Din (Sri Racha area) with bedding planes 196/15 W (Strike/Dip). Grid reference 0711932 E 1450139 N.

rocks was found yet.

A nonconformity is obviously distinguished by the contact of granites that exposed along the western boundary of the study area where much younger Quaternary sediments were noticed. Along this nonconformity, dykes that penetrated the adjacent rocks near the aureole of contact zone were observed.

4.4 Geochronology Interpretation

According to the structural details, there are at least three recognizable deformation phases which include two ductile deformation phases and a major brittle deformation. From the elongate conical or doubly-plunging folds, the plastic deformations could be noted. The oldest defomation (D_1) is characterized by somewhat elongate, upright to overturned folds with axial planes and fold axes trending NE-SW to nearly N-S direction. These folds become gently to moderately doubly plunging by the later D_2 ductile deformation and cause the regional structures to develop a dome-basin pattern. The oldest deformation is thought to be originated together with the regional metamorphism (M_1) and later D_2 is characterized by NW-SE cross folds which occurred together with, or immediately followed by granite intrusion that caused a contact metamorphism (M_2). D_3 brittle deformation is the youngest phase which is represented by low-angle faults and is defined as reverse faulting based on the evidence of stratigraphic correlation and the difference in degree of metamorphism. The additional evidence from petrography that sheared cordierite porphyroblasts were found near a fault plane could indicate that the faulting occurred after granite intrusion.

4.5 The mechanism of geologic structures

A fold interference pattern of the study area is determined to be dome-basin pattern or Type I interference pattern of Ramsay's (1967). This pattern could be developed by two sets of folds that the previous folds are deflected to develop new folds with the general trend cross-cutting the first folds at a high angle. Although the planar form of the previous axial surfaces may not be severely disturbed, the second generation movement will lead to undulations of the hinges of the first folds, and the

production of culminations and depressions of these first folds. In the study area the first folds trend in northeast-southwest direction while the second folds trend in northwest-southeast direction, which is illustrated by the three-dimensional geometry (Figure 4.21) that the first fold geometry is shown in diagram A and the displacement pattern of the superimposed second system is indicated in the B diagrams.

The representative geologic structures is illustrated by the model in Figure 4.22 that shows the major folds trend in northeast-southwest direction as a result of simple buckle folding that derived from maximum compressive stress trending NW-SE direction. The superposing of minor northwest-southeast folds is possibly developed as the consequence of resultant folds by the first deformation that could disturb the pre-existing fold pattern and develop a dome-basin pattern. In contrast to the younger event of faulting, the maximum compressive stress is changed to ENE-WSW direction determining by the evidence of fault slip at Khao Hat Yao.
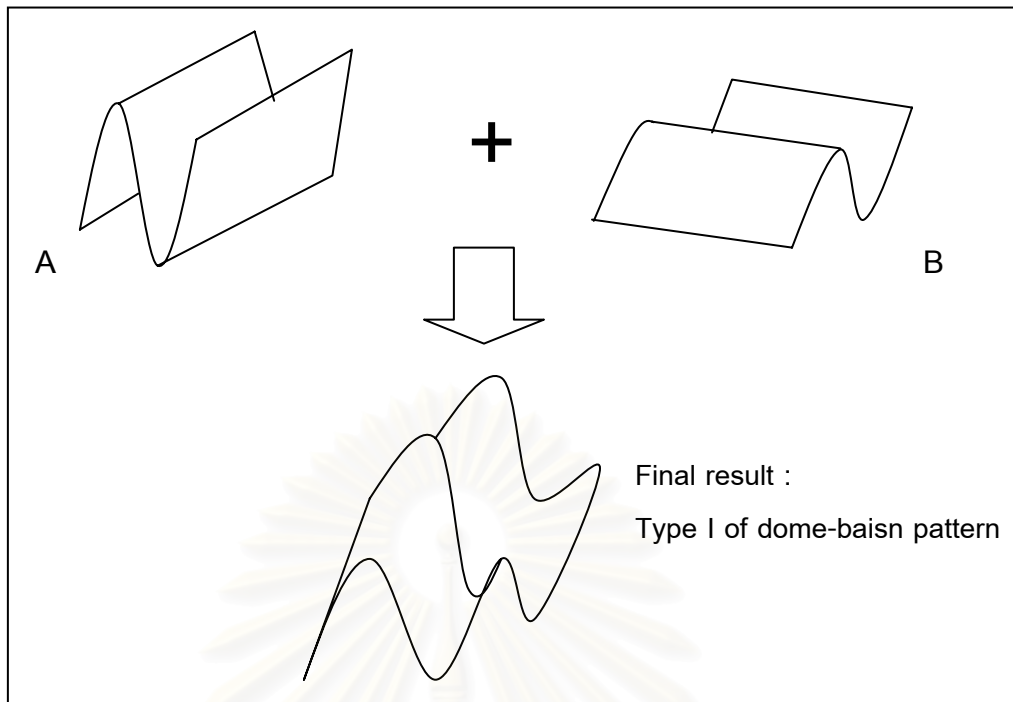
Figure 4.21 Illustration of three-dimensional fold Type I of dome-basin pattern (C) arising

by the superposition of shear folds (B) on pre-existing fold form (A).
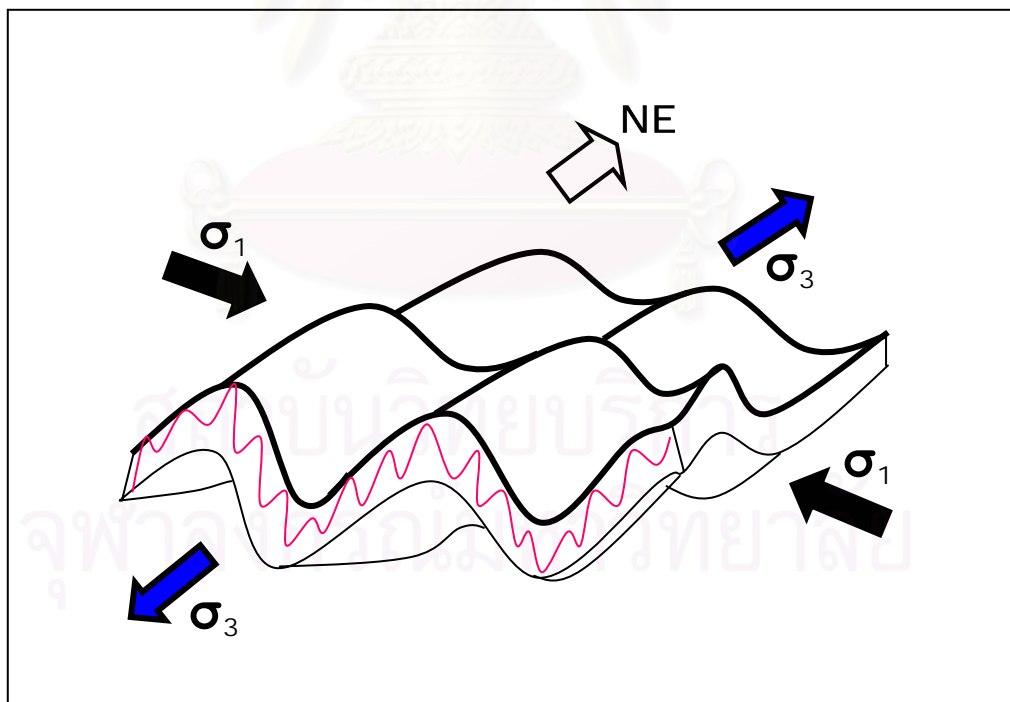
Figure 4.22 Three-dimensional structural model of the rock unit of study area illustrating

major trend of previous folding to the northeast and shear fold occurring in

hinge zone that develop as dome and basin pattern in response.

CHAPTER V

MICROSTRUCTURE AND METAMORPHISM

This chapter explains the examination of mineral assemblages in the rock units in order to elucidate the metamorphism having been occurred in the study area. The deformation mechanisms are observed by the representative microstructures found under petrographic microscope.

5.1 Metamorphic Petrology

The sedimentary units in the study area are made mainly of pelitic rocks interbedded with fine to medium sandstone and lens of carbonate rocks in Sattahip area and mostly of quartz tectonites (quartzites) in Sri Racha area. These rocks show evidences of metamorphic experience and deformation. In order to elucidate the P-T condition and metamorphism, the mineral assemblages together with important index minerals and other metamorphic minerals in these rocks were studied as below.

5.1.1 Andalusite

The index mineral found in pelites is andalusite. Although andalusite slate is found only at Khao Leam Kham, the euhedral andalusite crystals are noticed both in hand specimens and thinsections. Petrographically andalusite porphyroblasts are of obviously chiastolite variety containing graphite inclusions which are symmetrically arranged to form a weak cross (Figure 5.1). Notably most porphyroblasts illustrate the alteration rims (Figure 5.2). The relationship between quartz veinlets whose orientation is compatible with the foliation of the matrix been cross-cut by the andalusite porphyloblasts unmistakenly indicates s a chronologic interpretation of the later-formed andalusite (Figure 5.3).

The three common polymorphs of Al_2SiO_5 are andalusite, silimanite and kyanite. The stability relations of the three polymorphs have been determined experimentally (Holdaway, 1971) to illustrate the lowest pressure condition of andalusite stable field as compared with silimanite and kyanite, however experiencing higher temperature than
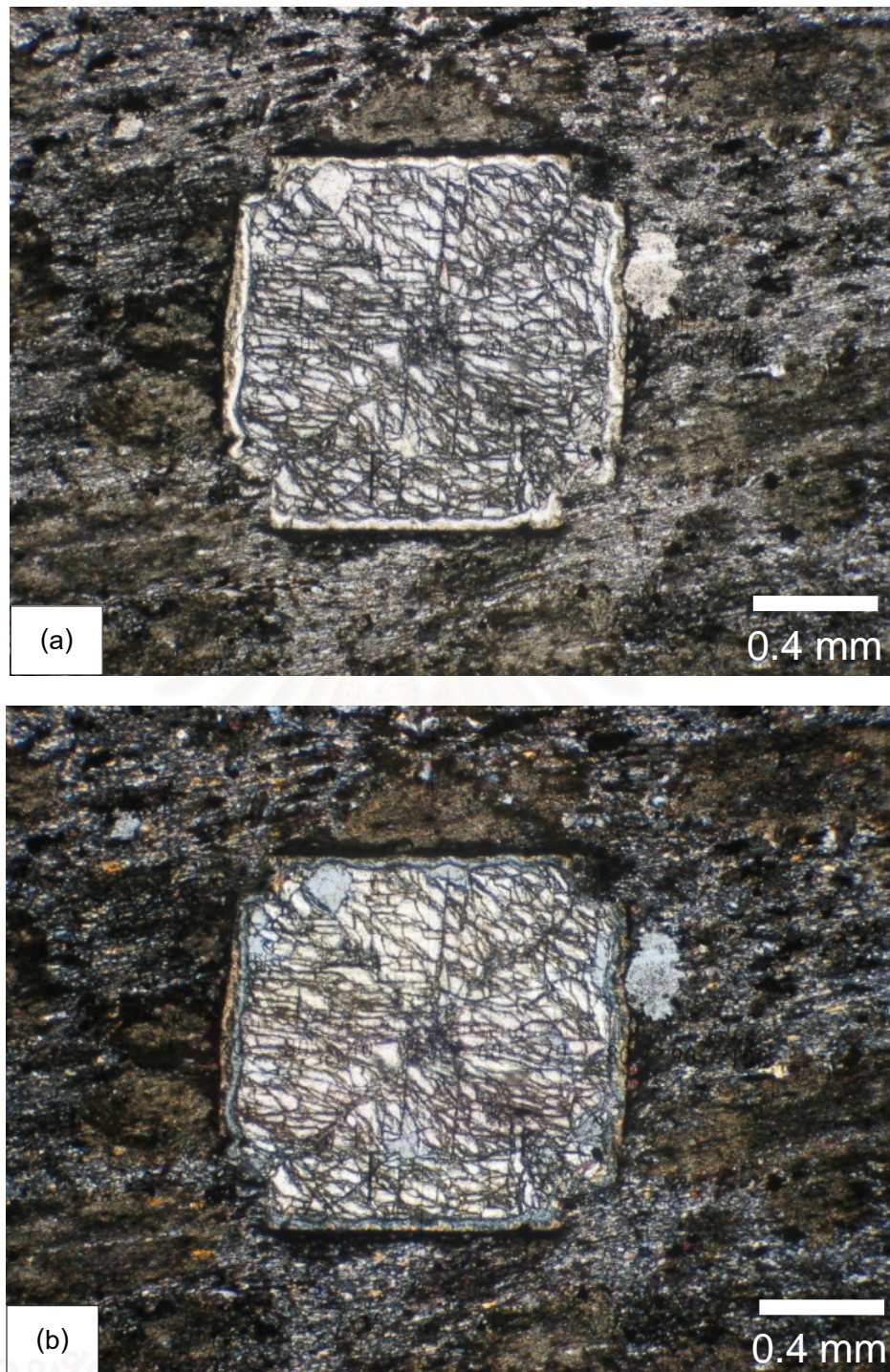
Figure 5.1 Photomicrograph of chiastolite variety of andalusite found at Khao Laem

Kham, (a) uncrossed nicols and (b) crossed nicols.
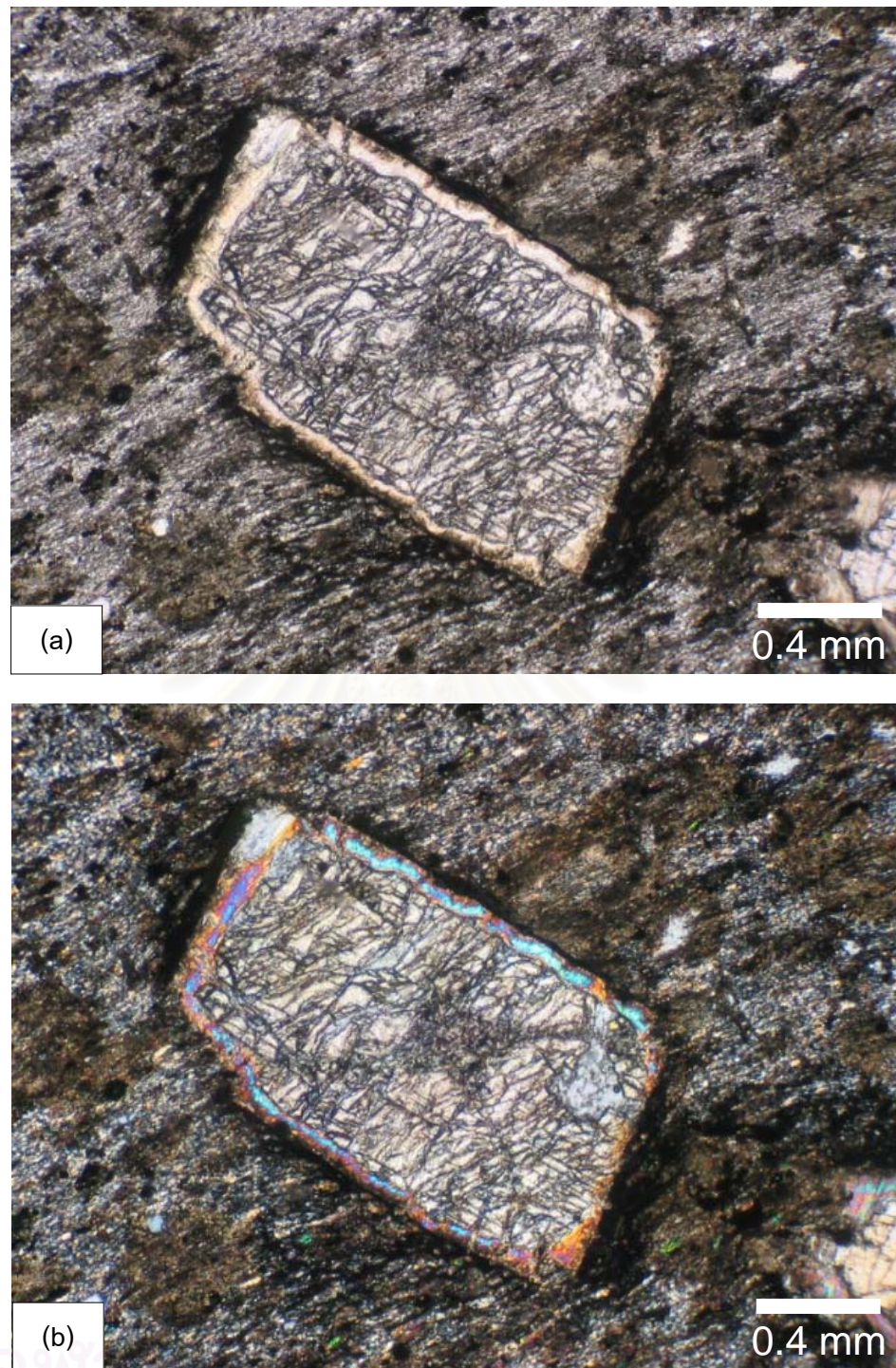
Figure 5.2 Photomicrograph of alteration rim of andalusite porphyroblast which also illustrates chiastolite characteristics, (a) uncrossed nicols and (b) crossed nicols.
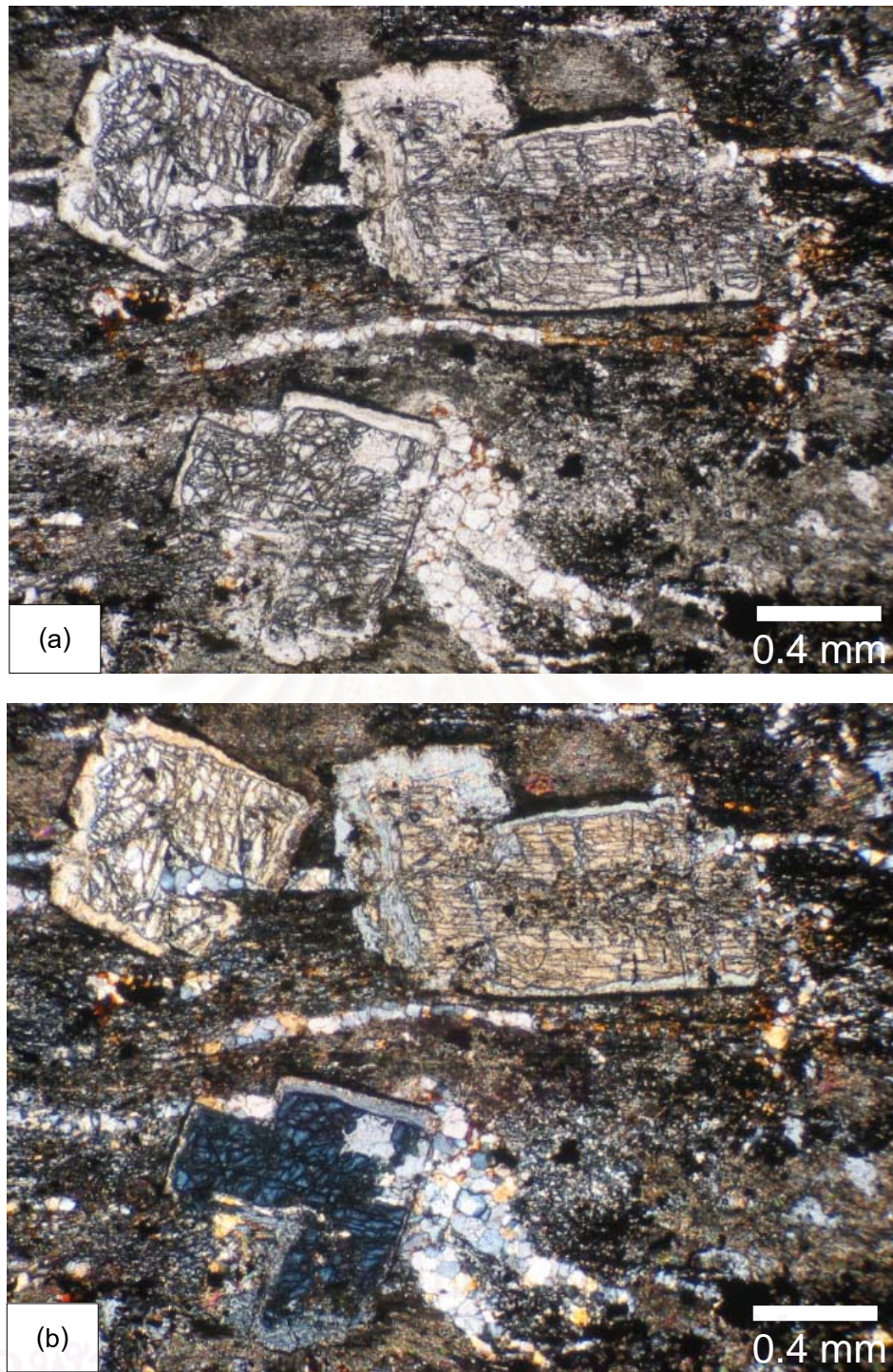
Figure 5.3 Photomicrograph illustrating cross-cut relationships by which quartz veinlets are cross-cut or superimposed by andalusite crystals, (a) uncrossed nicols and (b) crossed nicols.

kyanite (Figure 5.4). Also andalusite is frequently found in an aureole of a contact metamorphism and generally coexists with cordierite. Moreover andalusite can be found in an association with kyanite or sillimanite, or both, in a regionally metamorphosed terrane (Klein and Hurlbut, 1993). At Khao Laem Kham andalusites are found as chiastolite varieties containing black carbonaceous impurities forming a black cross in the section normal to the longer axis of crystals. The porphyroblasts of chastolite here commonly show rim of shimmer aggregates which are probably muscovite. Pseudomorphs of fine-grained muscovite (sericite) after andalusite are common if subjected to hydrothermal and diaphthoritic alteration (Pichler and others, 1997).

The phase relationship of the three Al_2SiO_5 polymorphs is a useful indicator of pressure in the temperature range 400-700°C. A division of progressive regional metamorphisms proposed by Miyashiro (1994) can be grouped into three metamorphic facies series based on P/T ratio, with the reference to the stability relations of the Al_2SiO_5 polymorphs, glaucophanic amphibole and jadeite + quartz. These are low-P/T type (or andalusite-sillimanite series), medium-P/T type (or kyanite-sillimanite series) and high-P/T type (or glaucophanic metamorphism). The appearance of andalusite in the study area thus can be categorized in andalusite zone of the low-P/T regional metamorphism (low-P/T type or andalusite-sillimanite series), as similar to the Ryoke metamorphic belt in Japan and the Buchan region of the Scottish Highland, both of which belong to this series. This low-P/T type is produced in the crust where intense heating occurs at a relatively shallow depth. Metamorphic regions of the low-P/T type are usually closely accompanied by abundant granitoid intrusions. In an arc area, some are syn- or late-metamorphic intrusions within the pertinent metamorphic belts, whereas others are post-metamorphic intrusions into the inside as well as the outside of the belts (Miyashiro, 1994). In the regions showing progressive metamorphism of pelitic rocks, the amphibolite facies usually includes the andalusite and the sillimanite-muscovite zone in the low-P/T type. Metapelites commonly contain andalusite and cordierite in the low-pressure part.

However the metamorphic facies observed in the contact aureoles may include the greenschist facies, amphiolite facies with andalusite, kayanite and sillimanite,

Figure 5.4 Pressure-temperature diagram illustrating the stability fields of andalusite, kyanite and sillimanite (Modified after Holdaway, 1971).
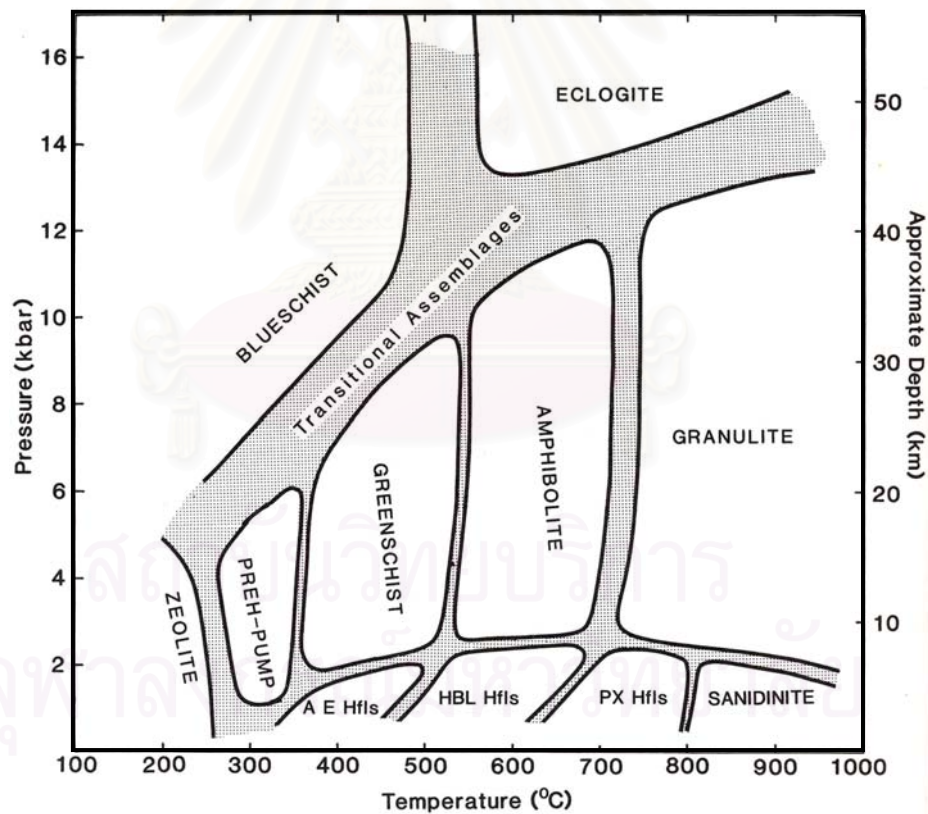
Figure 5.5 Pressure-temperature diagram showing the fields of the various metamorphic facies (After Yardley, 1990). Abbreviations used are: Hfls = hornfels, AE = albite-epidote, HBL = hornblende, PX = pyroxene, PREH-PUMP = Prehnite-pumpellyite.

pyroxene-hornfels facies, and granulite facies, among which the amphibolite facies with andalusite is probably the most widespread (Miyashiro 1973). Andalusite observed at Khao Laem Kham is also assumed to be the stable Al_2SiO_5 mineral which is usually occurred in both hornblende-hornfels and pyroxene-hornfels facies depicted by metamorphic facies (Figure 5.5). In many contact aureoles, andalusite is stable up to the highest grade in contradict to andalusite in low-P/T regional metamorphism which occurs only in the lower temperature zones.

Andalusite in the study area was thought to generally associate the contact aureole around the granitic intrusive body, near where the occurrence of andalusite is noted.

5.1.2 Cordierite

Cordierite porphyroblast in the sequences of metamorphic zones in north-east Scotland have been described by Harte and Hudson (1979) as a good example of distinctly low pressure metamorphism, fairly typical in many thermal aureoles. Although the metamorphism here is established as regional, magmatic heat input is also the important factor. The cordierite zone is derived from continuous reaction of

$$\text{chlorite} + \text{muscovite} \longrightarrow \text{cordierite} + \text{biotite} + \text{quartz} + H_2O$$

while andalusite becomes a possible phase in most pelite compositions at low pressure as a result of the discontinuous reaction as following,

$$\text{chlorite} + \text{muscovite} + \text{quartz} \longrightarrow \text{cordierite} + \text{andalusite} + \text{biotite} + H_2O$$

In this andalusite zone, it is possible for the coexistence of cordierite and andalusite in common pelite compositions that plot below chlorite on the AFM diagram. However it could be presented in high graded regional-metamorphosed metapelites too.

Pseudohexagonal cordierite crystals (Figure 5.6) are found as porphyroblasts in spotted slate at a hill located to the east of Khao Sattahip. These cordierite porphyroblasts were also found in spotted slate at Khao Mon. Here the mineral appears

to be shear porphyroblasts (Figure 5.7) when approaching the fault zone of this pelitic slate. Cordierite could be considered as an index mineral for the anatectic origin of the host rock, or being contaminated by Al-rich contact rocks. It is regularly formed in contact (thermal) metamorphic rocks. Cordierite porphyroblasts in the outer contact aureole in the study area are knotted and commonly occur in cordierite-hornfels host rock.

5.1.3 Chlorite

Chlorite is a common mineral in metamorphic rocks and it is a diagnostic mineral of greenschist facies. Greenschist-facies rocks occur in the lowest-temperature zones in many regional metamorphic complexes and this facies is represented by chlorite and biotite zones in ordinary metapelitic regions (Miyashiro, 1994). However chlorite also occurs in rocks of lower contact metamorphism categorized in albite-epidote-hornfels facies which is typical of the outermost parts of contact aureoles (Bates and Jackson, 1980). In Sattahip area, chlorite is observed in metapsammite at Ban Sattahip (Figure 5.8). Petrographically chlorite is characterized as flaky pale green crystals with a weak pleochroism. A noted mineral in the assemblages is twinned albite (Figure 5.9).

The occurrence of chlorite in the study area indicates the greenschist facies of the low-grade metamorphic rock which is though to be occurred in the outermost rim of contact aureoles next to the andalusite zone at Khao Laem Kham.

5.1.4 Epidote

Epidote observed in caclsilicate rocks at Khao Chi On is characterized by its fine granulars, peculiar green turquoise and bright blue color with intensive anomalous interference color (Figure 5.10). Epidote is typically a mineral of the greenschist facies found in low-grade regional metamorphic rocks and widely distributed in contact-metamorphic rocks. Marly to calcareous clay-rich original rocks are chemically suitable for epidote growth (Pichler and others, 1997). The metamorphic facies (After Yardley, 1988) is compatible with albite-epidote hornfels facies (Figure 5.5).

78
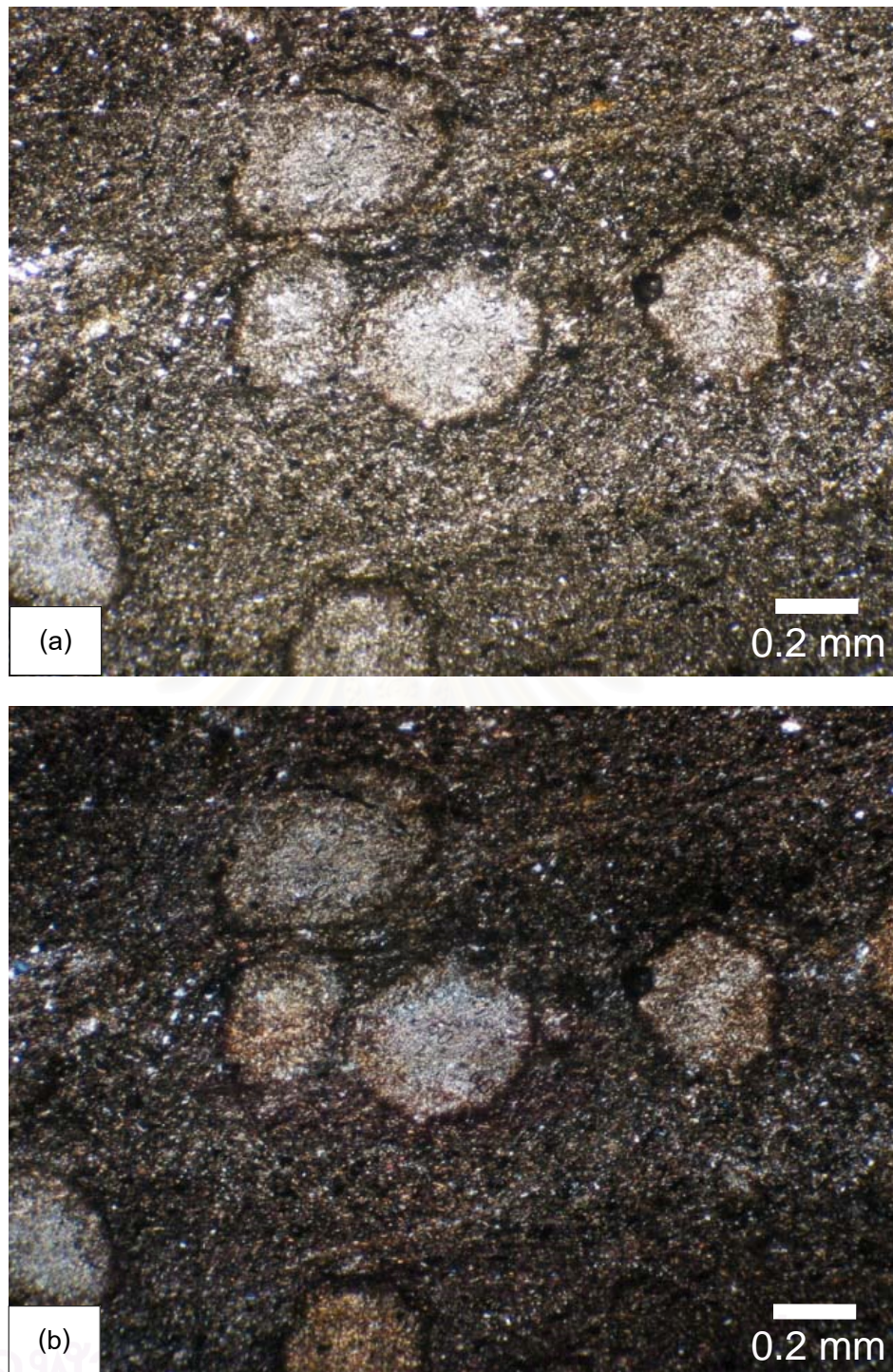
Figure 5.6 Pseudohexagonal cordierite spots in spotted slate near Khao Sattahip at Grid

reference 0709246 E 1404142 N, (a) uncrossed nicols and (b) crossed nicols.
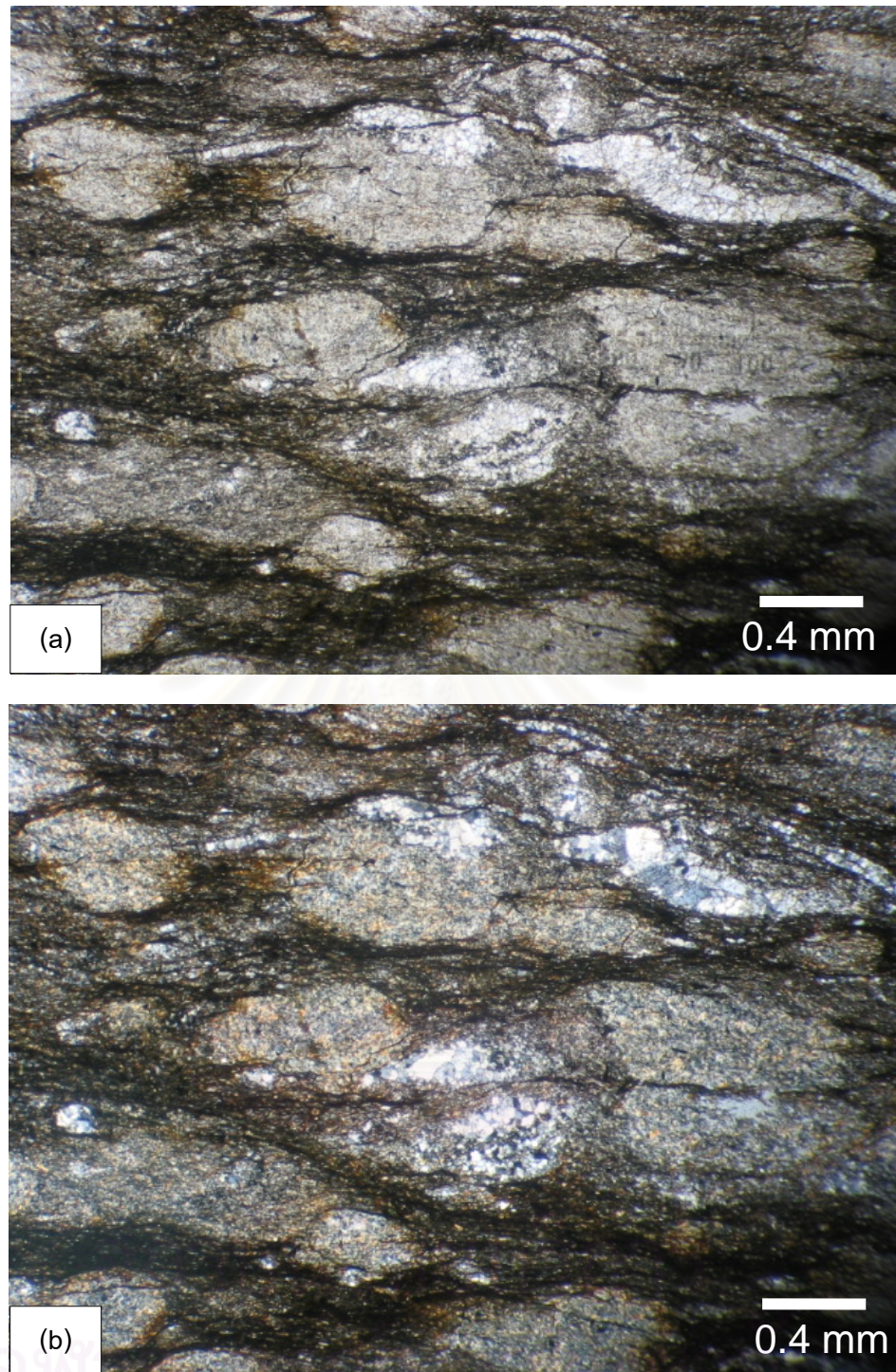
Figure 5.7 Sheared cordierite porphyroblasts in spotted slate at Khao Mon near fault plane at Grid reference 0709186 E 1401189 N, (a) uncrossed nicols and (b) crossed nicols.

0.2 mm

(a)

0.2 mm

(b)
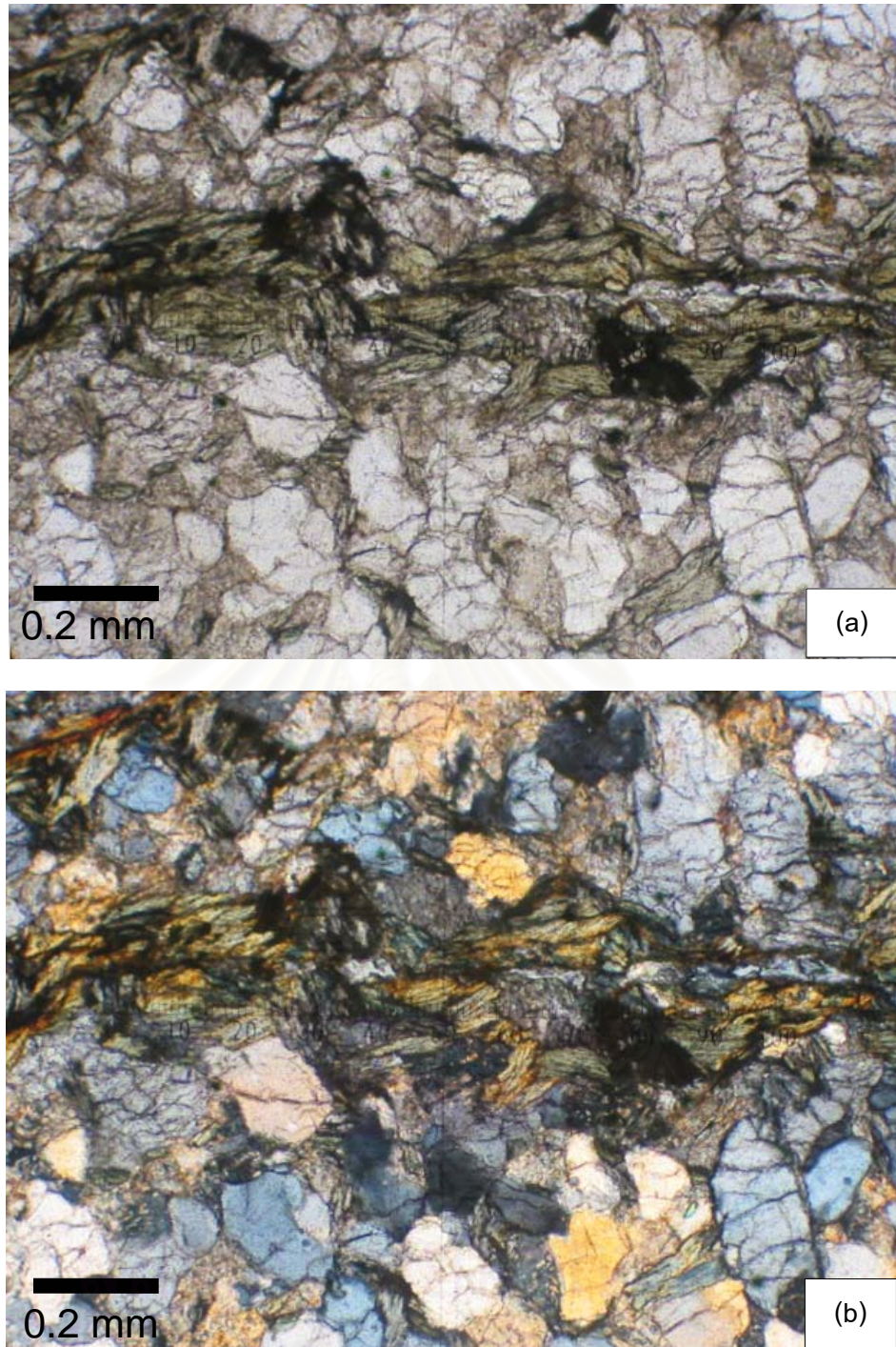
Figure 5.8 Photomicrograph of chlorite-rich layer in metaquartzo-feldsparthic rock, (a) uncrossed nicols and (b) crossed nicols. Grid reference 0705712 E 1399944 N.
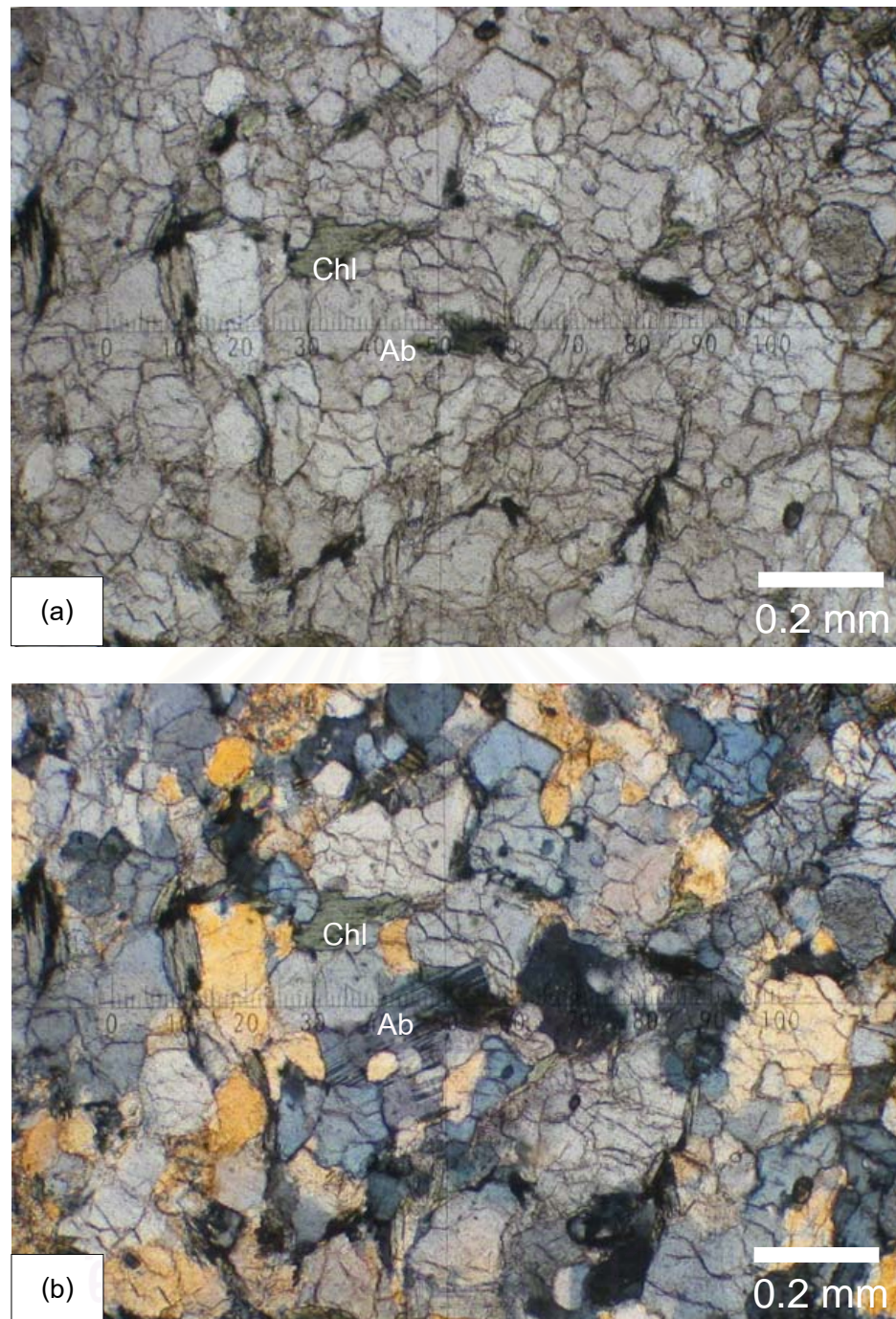
Figure 5.9 Photomicrograph showing mineral assemblage of albite (Ab) together with
chlorite (Chl) in metaquartzo-feldsparthic rock, (a) uncrossed nicols and (b)
crossed nicols. Grid reference 0705712 E 1399944 N.
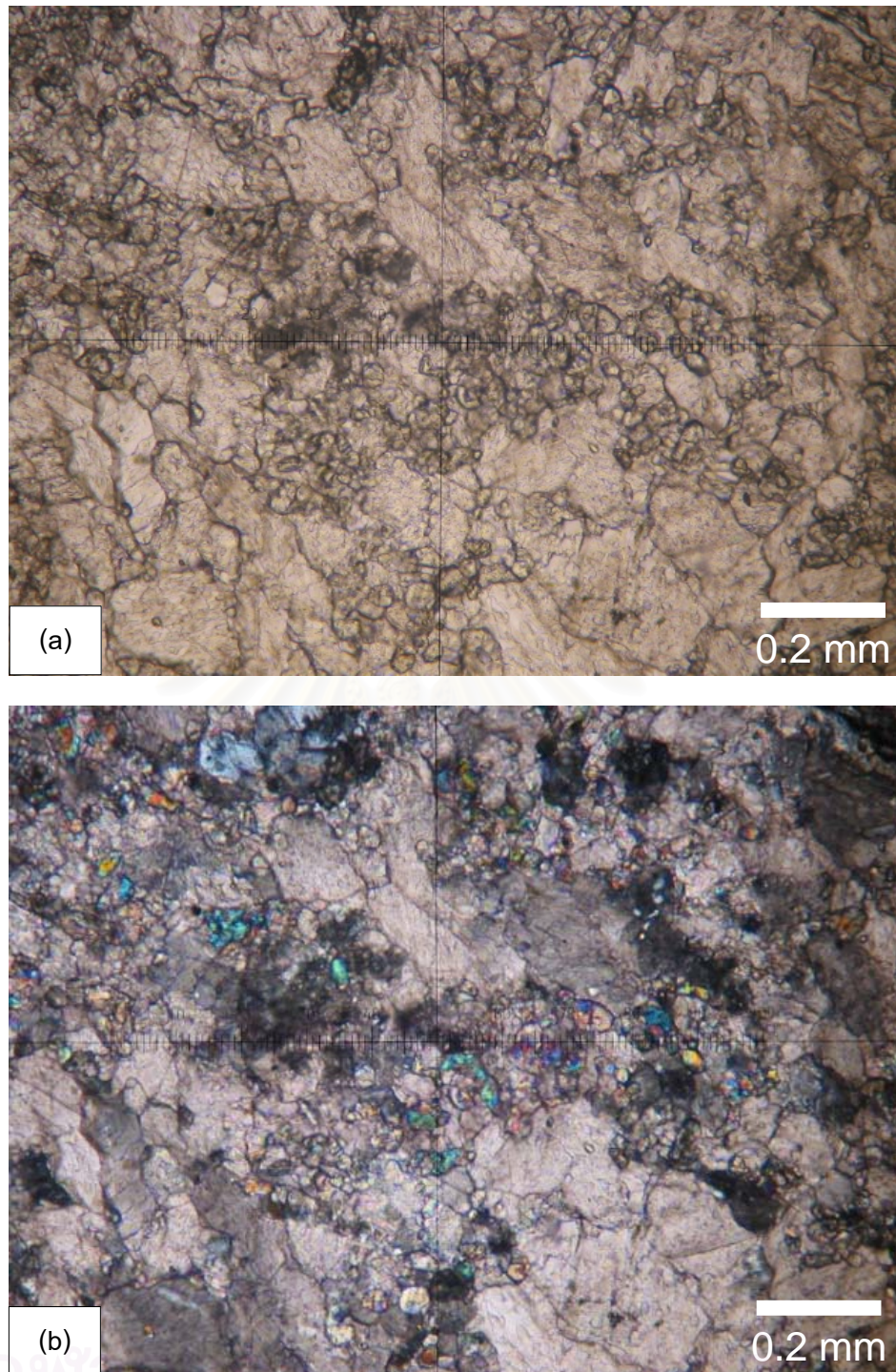
Figure 5.10 Photomicrograph of green- and blue intensive interference colors of epidote

crystals at Khao Chi On, (a) uncrossed nicols and (b) crossed nicols. Grid

reference 0713946 E 1411668 N.

5.1.5 Micaceous minerals

In Sri Racha area, the minerals used to roughly characterize a range of metamorphic grade are micas. Muscovite and/or sericite are commonly found in these deformed quart-rich metasandstones, ranging from massive quartzite to micaceous quartzite. Petrographically there are two characteristics of micas found in these quartz tectonites. The first one is tiny flakes or elongate grains of white mica which show preferred orientation as lineation (Figure 5.11) and/or conformable to bedding foliation plane (Figure 5.12). These mica crystals are believed to be originated during the regional metamorphism. Contrarily another characteristic of mica is that the crystals are formed as decussate grain, especially in rocks with higher clay impurity, without preferred orientation (Figures 5.13 and 5.14). This perhaps is due to the influence of contact metamorphism.

5.2 Deformation Mechanisms

Microstructural study of the rock specimens is to furnish and elucidate the deformation processes in deformed rocks. Quartz tectonites of Sri Racha area received a special emphasis on the grain-scale microstructures to observe and find out what deformation mechanisms of deformed rocks they had experienced.

Quart tectonite specimens from four localities in Sri Racha area were collected and prepared for both regular thinsections and orientated thinsections for microstructural study. The deformation mechanisms are judged from the different grain-scale microstructures being exhibited.

5.2.1 Recovery

Passchier and Trouw (1996) speculated that when the crystal is free from dislocation, the internal strain energy is at its minimum. If a crystal is deformed and induced dislocations, its internal energy is increased by local changes in the distance between atoms. The increase in internal energy is proportional to the increase in total length of dislocations per volume of crystalline material, also known as the dislocation density. Dislocations and dislocation tangles are formed in response to imposed
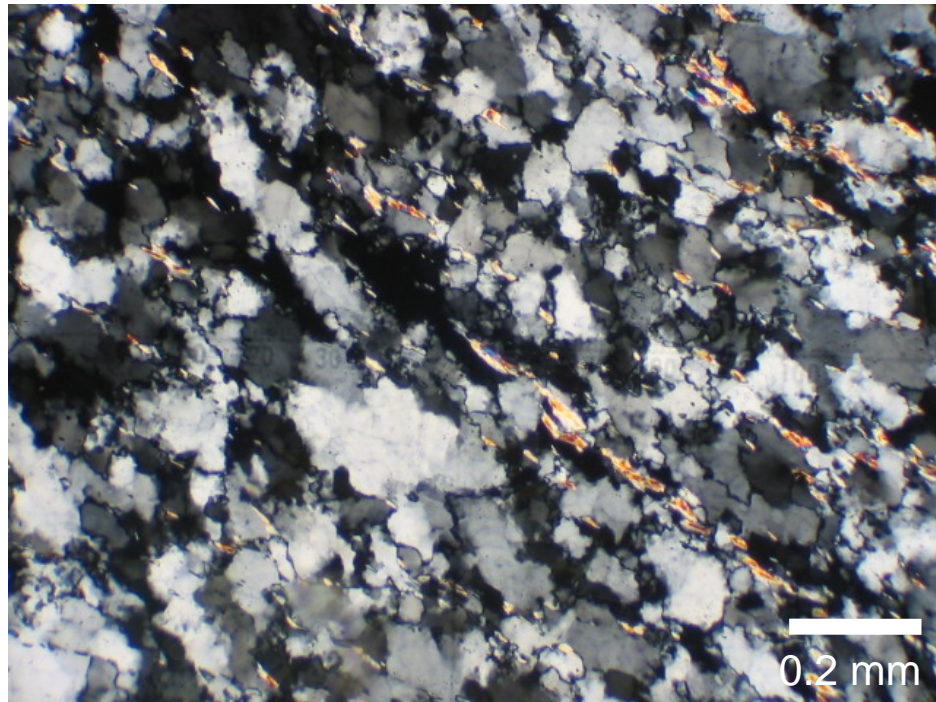
Figure 5.11 Photomicrograph of micaceous quartzite at Khao Khwang showing lineation indicated by tiny sericite flakes, grid reference 0706164 E 1452192 N
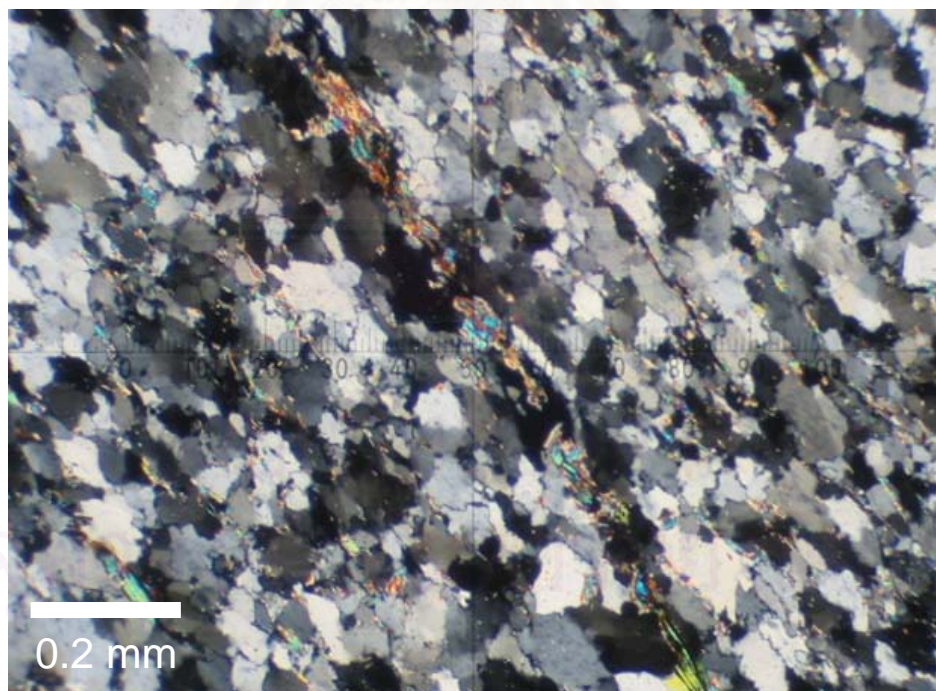
Figure 5.12 Photomicrograph of micaceous quartzite at Khao Ban Uttaphong showing the foliation by lineation of fine-grain mica. Grid reference 0706164 E 1452192 N.
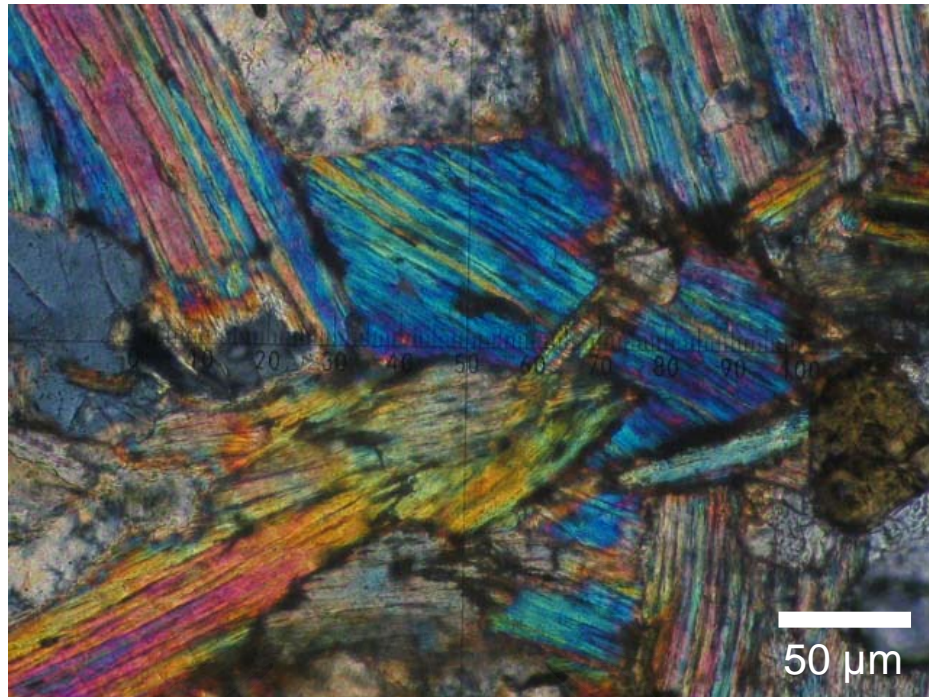
Figure 5.13 Photomicrograph of polygonal grain shape of muscovite in micaceous
quartzite at Ban Noen Uma. The mineral was perhaps formed by the
process of static recrystallization. Grid reference 0709300 E 1454159 N.
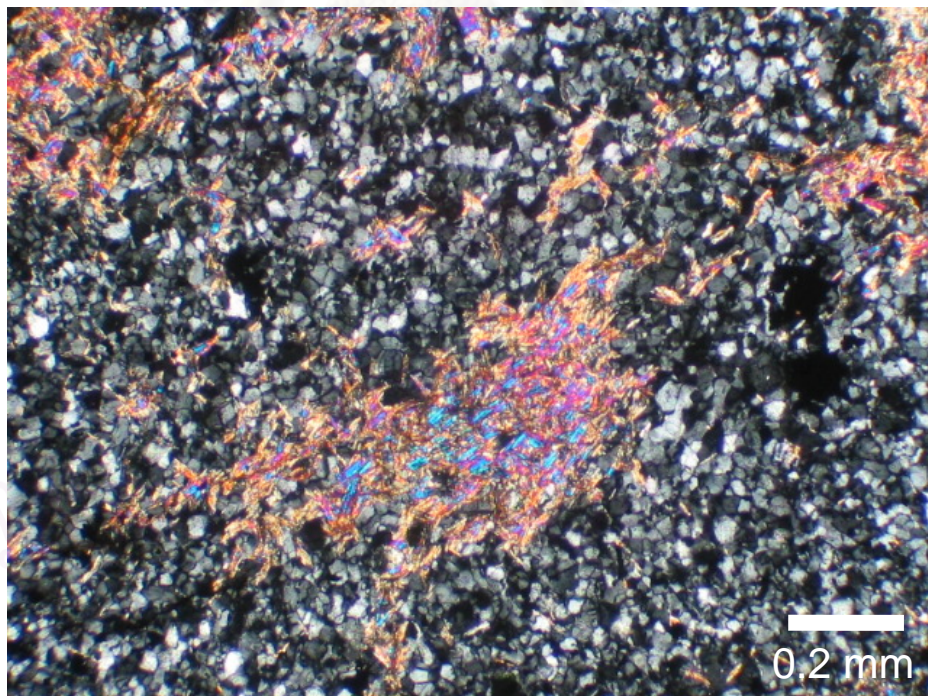
Figure 5.14 Photomicrograph of polygonal grain shape of muscovite in micaceous
quartzite near Ban Khao Uttaphong. The mineral was perhaps formed by the
process of static recrystallization. Grid reference 0708288 E 1452622 N.

differential stress. Other processes tend to shorten, order or destroy the dislocations in order to decrease the total dislocation length and hence the internal strain energy of crystals and therefore operate following the thermodynamic principle to minimize total free energy in a system. During deformation, disordering and ordering mechanisms will compete while after deformation stops, ordering mechanisms progress towards an equilibrium situation with the shortest possible length of dislocations in the crystal lattice. The process of these ordering mechanisms is known in the general term of recovery.

In response to recovery, dislocations tend to concentrate in planar zones in the crystal, decreasing dislocation density in other parts. This results in the occurrence of zones in the crystal which have approximately uniform extinction, and which grade over a small distance into other similar crystal sectors with a slightly different orientation. These transition zones are known as deformation bands. Figure 5.15 illustrates such deformation bands found in quartz tectonite at khao Leam Chabang, which can be regarded as a transitional stage between undulous extinction and subgrain boundaries as noted by Passchier and Trouw (1996).

5.2.2 Recrystallization

The process that removes the internal strain energy of grains that remains after recovery is called recrystallization. During recrystallization, high-angle grain boundaries are formed that separate relatively strain-free grains from each other. The characteristic of recrystallized microstructure is grains without undulous extinction and with relatively straight grain boundaries that meet at angles of approximately 120° (Van der Pluijm and Marshak, 1997). This process can be divided into dynamic recrystallization and static recrystallization as the following.

Dynamic Recrystallization

This is an important mechanism in recrystallization of rocks during deformation which is composed of two major processes (Passchier and Trouw, 1996), known as grain boundary migration recrystallization (GBM) and subgrain rotation recrystallization (SR). Dynamic recrystallization can be used as a qualitative indicator of the temperature

conditions during deformation based on experimental work which is corresponded to field observation , for example, >300°C for calcite, >350°C for quartz, and >450°C for feldspar (Van der Pluijm and Marshak, 1997).

Jessell (1987) stated four microstructures indicating movement direction of a migrating grain boundary during dynamic recrystallization as pinning, window, dragging microstructures and left-over grains. These microstuctures could be found in the present study area as shown in Figure 5.16. Furthermore, if a grain is almost completely replaced by a neighbor,left-over grains, all with identical orientation may indicate the presence of an originally larger grain (Urai, 1983; Jessell, 1986). The grain boundary can also bulge into the crystal with high dislocation density and form new independent crystal, this process is known as bulging. Such process could be observed in this study as in Figures 5.17 and 5.18. It is also possible, though probably less common in rocks (Drury and Urai, 1990) that a small dislocation-free core nucleates inside a strong deformed grain with high density of dislocation tangles, and grows at the cost of the old crystal. This is as seen in this study in Figure 5.19.

Static Recrystallization

If temperature was relatively high when deformation stopped or if much water was present along grain boundaries, recovery, recrystallization and grain boundary area reduction may continue in absence of deformation until a minimum internal energy configuration is obtained. This combined process is known as static recrystallization (Passchier and Trouw, 1996).

The principal mechanism of static recrystallization occurring after the differential stress is removed or after deformation has stopped is grain boundary area reduction (GBAR) which is characteristic by the presence of crystals with straight or smoothly curved grain boundaries known as a polygonal fabric developed in response to grain boundary area reduction. Figure 5.20 illustrates such process as observed in this study. A decrease in the total surface area of grain boundaries in a rock can reduce this internal free energy by this process and its effect is more obvious and may become dominant after deformation ceased when compare to GBM or SR recrystallization, especially at high temperature (Bons and Urai 1992).
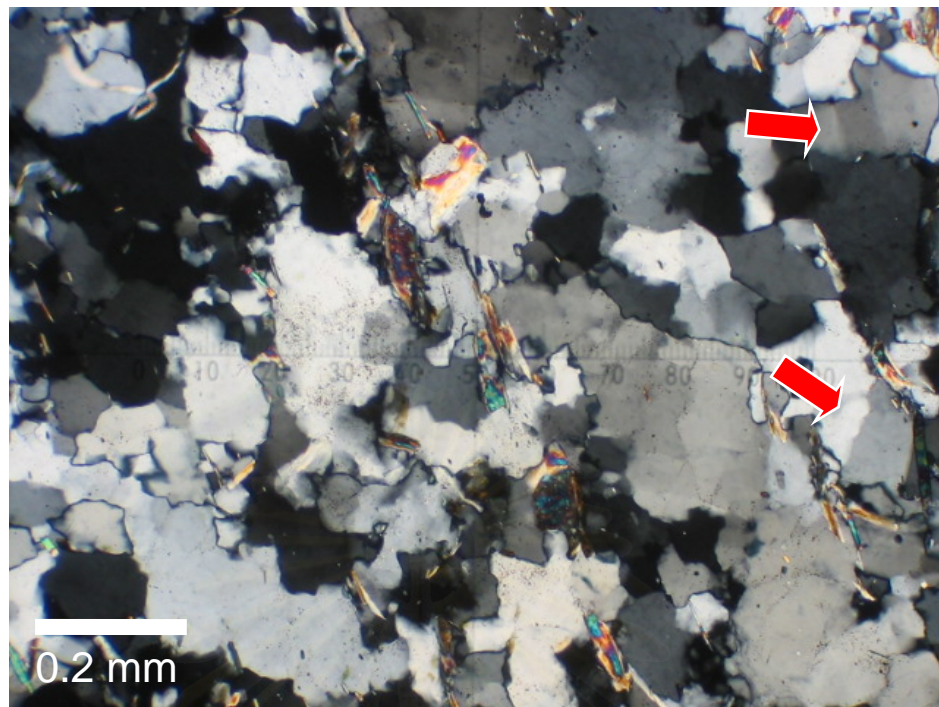
Figure 5.15 Photomicrograph of deformation bands in quartz grains in micaceous

quartztie at Khao Leam Chabang. Grid reference 0703565 E 1446204 N.
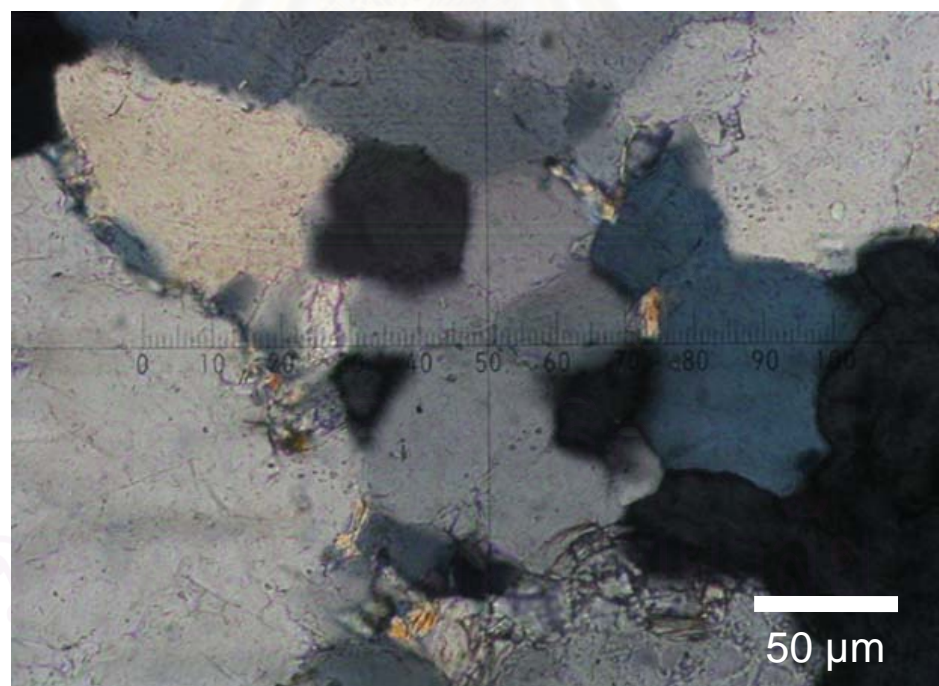
Figure 5.16 Photomicrograph of left-over grains which is almost replaced by growing of

the light grain with lower dislocation density into the higher one. Thinsection

of quartzite at Khao Bo Ya. Grid reference 0704193 E 1448324 N.
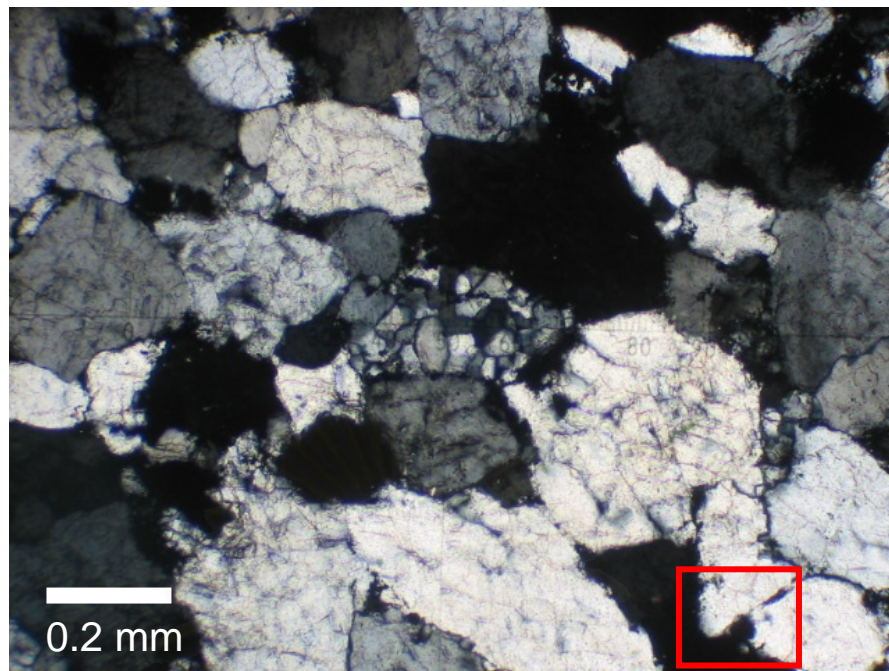
Figure 5.17 Photomicrograph of grain boundary migration of deformed medium-grain
grayish black sandstone at Rong Rian Navikkayothin Burana (Sattahip II)
showing the grain is consumed by bulging of neighboring grain. Grid
reference 0704919 E 1403850 N.
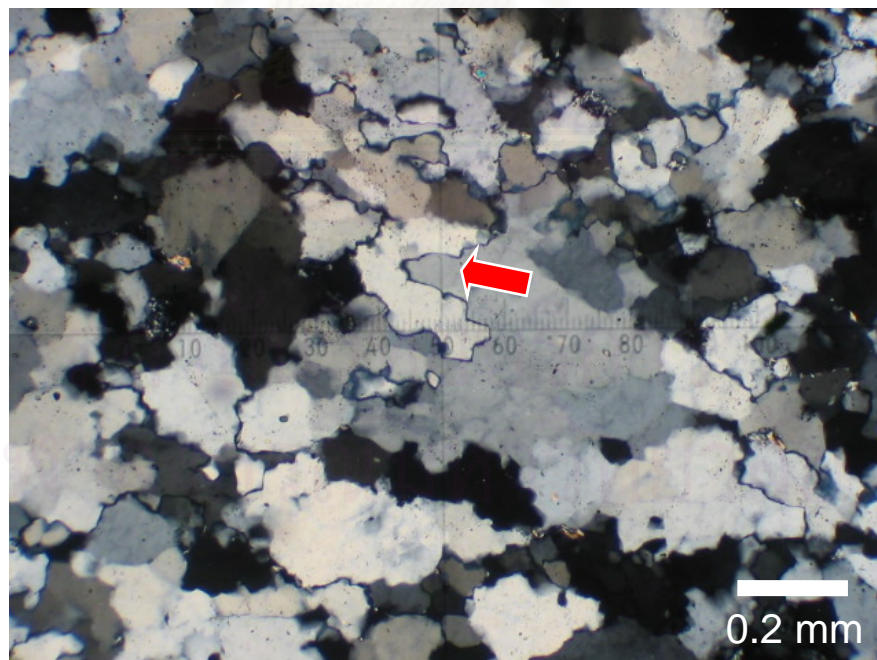
Figure 5.18 Photomicrograph illustrating that the grain with higher dislocation density is
consumed by bulging of the less deformation at Khao Bo Ya. Grid reference
0704193 E 1448324 N.
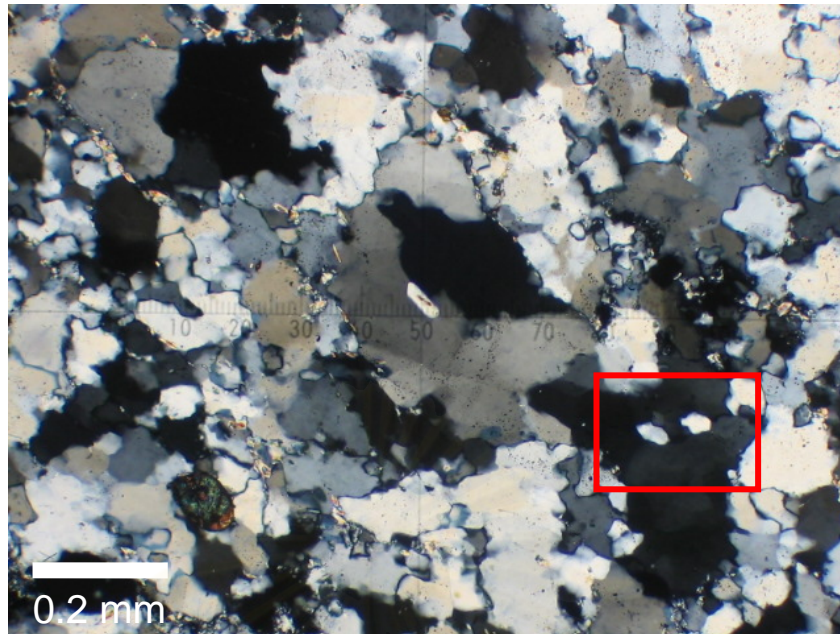
Figure 5.19 Photomicrograph of a small dislocation-free core nucleation in a strongly
deformed grain. Thinsection of quartzite at Khao Bo Ya. Grid reference
0704193 E 1448324 N.
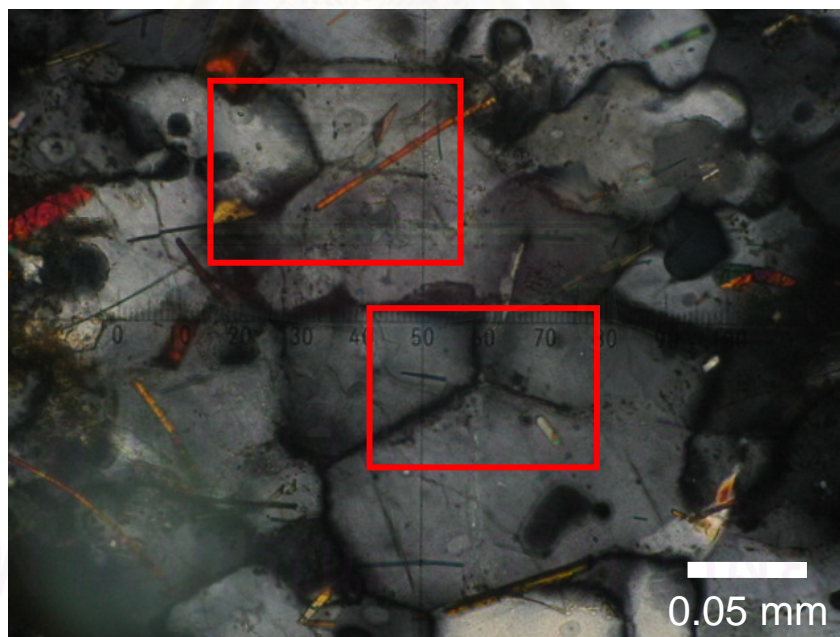
Figure 5.20 Photomicrograph of developing polygonal and some curved grains
originated by the process of grain boundary area reduction (GBAR) through
grain boundary adjustment and grain growth, resulting in a decrease in
grain boundary energy. Thinsection of micaceous quartzite at Ban Noen
Uma. Grid reference 0709300 E 1454159 N.

CHAPTER VI

CRYSTALLOGRAPHIC PREFERRED ORIENTATION STUDY

Four orientated thinsections of quartz tectonite were determined for the crystallographic preferred orientation. The optic axes of quartz grains were studied by using a petrographic microscope equipped with universal stage assemblage. The optic axis orientation is meant to veritfy the relationship between quartz fabrics and the regional geologic structures in Sri Racha area.

6.1 Introduction of Crystallographic Preferred Orientation (CPO)

It is noted that the crystallographic preferred orientation of (CPO)many minerals in deformed rocks is not randomly distributed but arranged systematically. In the case of minerals with equant grain shape, dislocation creep seems to be the most important mechanism (Passchier and Trouw, 1996). They further noted that dislocation creep changes the shape of a crystal and the interaction with neighboring crystals may result in its rotation with respect to the instantaneous stretching of bulk flow. If deformation starts in a crystalline aggregate with random initial orientation, the resultant of some deformation will be a preferred orientation. The CPO pattern is formed due to dislocation glide on slip planes of specific mineral. At low differential stress, only one slip system may be active, but at higher differential stress, several slip systems can operate simultaneously. In silicates, however, which usually have low crystal symmetry, fewer slip systems are active and space problems are accommodated at low temperature by lattice bending, kinking, and fracturing and at high temperature by dynamic recrystallization or grain boundary sliding.

Theoretical study by Lister and Hobbs (1980) had indicated that the development of crystallographic fabrics in quartzites during plastic deformation involving intracrystaline glide is governed by three main factors as following, the strain path or kinematic frame work, the magnitude and symmetry of finite strain and the particular combination of crystallographic glide systems active during deformation. There are two important mechanisms by which a crystallographic preferred orientation

may develop based on experimental studies (Tullis and others, 1973). Firstly, at low homologous temperatures and/or high stain rates, fabrics may develop by rotation of inequant grains or by crystallographic slip within individual grains and resultant grain rotation. Secondly, under conditions where recrystallization is dominant, fabrics may be associated with the actual recrystallization process. Under conditions of plastic deformation of polycrystalline material where intracrystalline slip plays an important role, the crystal axes may tend to rotate and a pattern of preferred orientation can develop. Because the crystal structure of a crystalline material deforming through the conservative migration of dislocations remains more or less undistorted, though the grains themselves undergo gross changes in shape. Thus, the crystal axes act as an internal reference frame during deformation (Lister and Hobbs, 1980).

6.2 C-axis Lattice Preferred Orientation (LPO) of Quartz

The four orientated samples of quartz tectonites were all collected from Sri Racha area (Figure 6.1) and were prepared for orientated thinsections for microfabric study. As no tectonic axes were obvious in these hand-specimens, the orientated thinsections hence were prepared in perpendicularly to the bedding plane. The orientation of quartz c-axes was determined by using a petrographic microscope equipped with a universal stage assemblage and analyzed on equal area, lower-hemisphere stereographic projection. Measurement of quartz c-axes is possible in aggregates with a grain size larger than 20 µm across. Strong internal deformation such as undulose extinction inhibits accurate measurement thus referred those grains are abandon for measurement.

Quartz c-axis fabrics of each sample are displayed as linear data in stereogram with density contours in order to illustrate the present orientation in the nature by trend and plunge. The measurement is determined regardless of reference fabric elements, foliation and lineation, which is associated with deformation that caused the preferred orientation of the c-axes, because the appropriated specimens selected to microfabric study are massive to bedded quartzites, excluding SM1 where micaceous layers are presented, leading to the difficulty of clear foliation or lineation indicator exception of
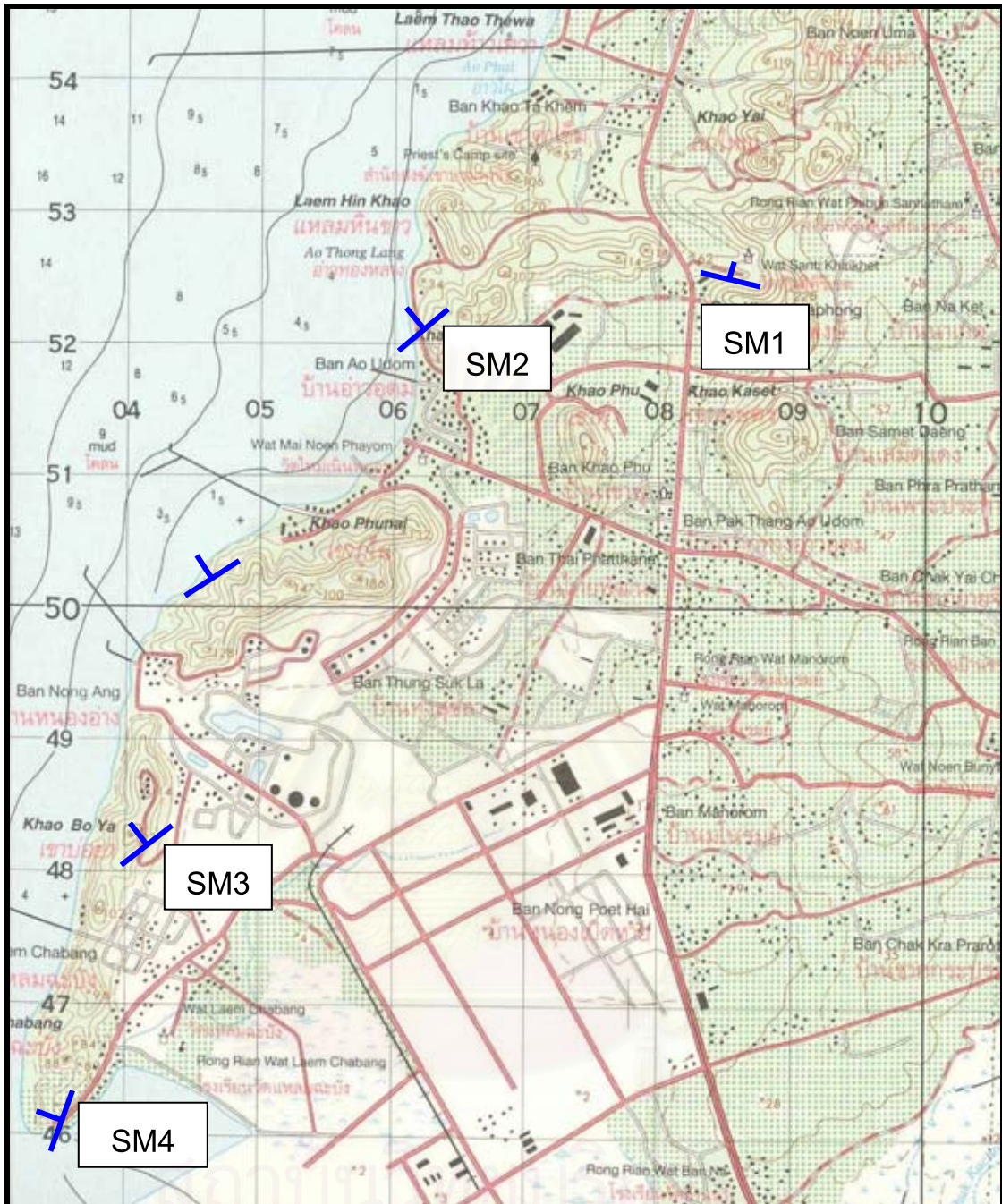
Figure 6.1 Location map of orientated samples in Sri Racha area. The specimens were

collected at Khao Ban Uttaphong (SM1, Grid reference 47708407 E 1452507

N, bedding plane 278$^{°}$/62$^{°}$ N), Khao Khawang (SM2, Grid reference

47706164 E 1452192 N, bedding plane 224$^{°}$/35$^{°}$ NW), Khao Bo Ya (SM3,

Grid reference 47704193 E 1448324 N, bedding plane 232$^{°}$/72$^{°}$ NW) and

Khao Leam Chabang (SM4, Grid refernce 47703565 E 1446204 N, bedding

plane 200$^{°}$/45$^{°}$ NW).

bedding planes of each specimen that successfully measured in the field. The great – circles representing the statistic significance of bedding plane were added into each stereonet plot in order to determine whether there is any relationship between quartz c-axis pattern and reference bedding planar structure in specific location.

Orientated quartz tectonite samples are mostly collected from the unit of quartzite that is believed to be experienced metamorphism of the same event. The SM1, SM2, SM3, and SM4 are picked from inclined beds of micaceous quartzite and bedded to massive quartzite which is believed to be a part of macroscopic fold limb.

Quartz c-axis preferred orientation of SM1 (Figure 6.2) shows the maximum density at $044^{\circ}/24^{\circ}$ (trend/plunge). The fabric pattern is probably characterized as small-circle or conical distributions where the vortex axis is counted to be $086^{\circ}/40^{\circ}$. Two compatible quartz c-axis fabrics belonging to SM2 and SM3 (Figures 6.3 and 6.4) display the obvious point-maxima defined by the maximum density at $60^{\circ}/36^{\circ}$ and $073^{\circ}/36^{\circ}$ respectively. Analogy to quartz c-axis pattern of SM4 (Figure 6.5), it shows different style of fabric when comparing to the fabric patterns of samples mentioned above. The pattern seems to be a great circle and the maximum density is concentrated at $190^{\circ}/54^{\circ}$ (trend/plunge). This unique fabric belonging to SM4 may be due to uneven measurement of quartz c-axis. It must be admitted that several quartz grains in this thinsection of SM4 are not successfully found and have to be skipped for c-axis measurement which may result as incomplete plotting and inaccurate interpretation of fabric pattern. For further discussion, quartz c-axis pattern of SM4 would be abandoned based on the reason described above. When gathering linear data of quartz c-axes of SM1, SM2, and SM3, the contouring shows the strong point maxima pattern indicated by the maximum density at $67^{\circ}/36^{\circ}$ (Figure 6.6).

In a case that the orientation of reference fabric elements (foliation and lineation) are not indicated, the c-axis fabric is insufficient for interpretation about associated deformation that cause the preferred orientation of c-axes. However it is obviously shown that the strong preferred orientation of quartz c-axis belonging to SM1, SM2, and SM3 are scattering in NE to SE quadrants where the point maximum trending ENE
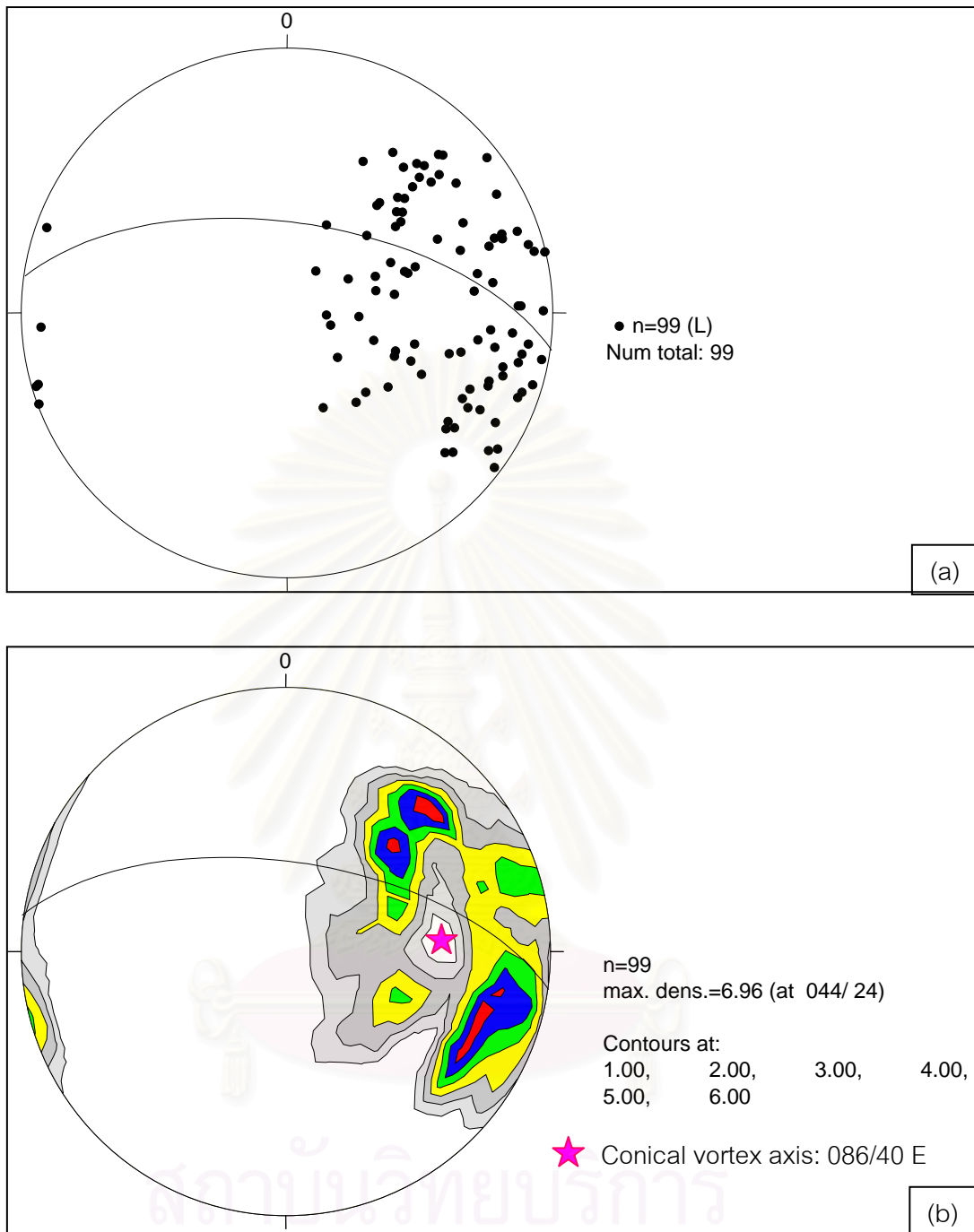
Figure 6.2 Pole diagram (a) and contouring (b) of quartz c-axis fabric of SM1 with additional great circle representing the bedding plane: 278°/62° N. The maximum density of contouring is at 44°/24° (trend/plunge) and a conical vortex axis is at 86°/40° (n= number of plotting, max. dens.= maximum density of contouring). Contour lines are at the specified percentage of total population.
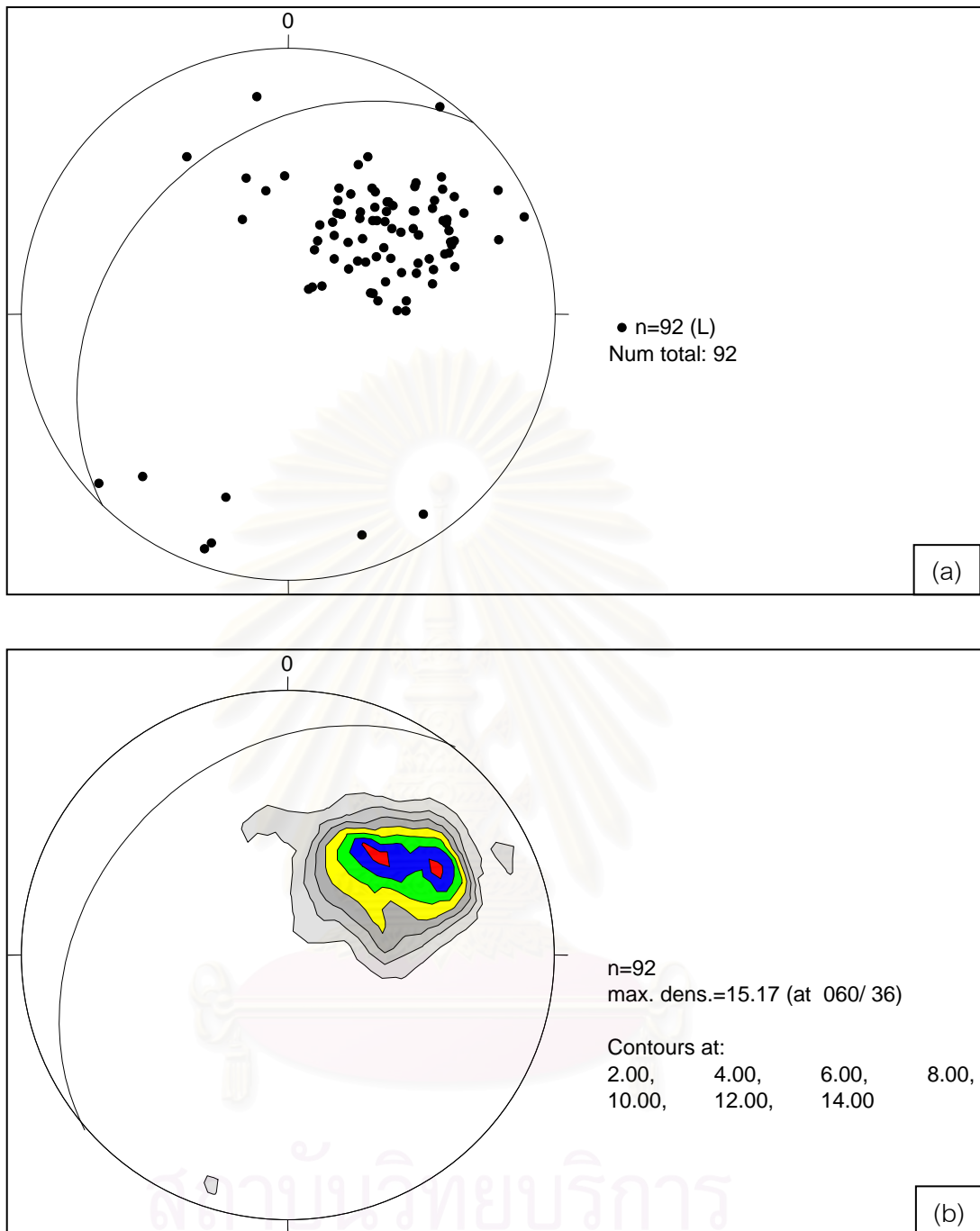
Figure 6.3 Pole diagram (a) and contouring (b) of quartz c-axis fabric of SM2 with

additional great circle representing the bedding plane: 224°/35°NW. The

maximum density of contouring is at 60°/36° (trend/plunge), n= number of

plotting, max. dens.= maximum density of contouring. Contour lines are at the

specified percentage of total population.
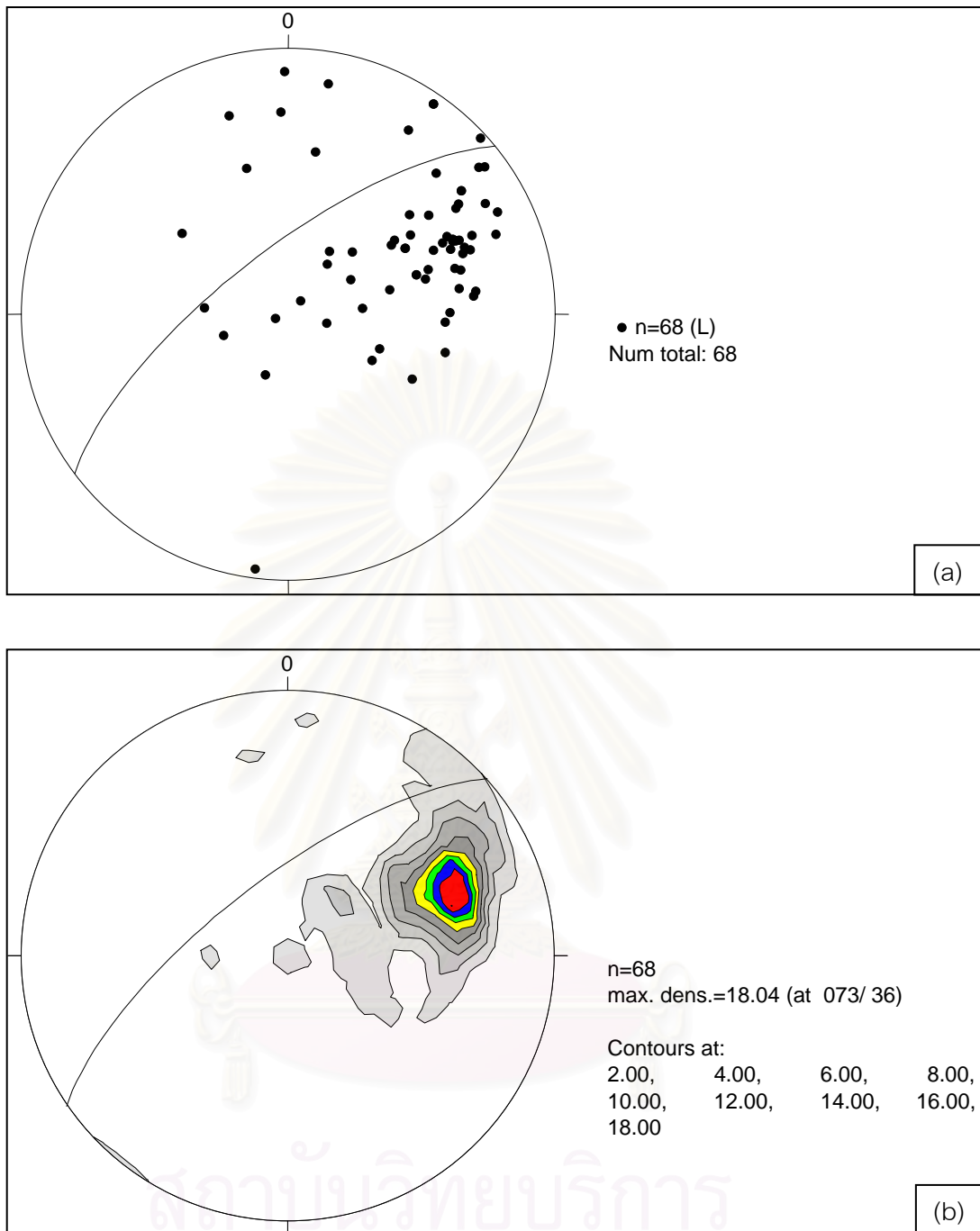
Figure 6.4 Pole diagram (a) and contouring (b) of quartz c-axis fabric of SM3 with

additional great circle representing the bedding plane: 232°/72°NW. The

maximum density of contouring is at 73°/36° (trend/plunge), n= number of

plotting, max. dens.= maximum density of contouring. Contour lines are at the

specified percentage of total population.
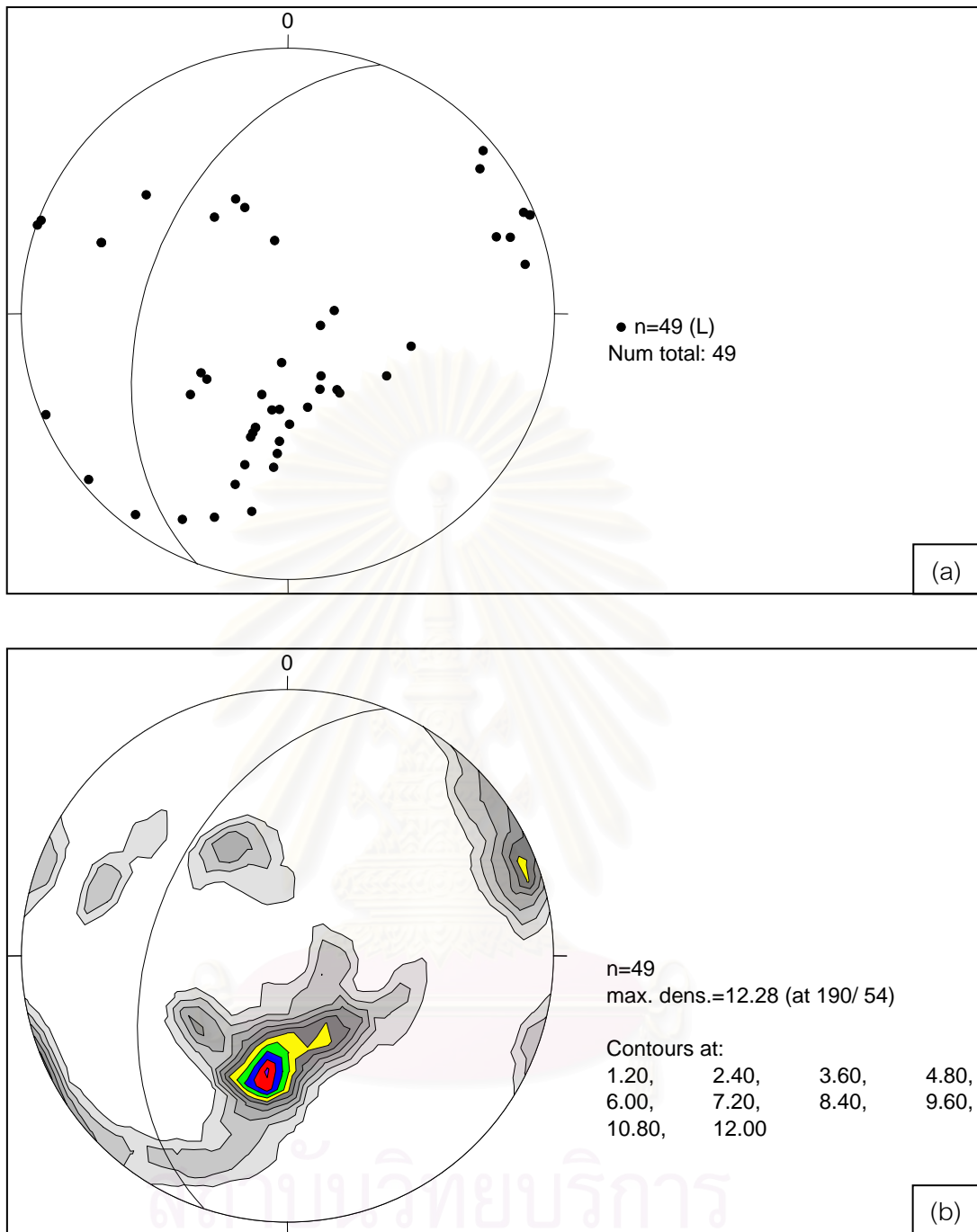
Figure 6.5 Pole diagram (a) and contouring (b) of quartz c-axis fabric of SM4 with

additional great circle representing the bedding plane: 200°/45° NW. The

maximum density of contouring is at 190°/54° (trend/plunge), n= number of

plotting, max. dens.= maximum density of contouring. Contour lines are at the

specified percentage of total population.

direction with moderate plunging considering from pole diagram of Figure 6.6. The patterns of quartz c-axis fabric described above are point maxima and small-circle patterns. This result may be implied to be the effect of coaxial deformation where the axial symmetry is recognizable.

However there is possibility to determine the optic axial fabric with respect to a reference frame of foliation and lineation as the fabric elements of SM1 have been successfully made. Microscopical trace of foliation obviously illustrated in micaceous quartzite thinsections, being prepared perpendicularly to bedding plane, defined by subparallel mica flakes as shown in Figure 6.7 had illustrated so. The orientations of foliation and fold axis derived by stereographic projection technique are $65°/69°$ SE (strike/dip) and $79°/32°$ (trend/plunge) repectively (Figure 6.8). It is noted that the c-axis LPO patterns of SM1, SM2, and SM3 conforms the fold axis derived from fabric elements of SM1 (Figure 6.9).

In stereograms, standard presentation of LPO patterns is with the Y-direction of finite strain vertical and X and Z directions along the EW and NS axes. This implies that a corresponding foliation and lineation are presented in the diagram as an E-W-trending vertical plane (S_r) and horizontal line repectively. L_r is usually a stretching or mineral lineation (Passchier and Trouw, 1996). According to SM1 the reference foliation (S_r) orientation is $65°/69°$ SW (strike/dip) and reference lineation fold axis (L_r) is $79°/32°$ (trend/plunge), which is thought to correspond the original quartz-dimensional preferred orientation and subsequently obliterated by the influence of younger granite intrusion. The pole diagram of quartz c-axis pattern with respect to a reference frame is shown in Figure 6.10. Quartz c-axes are concentrated near the X-direction of finite strain that represented here as L_r. The LPO pattern gives rise to a $30°$-$40°$ small-circle girdle of c-axes around X-direction representative of a fold axis.

6.3 Geological Implications of Quartz c-axes fabric

The result of quartz c-axis study regardless of the reference frame of fabric elements shows a conformed orientation with the fold axis derived from SM1 (Figure 6.8 b)
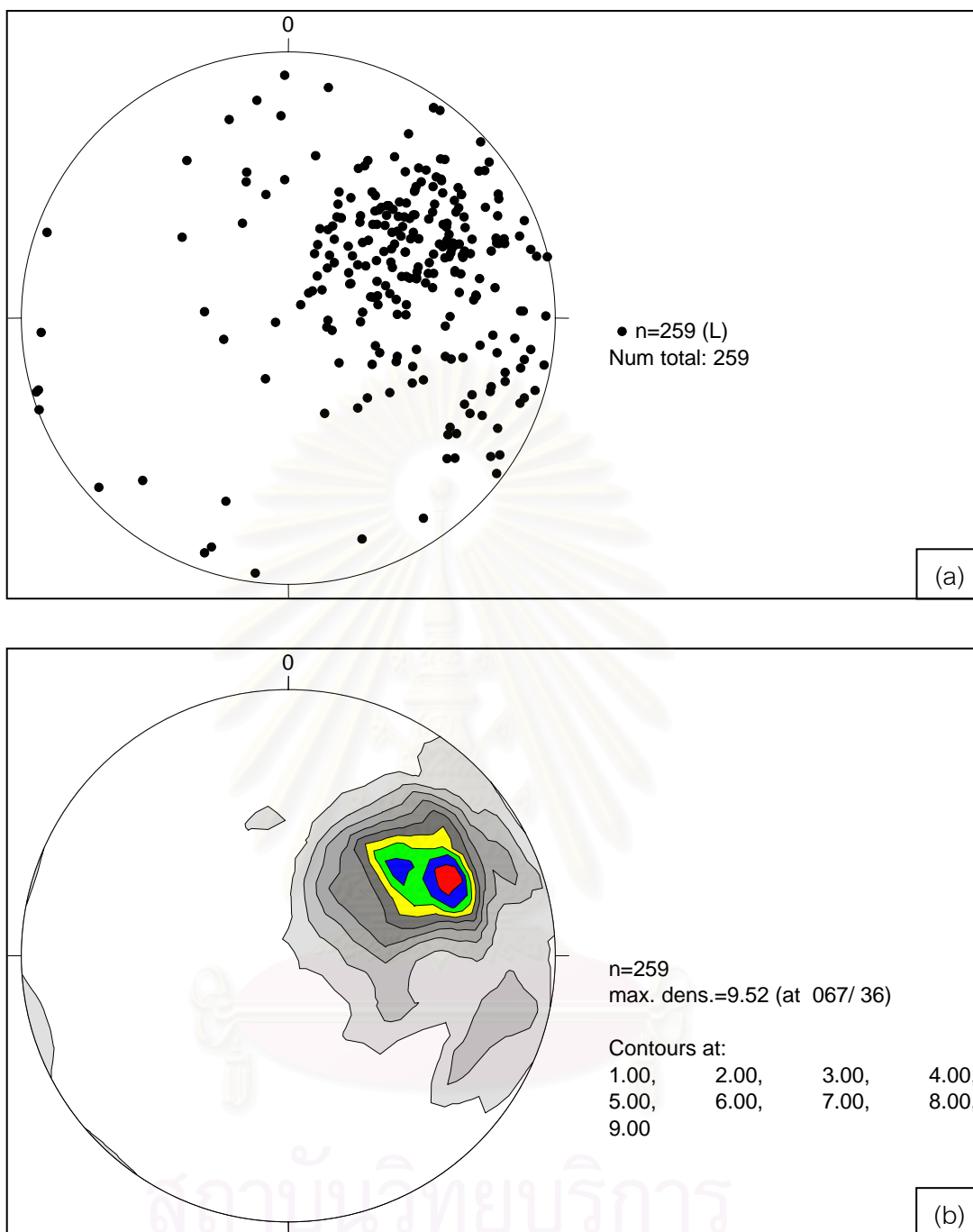
Figure 6.6 Pole diagram (a) and contouring (b) of gathering quartz c-axis fabric of SM1, SM2, and SM3. Point maxima shows the maximum density of contouring at 67°/36° (trend/plunge), n= number of plotting, max. dens.= maximum density of contouring. Contour lines are at the specified percentage of total population.
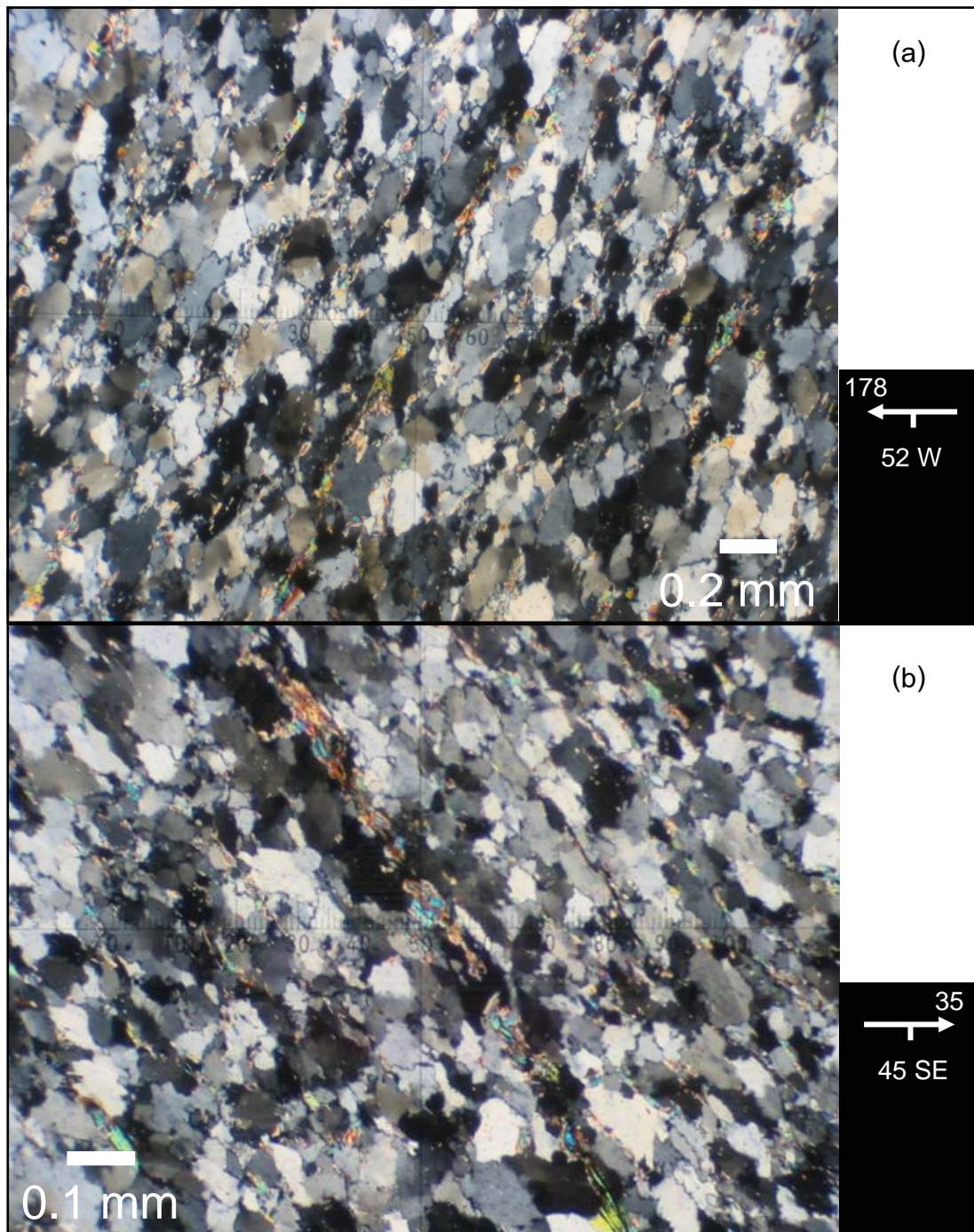
Figure 6.7 Photomicrograph of foliation in sample SM1 defined by subparallel mica
flakes which are illustrated in two orientate thinsections cutting in different
direction and are used to analyze for the orientation of foliation by
stereographic projection technique in (See further Figure 6.8a).
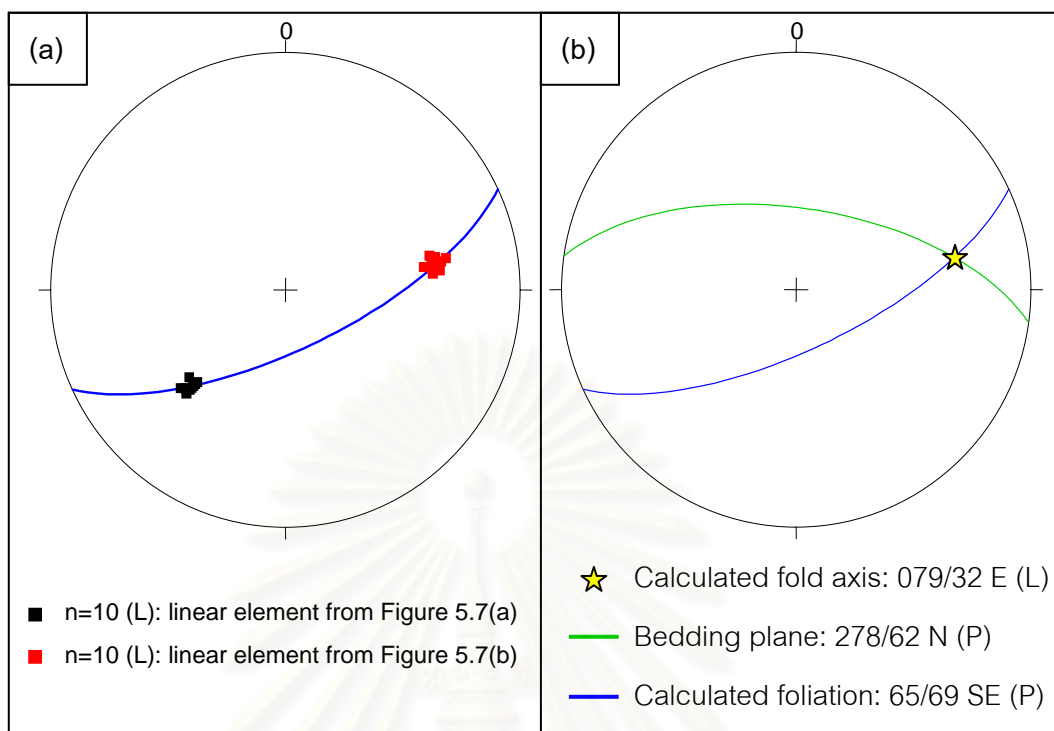
Figure 6.8 Stereonet plot showing (a) foliation plane of SM1 calculated from the fabric

elements shown in Figure 5.7 that strike ENE and steeply dipping to SSE, and

(b) fold axis (yellow star) trending to ENE direction with moderately plunging value.
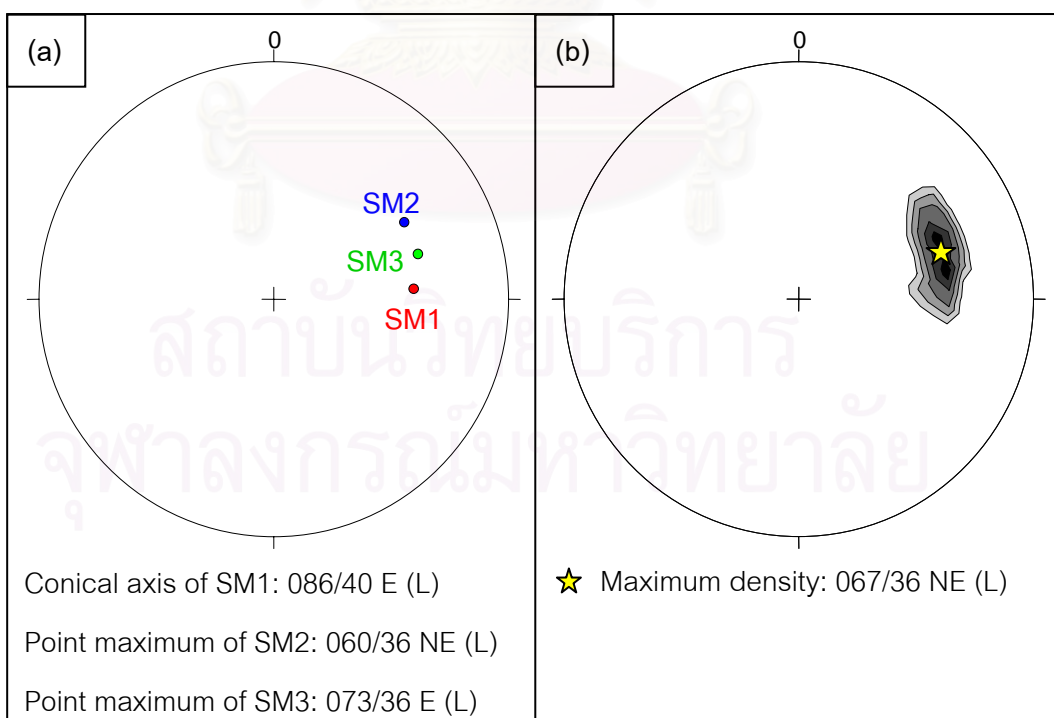
Figure 6.9 Stereogram plotted the conical vortex axis of SM1 and 2 point maxima of

quartz c-axis patterns from SM2, and SM3 (a) showing maximum density

(b) at 67°/36° (trend/plunge) which is conformable to fold axis.
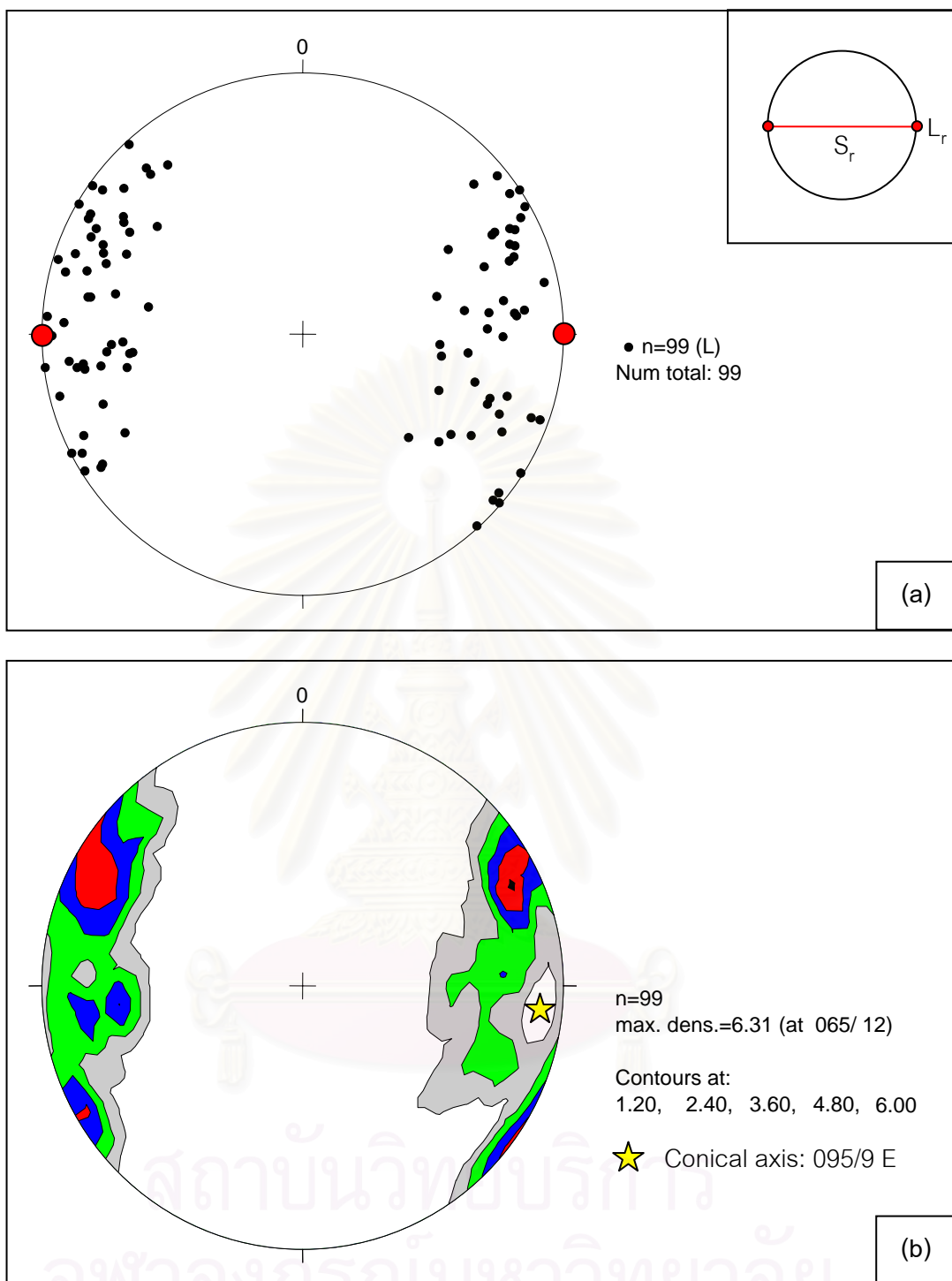
Figure 6.10 Pole diagram (a) and contouring (b) of quartz c-axis fabric of SM1 respect to

S_r foliation (red line in inset) and L_r fold axis (red dots). The maximum point

from contouring is 65°/12° (trend/plunge) and a conical vortex axis (yellow

star) is at 95°/9° (n= number of plotting, max. dens.=maximum density of

contouring).

and the single point maximum of quartz c axes (Figure 6.6) in ENE trending with moderate plunging ($67^{\circ}/36^{\circ}$). In addition to standard presentation of LPO patterns regarding to reference frame, the c-axis fabric of SM1, where fold axis and axial foliation are known, is accomplished under this condition. Quartz c axes are aligned as small-circle around fold axis direction that corresponds to the principal extension direction (X-direction of finite strain).

In case that the fold axis determining from SM1 is postulated to be the representative of mesoscopic folds that are the composite folds of a larger macroscopic fold in Sri Racha area, the maximum shortening direction is supposed to be in WNW-ESE direction which is closed to the NW-SE maximum shortening direction in Sattahip area.

The related quartz c-axis study was done by Mainprice and others (1986) who mentioned that c-axis concentrating near the X-direction of finite strain is caused by the prism <c> slip that is activated at temperatures higher than 700°C. However the activation of slip systems of quartz is sensitive to the metamorphic and deformation conditions. The interpretation of the P-T condition should be carefully determined and should not be too early to establish. Law (1986) studied c-axis fabrics from Roche Maurice quartzite in western Brittany and concluded that quartz c-axis fabrics confirm, by analogy with theoretical and experimental studies, that the minor fold hinge are aligned parallel to the principal extension direction (X).

CHAPTER VII

TECTONIC DISCUSSION

7.1 The Deformation History and Tectonic Implication

It is generally accepted that eastern Thailand was a part of terrane beingdeveloped from the welding of Shan-Thai and Indochina terranes along the Nan-Uttaradit Suture. Various opinions on the episode of suturing between Shan-Thai terrane and Indochina terrane have been suggested. According to Bunopas and Vella (1978 and 1983), suturing was purposed to be in middle to late Triassic.

In late Permian, the Shan-Thai terrane began its collision with Cathaysialand and the suturing to Indochina terrane was largely completed by the late Triassic (Bunopas, 1981, and Chaodumrong, 1992). The I-and S-type granites generated during the late Triassic to Early Jurassic (Cobbling and others, 1986) also supported late Triasssic collision. After the collision, the Shan-Thai became a stable landmass. Therefore, in Jurassic it was less affected by tectonism than in Triassic and the youngest marine rocks were formed before the welded terrane became a continental mass. During Cenozoic, most of the tectonic features were mainly the consequence of the Indian-Eurasian collision (Monar and Tapponier, 1975). There were several strike-slip faults activated successively as Indian terrane moved northward against Eurasian terrane, i.e., the Red River Fault was activated. Consequently, the Southeast Asian Crustal block was rotated clockwise and then extruded several hundreds kilometers southeastward (Achache and others, 1983). The extension and rotation of Southeast Asian crustal block resulted in a series of extensional basins extending from the Gulf of Thailand to the South China Sea (Harder, 1991).

According to the present detailed descriptive structural study, metamorphic petrology and microfabric analysis, the study area had experienced at least three deformation phases and two episodes of metamorphism. The representative of the first deformation (D_1) is F_1 mesoscopic folds that produced L_1 fold axes majorly in the direction of NE-SW to nearly N-S. A regional metamorphism (M_1) is proposed to

accompany this phase of deformation as based on the evidence of microfabric analysis that shows the strong preferred orientation of quartz c-axes comforming the fold axis orientation. The preferred orientation of quartz c-axes perhaps has some connection between the crystal growth and deformation, i.e. metamorphism. The foliation defined by alignment of mica flakes is thought to be a response to the stress field too. The dynamothermal D_1 deformation phase and M_1 regional metamorphism are believed to occur during an orogenic event probably in Permo-Carboniferous age.

The D_2 deformation phase is characterized by the NW-SE cross folds superimposing on the previous F_1 folds to form an interference-fold pattern of Ramsay's (1967) Type-1. D_2 may be occurred together with, or immediately followed by a granite intrusion. The occurrence of cordierite and andalusite porphyroblasts is a product of this metamorphic event. Granite in the study area is believed to be a portion of Rayong - Bang Lamung batholith which intruded the Paleozoic country rocks in Late Triassic. This event is believed to cause a contact metamorphism (M_2) superimposed on the former regional metamorphism expecially in an aureole around the intrusive body. An occurrence of the metamorphic minerals, andalusite found at Khao Leam Kham and nodular cordierite observed at Khao Mon, indicates a low-pressure metamorphic condition, thus contact metamorphism, and is believed to be originated as a post-tectonic recrystallization. Besides, in Sri Racha area, flakes of mica in micaceous quartzite show the reaction rims and engulfed by quartz recrystallization (Figure 7.1). The metamorphic reaction is well defined in Figure 7.2. The coexistence of andalusite with K-feldspar and sericite may be derived from the reaction below.

$$\text{Muscovite} + \text{Quartz} \longleftrightarrow \text{K-feldspar} + Al_2SiO_5 + H_2O$$
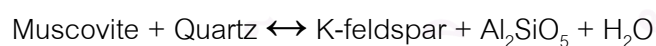
Anestimated pressure range of this reaction, according to the work of Stipp and others (2002), is 2.5-3 kb and the temperature interval is defined at $620 \pm 20\,^\circ C$. This is probably due to the contact metamorphism to originate andalusite and K-feldspar after reaction of pre-existing of quartz and muscovite. Muscovite at the core of andalusite seems to be engulfed by growth of andalusite that indicates the higher dislocation density of muscovite crystal that possibly formed during the former regional
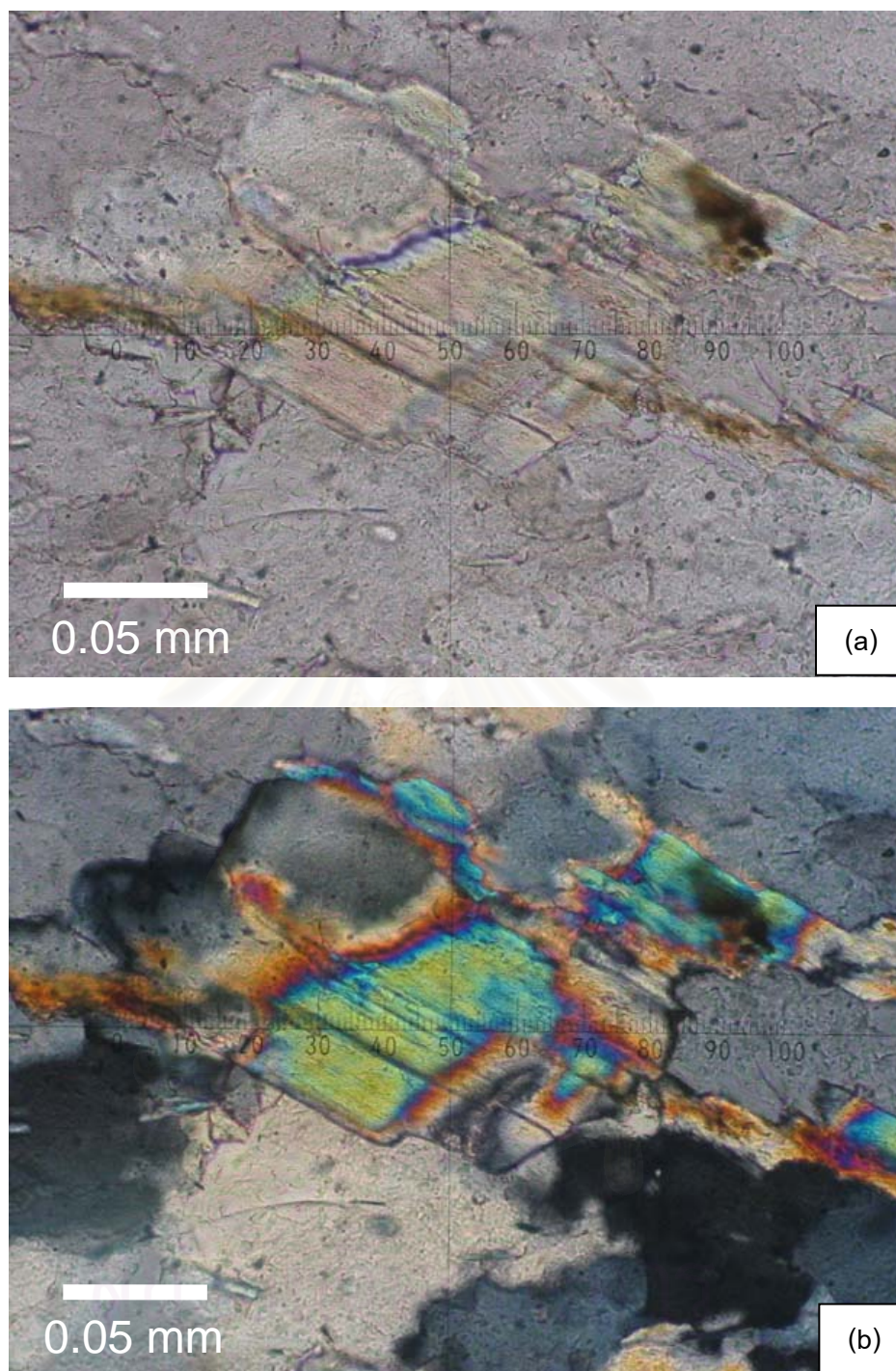
Figure 7.1 Photomicrograph of the alteration rim of mica flakes that are engulfed by a
new quartz recrystallization. Thinsection from Khao Ban Uttaphong, (a) in
planed polarized light and (b) in crossed polarized light. (Grid reference
0706164 E 1452192 N).
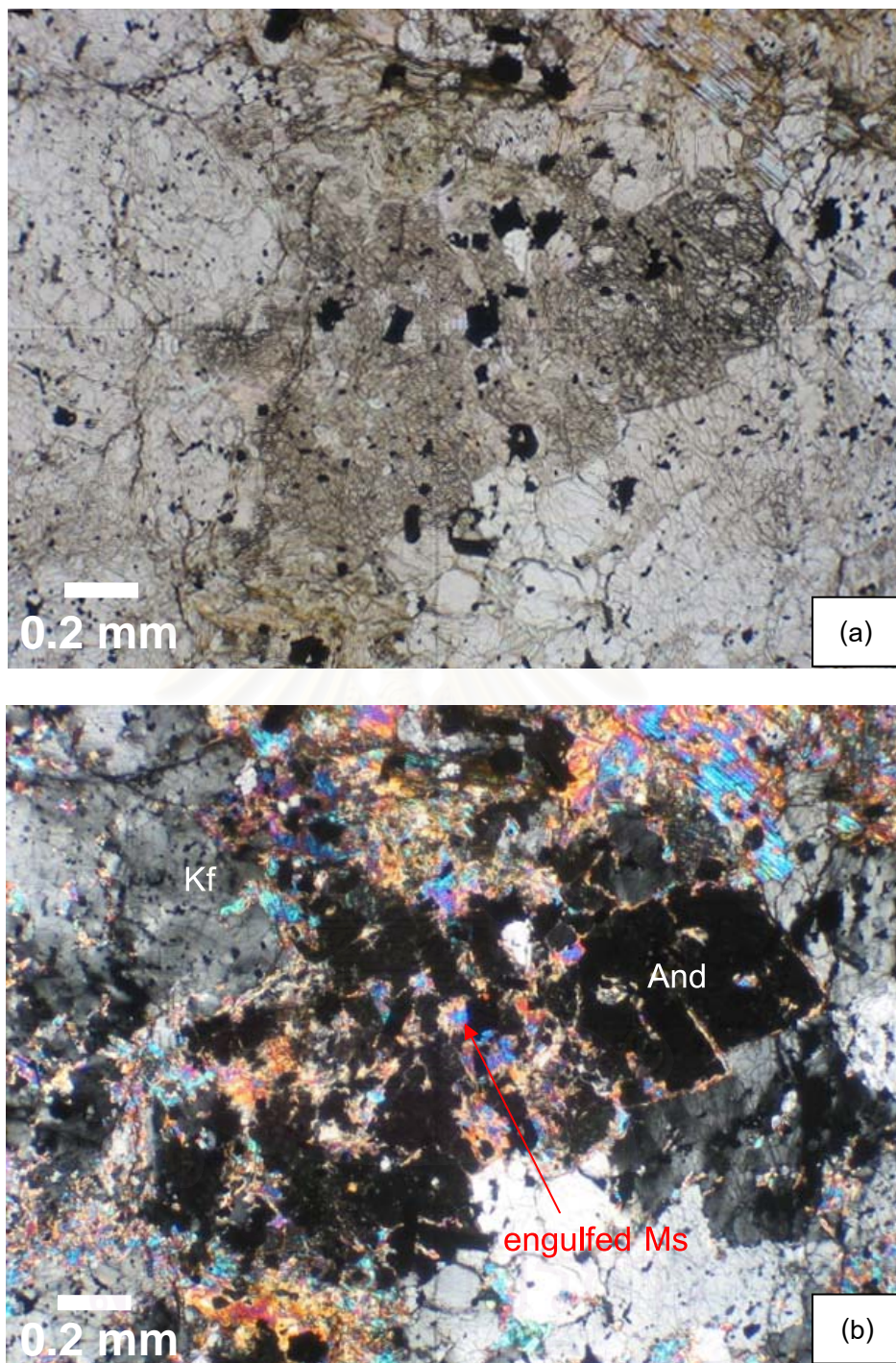
Figure 7.2 Photomicrograph of the coexistence of andalusite (and) and K-feldspar (Kf)

after inferred reaction of quartz and muscovite (Ms, sericite), (a) in planed

polarized light and (b) in crossed polarized light. Specimen is from Wat Santi

Khirikhet, (Grid reference 0708288 E 1452622 N).

metamorphism. The mineral assemblage of K-feldspar, quartz, biotite and chlorite (Figure 7.3) may be occurred by the reaction mentioned below with the estimate stable temperature of 380°C. This is similar to the works of Winkler (1979) and Yardley (1989) for existing together of biotite and muscovite.

Chlorite + K-feldspar $\longleftrightarrow$ Muscovite + Biotite + Quartz.

The youngest deformation event, D3, is a brittle deformation of thrusting that is obviously exhibited in Sattahip area. The evidence of thrust is characterized by a placing the older metamorphosed strata along a flat-lying fault onto the younger unmetamorphosed strata depicted in Figure 3.55. Although no evidence to elucidate the thrusts in Sri Racha area, a low angle fracture plane found at Khao Yai Si is possibly originated as the same mechanism to that in Sattahip area. The slip direction of the whole fault system still is controversial though it locally found the evidence of reverse fault moving from ENE to WSW.

All folding events discussed above are believed to be the plastic deformations occurred in association with an orogenic process probably in Permo-Carboniferous time. The relative age of faulting is believed to be younger than Triassic granitic intrusion because this fault was not cut across by this granite intrusion based on field investigation. Instead the fault cut the aplitic dykes, perhaps formed during the major igneous intrusion. Accounting to faulting process it could be occurred in period of Middle-to Late Mesozoic, or even of very early Tertiary time. The estimated youngest age for this faulting should not be younger than an inferred-Tertiary alluvial-fan unit lying at Khao Din in Sri Racha area further to the east beyond the limit of this study area which has never been affected by this faulting event.

7.2 Microstructure and Quart c-axis Implication

The strong point maxima of quartz optic axes had possibly taken place during deformation and believe to be the effect of syn-tectonic crystallization during the M_1 regional metamorphism. The origin of this lattice preferred orientation is thought to be caused by rotation of gliding because the glide planes regularly orientate to some
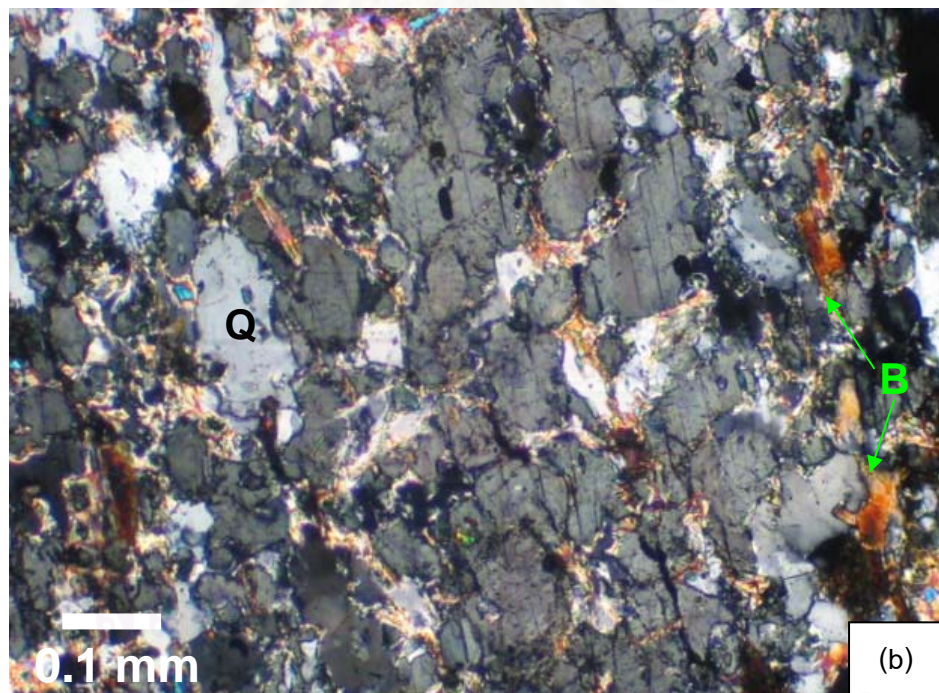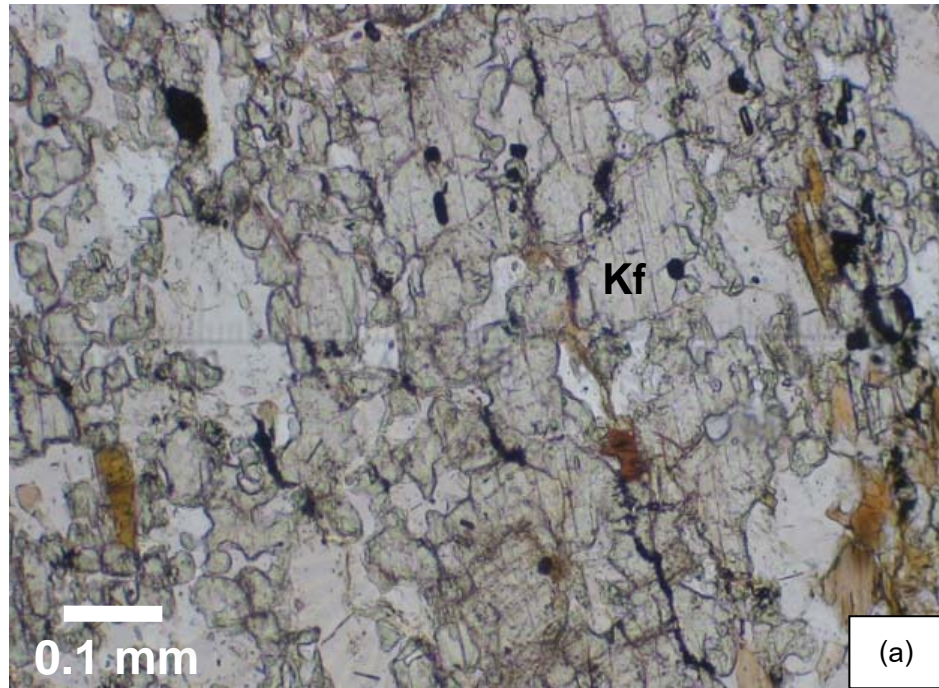
Figure 7.3 Photomicrograph showing mineral assemblages composing of K-feldspar

(Kf), quartz (Q), muscovite (Ms) and biotite (B), (a) planed polarizer and (b)

crossed polarizer (Grid reference 0709300 E 1454159 N).

special position with respect to the stress. When crystals have a single glide plane, the slip plane and/or slip direction is parallel to each other, and the slip plane is perpendicular to the principal stress axis in non-rotational strain or parallel to the movement surface in simple shear (Spry, 1969). Quartz is a hexagonal mineral where the optic axis or C - crystallographic axis is normal to the glide plane. However slip systems of quartz can be more than one. The interpretation of what glide system is active during deformation is still controversially. The fold axis represented by the intersection lines between foliation plane and bedding plane of SM1 is compatible with the fold axis of macroscopic structure in Sattahip area. Although no foliation plane was recognized in SM2 and SM3, surprisingly the fabric patterns of quart c-axis in SM2 and SM3 that illustrate very significant point maxima are conformable to SM1. If the fold axis defined by structural element of SM1 is representative of macroscopic fold of Sri Racha area, the interpretation that the structural pattern of these two areas be simultaneously originated by the same event of regional metamorphism mention above thus becomes more practical.

In Sri Racha area, orientated samples of quartz tectonite were used to study for the microstructures and further referred to deformation mechanism. The c-axis preferred orientation of quartz is considered to be the dynamic recrystallization under the specific stress field that is believed to be synchronous to the regional metamorphism taken place during an orogenic event. Thermal metamorphism that superimposed onto these quartz fabrics could disturb the original dimensional preferred orientation of quartz grains by recovery, bulging, or grain boundary migration in response to the heat adding to the system. However the effect of thermal metamorphism superimposed on regional is solely obliterated the trace of dimensional preferred orientation of quart but a c-axis preferred orientation is always retained.

7.3 Age Determination

According to the geological map of Thailand, scale 1:1,000,000 that is the latest version in 1999 (Department of Mineral Resource, 1999), the study area is underlain by the rock unit defined as CP unit which indicating Carboniferous-Permian in age. This

rock sequence belonging to Shan-Thai terrane generally started from siliciclastic-carbonaceous, sandstone-mudstone, with minor chert and argillaceous limestone lenses in the lower part. This lower part grades to well bedded chert, siliceous shale, carbonaceous shale, sandy shale and more argillaceous limestone in the upper part (Salyapongse and others, 1997). The known Middle Permian section includes bedded sequence of sandstone, sandy shale, chert and small lenticular limestone at Khao Rewadee where Middle Permian fusulinids, calcisphere, small foraminiferas and algae were found (Bunopas, 1981). At Amphoe Klaeng areas where rock succession is also mapped as CP unit, the radiolarian of Upper Permian was also found at Khao Wang Chik near Klaeng (Sashida and other, 2000).

Quartzites in Sri Racha area underlies limestone at Khao Rewadee and thus considered to be in Carboniferous-Permian age as based on the stratigraphic correlation. However a fossil of nautiloid was found in limestone at Ko Si Chang and identified by R. Ingavat as Multicameroceras which indicated Early-Middle Ordovician age (Nakinbodee and others, 1976). Because Si Chang limestone overlies quartzite and quartz schist that are similar to quartzite found in main land Sri Racha, the age of these rock units is thus confusing. However the evidence of fossils is unclear because rocks are so deformed and disturbed by younger granite intrusion that may cause the fossils to be deformed and recrystallized.

In the present study, however fossil records described at Khao Rewadee had never been found. Only recrystallized radiolarian in bedded chert was found at Khao Plu Taluang (Figure 7.4). The age of rocks in study area thus could be pre-Permian, or as old as Ordovician if the discussion above is valid.

7.4 Related report discussion on geologic evolution

The report of mantled gneiss dome in Thailand stated by Macdonald and others (1993) was pointed to the basement complexes in Thailand, especially in the northwestern mountain range. There, the representative large-scale mantled gneiss dome is composing of a core of granite migmatites or gneisses overlain by a layered metasedimentary or metavolcanic cover, or mantle. Many gneiss domes record positive
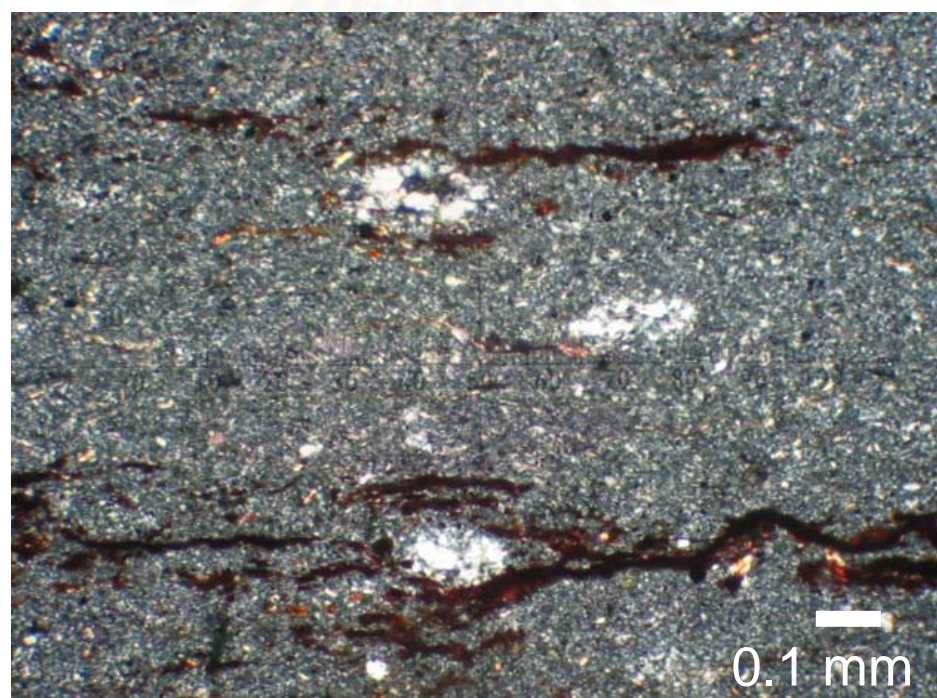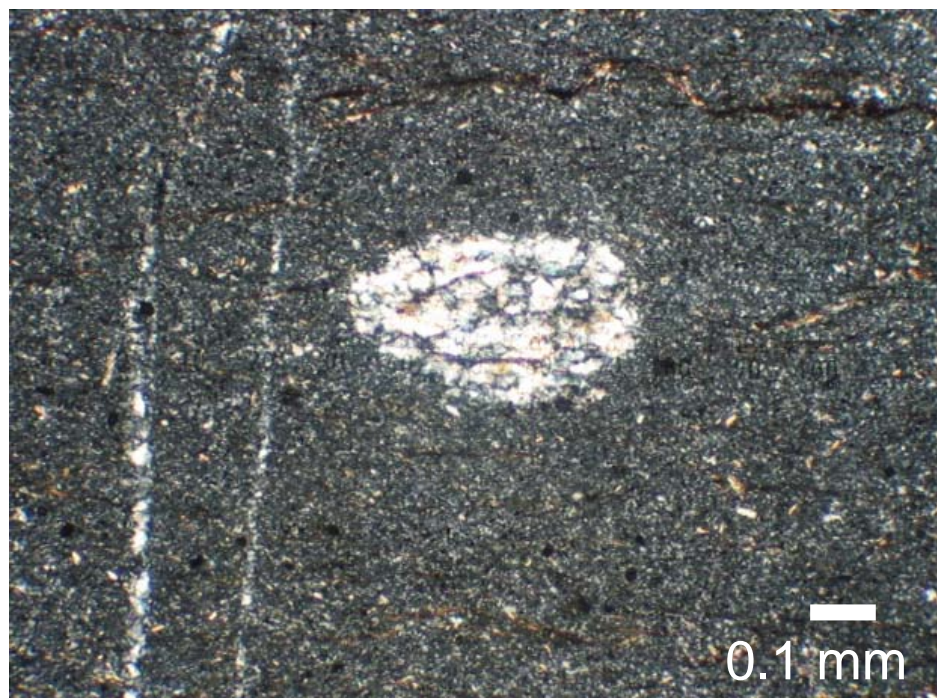
Figure 7.4 Photomicrograph of recrystallized radiolarian in chert bed at Khao Plu

Taluang (Grid reference 0713935 E 14004803 N).

.

feedback between decompression and partial melting of orogenic middle crust. In exhumed orogens, the signature of the rapid ascent of partially molten crust is a gneiss dome cored by mignatite ± granite (Teyssier and Whitney, 2002). However this process is still the least understood and needed more researching. The application of the concept to the preset study area is henceforth beyond the writer's attempt.

CHAPTER VIII

CONCLUSIONS AND RECOMMENDATION

Regionally there are two main lithologic units in the study area including sedimentary and metasedimentary rocks, and granitic rocks. The emphasis of this study is paid on the rock unit which is known as the low-grade metamorphic rocks consisting of metapelites, metapsammite found generally in Sattahip area, and quartzites interbedded with quartz schist regularly found in Sri Racha area. This rock unit is believed to be Lower Paleozoic and possibly as young as Carboniferous-Permian in age. These rocks were later intruded by younger granite which is believed to be of Triassic period. North-south trending of granite batholith exposing along the eastern edge of the study area is marked as the eastern limit for the present study. The general tectonic setting for this area is still under debation.

According to the present detailed structural study however, it could be summarized that there are at least two metamorphic events and three episodes of deformation being occurred in this area. The oldest deformation (D_1) is represented by the tight isoclinal folds that furnish the fold axes (L_1) trending dominantly in NE-SW to nearly N-S directions. The evidence from microscopic structure is derived from quartz c-axis fabric that has a strong preferred orientation. Such orientation might be caused by the recrystallization and rearrangement of c axes in accordance to the stress field and its effect is thought to be simultaneous to the first regional metamorphic event (M_1). The D_2 deformation produces the fold axes trending in NW-SE direction superposing on the former folds and creates plunging to the L_1 fold axes. D_2 deformation is believed to be developed together with or immediately followed by the granitic intrusion that causes the contact metamorphism M_2. In term of metamorphic petrology, the andalusite and cordierite porphyroblasts which are the indicators of contact metamorphism crosscut on the older foliation that could be imply the younger event of this metamorphism. The representative of the latest deformation D_3 is the brittle deformation of low to moderate angle faulting where locally drags the older metamorphic rock sequence to overlie the non-metamorphosed rocks which is believed to be younger in age based on the degree of metamorphism.

By the fact that rocks have been multiply deformed, the fold pattern in regional scale, based on the study of mesoscopic analysis, is the refolded fold of dome-basin pattern, Type-1 interference folds of Ramsay's (1967). The oldest deformation is believed to be the strongest deformation by the fact that the folding is still preserved the NE-SW trending with small amount of NW-SE direction. These geologic structures indicate the finite NW-SE compressive stress that causes the NE-SW trend of major fold with locally extensional joints and minor normal faults that are the effect of concurrently extensional mechanism along the fold trend.

The D_1 and M_1 is thought to occur tectonically in the Permo-Triassic orogeny and the effect of late Triassic (Rayong-Bang Lamung granite) granite intrusion is subsequently occurred during or immediately after the D_2 refolding event. The reversed fault that is believed to be the effect of D_3 is possibly taken place after the late Triassic Rayong-Bang Lamung granite intrusion. In addition to the local evidence of inferred Tertiary sequence at Khao Din, it could imply that the metamorphic events and episodes of deformation are all pre-Tertiary in age as D_1, M_1, D_2 and M_2 should have taken place in pre-late Triassic age and M_3 is occurred during late Triassic to pre-Tertiary.

From this study, the further study should be extended to the other related geologic studies in this area. According to the present study that emphasizes only on to the construction of aerial the geologic structural model of this area, the details study of original rock unit is not attempted, especially prior to the metamorphic episodes. Also the rock sequence at Khao Din in Sri Racha area, by which the author suggests to be Tertiary alluvial fan unit, has to be checked. Moreover the study of microfabric analysis should be carefully interpreted. To understand the mechanism of slip planes activated during deformation and the pressure-temperature condition that causes the specific pattern on quartz c axes, the well understanding of the processes in which microsturctures developed is important and analogue experiment should be performed in order to compare the deformation pattern from the experiment to the nature condition. In this study quartz c axes in quartz tectonites were investigated in order to observe the pattern of fabric that problably have some relationship with the mesoscopic structure. Because this part of the study is an additional detail in preliminary examination, there

are only four orientated samples for investigating the preferred orientation of quartz c axes. Although the outcomes are exciting as they show a maximum of c-axis orientation conforming the fold axis orientation, the orientated samples and c axes counting should be increased in number in order to gain accuracy.

The metamorphic terrane in the study area is believed to be a part of roof pendant or mantle of a gneiss dome where Rayong-Bang Lamung granites intruded into the Carboniferous-Permian country rocks, a thought of mantle-gneiss dome been mentioned by some researchers. In the case that inferred Precambrain sequence in eastern Thailand (Khao Chao) is thought to be originated by the process of decompression and doming, the low-graded metamorphic rocks in the study area are possibly a part of mantle or the outer part of a domal structure by this mechanism. To prove about the tectonic setting, more studies must be done with special attention. The mantle gneiss dome had been noted to commonly associate an orogenic event. Perhaps it is a case in this area too.

REFERENCES

Achache, J., Courtillot, V. and Besse, J. 1983. Paleomagnetic constraints on the Late Cretaceous and Ceonzoic tectonics of Southeastern Asia. <u>Earth and Planetary Science Letters</u> 63: 123-136.

Areesiri, S. 1983. Genetic consideration of amphibolite and related rocks of Bo Kwong Thong, Amphoe Phanat Nikom, Changwa Chon Buri. <u>Proceddings of the Annual Technical Meeting</u>. Department of Geological Science, Chiangmai University: 81-100.

Barr, S. M., and MacDonald, A. S. 1991. Toward a late Paleozoic-early Mesozoic tectonic model for Thailand. <u>Journal of Thai Geosciences</u> 1: 11-22.

Baum, F., Braun, E. V., Hess, A., Koh, K. E., Kruse, G., Guarch, H., and Siebenhuener, M., 1970. On the geology of northern Thailand. <u>Beiheft Geol. Jahrb</u> 102: 23p.

Bons, P. D., and Urai, J. L. 1992. Syndeformational grain growth: microstructures and kinetics. <u>Journal of Structural geology</u> 14: 1101-1109.

Bunjitradulya, S. 1978. A review of the lower Paleozoic rocks of Thailand. In P. Nutalaya (ed), <u>Proceedings of the third regional conference</u>: 721-728. Bangkok, Thailand.

Bunopas, S., and Vella, P. 1978. Late Paleozoic and Mesozoic structural evolution of Northern Thailand: A plate tectonic model. <u>Proceeding of the 3rd Regional Conference on Geology and Mineral Resources of Southeast Asia</u>: 187-197. Bangkok, Thailand.

Bunopas, S. 1981. <u>Paleogeographic History of Western Thailand and Adjacent parts of Southeast Asia: A Plate Tectonic Interpretation</u>. Ph.D. Thesis, Victoria University of Wellington, New Zealand.

Bunopas, S. 1983. Paleozoic succession in Thailand. In P. Nutalaya (ed.), <u>Proceedings of the Workshop on Stratigraphic Correlation of Thailand and Malaysia</u> 1: 39-76. Haad Yai, Thailand.

Buravas, S. 1959. Preliminary notes on the geology of Thailand, <u>Thai Science Bulletin</u>, Bangkok, 43p.

Burrett, C., Long, J., and Stait, B. 1990. Early-Middle Palaeozoic biogeography of Asian terranes derived from Gondwanaland. In W. S. McKerrow and C. R. Scotese

(eds.), Palaeozoic Palaeogeography and Biogeography, Geological Society Memoir 12: 163-174.

Campbell, K. V. 1975. Basement complex, Department of geological sciences, Chiang Mai University, Special Publications 1,1: 3-12

Chaodumrong, P., Salyapongse, S., Sarapirome, S., and Palang., P. 2002. Geology of SW Khorat Plateau and Eastern Thailand. Excursion Guidebook of The Symposium on Geology of Thailand: 68p. Bangkok, Thailand.

Darbyshire, D. P. F. 1988. Geochronology of Thai Granites: Southeast Asia Granite Project Natural Environment. Research Council, Isotope Geology Center report 88/5, 43p.

Department of Mineral Resources. 1999. Geologic map of Thailand, scale 1:1,000,000. Department of Mineral Resources, Bangkok.

Dheeradilok, F., and Lumjuan, A. 1978. Metamorphic facies map of Southeast Asia, scale 1:5,000,000. Geological Survey Division, Department of Mineral Resources, Bangkok, Thailand.

Dheeradilok, F., and Lumjuan, A. 1983. On the metamorphic and pre-Cambrian rocks of Thailand, Conference of Geological Mineral Resource, Thailand: 7p. Department of Mineral Resources, Thailand.

Drury, M. R., and Urai, J. L. 1990. Deformation-related recrystallization processes. Tectonophysics 172: 235-253.

Dunning, G. R., Macdonald, A. S., and Barr, S. M. 1995. Zircon and monazite U/Pb dating of the Doi Inthanon core complex, Northern Thailand: Implication for extension within the Indosinian Orogen. Tectonophysics 251: 197-213.

Emmons, R. C. 1959. The Universal Stage. Geological Society of America. Memoir 8.

Harder, S. H. 1991. Extensional tectonics in the Gulf of Thailand, and South China Sea. Proceeding of the Seventh Regional Conference on Geology, Mineral and Energy Resources of Southeast Asia (GEOSEA VII): Abstract Volume 47.

Harte, B., and Hudson, N. F. C. 1979. Pelitic facies series and the temperatures and pressures of Dalradian metamorphism in E Scotland. In A. J. Harris et al. (eds.), The Caledonides of the British Isles – Review: 323-337.

Hinthong, C., and Sarapirome, S. 1983. Some Studies of Chon Buri Carbonate Rocks on Potential Sources of Construction Material. Conference on Geology and Mineral Resources of Thailand: 1-5. Department of Mineral Resources, Bangkok.

Holdaway, M.J. 1971. Stability of andalusite and the aluminum silicate stability diagram. American Journal of Science 271: 97-131.

Javanaphet, C. 1969. Geologic map of Thailand, scale 1:1,000,000. Department of Mineral Resources, Bangkok.

Jessell, M. W. 1986. Grain boundary migration and fabric development I experimentally deformed octachloropropane. Journal of Structural Geology 8: 527-542.

Jessell, M. W. 1987. Grain-boundary migration microstructures in a naturally deformed quartzite. Journal of Structural Geology 9:1007-1014

Johannes, D. 2000. StereoNett Version 2.46 [computer program]. Available from: http://homepage.ruhr-uni-bochum.de/Johannes.P.Duyster/stereo/stereo1.htm

Klein, C., and Hurlbut, C. S. Jr. 1993. Manual of mineralogy (after James D. Dana). United States of America: John Wiley & Sons, pp. 455-459.

Koch, K. E. 1973. Geology of the Region Si Sawat-Thong Pha Phum-Sang Khlaburi (Kanchanaburi Province/Thailand). Bulletin of Geological Society of Malaysia 6: 177-185.

Law, R., D. 1986. Relationships between strain and quartz crystallographic fabrics in the Roche Maurice quartzites of Plougastel, western Brittany. Journal of Structural Geology 8: 493-515.

Lin, J. and Watt, D.R. 1988. Palaeomagnetic constraints on Himalayan-Tibetan tectonic evolution. Royal Society of London, Philosophical Transactions 326: 177-188.

Lister, G. S., and Hobbs, B. E. 1980. The simulation of fabric development during plastic deformation and its application to quartzite: the influence of deformation history. Journal of Structural Geology 3: 355-370.

Mainprice, D., H. 1986. Dominant c slip in naturally deformed quartz: implications for dramatic plastic softening at high temperature. Geology 14: 819-822.

Macdonald, A. S., Barr, S. M., Dunning, G. R., and Yaowanoiyothin, W. 1993. The Doi Inthanon metamorphic core complex in NW Thailand: Age and tectonic significance. Journal of southeast Asian Earth Sciences 1-4: 117-125.

Miyashiro, A. 1961. Evolution of metamorphic belts. Journal of Petrology 2: 277-311.

Miyashiro, A. 1973. Metamorphism and metamorphic belts. London: George Allen & Unwin, 492p.

Miyashiro, A. 1994. Metamorphic Petrology. London: UCL, 404p.

Nakapadungrat, S., BEckinsale, R.D., and Suensilpong, S. 1984. Geochronology and Geology of Thai granites. Conference on Application of Geology and the National Development: 75-93. Chulalongkorn University, Bangkok.

Nakapadungrat, S., and Putthapiban, P. 1992. Granites and associated mineralization in Thailand, In Ch. Piancharoen (ed.), National Conference on Geologic Resources of Thailand: Potential and Future: 153-171. Department of Mineral Resources, Bangkok, Thailand.

Nakinbodee, V., Maranate, S., and Chaturongkavanich, S. 1976. Geological map sheet Changwat Rayong (ND 47-16) and sheet Bangkok (ND 47-12), scale 1:250,000. Geological Survey Division, Department of Mineral resources, Bangkok, Thailand.

Passchier, C. W., and Trouw R. A. J. 1996. Microtectonics. Germany: Springer-Verlag Berlin Heidelberg, 288p.

Pichler, H., Schmitt-Riegraf, C., and Hoke, L., 1997, Rock-forming minerals in thin section, London: Chapman & Hall, pp. 148-153.

Piyasin, S. 1972. Geology of Lamphang sheet (NE 47-11), scale 1:250,000: Report of investigation 14, Department of Mineral Resources, Bangkok, Thailand: 98p.

Pongsapich, W., Charusiri, P., and Vedchakanchana, S. 1983. Reviews of Metamorphic Rocks of Thailand, In P. Nutalaya (ed.), Proceedings Workshop on Stratigraphic Correlation of Thailand and Malaysia: 244-252. Haad Yai, Thailand.

Putthapiban, P. and Salyapongse, S. 1993. Geology of Changwat Chon Buri. Geological Survey Division, Department o Mineral Resources (in Thai).

Ramsay, J.G. 1967. Folding and fracturing of rocks: New York, McGraw-Hill, 568 p.

Rhodes, B., Blum, J., Devine, T., and Ruangvatanasirikul, K. 1997. Geology of the Doi Sutep metamorphic complex and adjacent Chiang Mai basin. In P. Dheeradilok et al. (eds.), Proceddings of the International Conference on Stratigraphy and Tectonic Evolution of Southeast Asia and the South Pacific: 305-313. Department of Mineral Resources, Bangkok, Thailand.

Salyapongse, S., and Jungyusuk, N. 1980. Geological Map of Eastern Thailand, Scale 1:500,000. Department of Mineral Resources, Bangkok, Thailand.

Salyapongse, S., and Jungyusuk, N. 1981. Geological Map Explanation of Eastern Thailand, Scale 1:500,000: A supplementary note submitted to the seminar on 1:500,000 map compilation of Geological Survey Division. Chiang Mai.

Salyapongse, S. 1992. Foliated contact metamorphic rock of the eastern gulf, Thailand. Journal of Thai Geoscience 2, 1: 35-42

Salyapongse, S., Fontaine, H., Patthapiban, P., and Lamjuan, A. 1997. Geology of the Eastern Thailand. Guidebook for excursion of the International Conference on Stratigraphy and Tectonic Evolution of Southeast Asia and the South Pacific: 69p. Bangkok, Thailand.

Sashida, K., Salyapongse, S. and Nakornsri, N., 2000. Latest Permian radiolarian fauna from Klaeng, eastern Thailand. Micropaleontology 46, 3: 245-263.

Spry, A. 1969. Metamorphic textures. 1st ed. Great Britain: Pergamon Press Ltd. p 215

Sripatanawat, V., 1972. The distribution of rock units of Map 1:250,000, Changwat Nakorn Sawan. Geol. Soc. Thailand Newsl 5, 5-6: 17-19.

Stipp, M., Stünitz, H., Heilbronner, R., and Schmid, S. M. (2002) The eastern Tonale fault zone: a 'natural laboratory' for crystal plastic deformation of quartz over a temperature range from 250 to 700°C. Journal of Structural Geology 24: 1861-1884.

Suriyachai, P. and Salyapongse, S. 1995. Description of the geologic units in King Amphoe Plauk Daeng, Ban Noen Krapok and Ban Chom Phon Map sheets. Geological Survey Division: 8p. Department of Mineral Resources, Bangkok, Thailand.

Suwanasing, A. 1973. Geology and Mineral Deposits in The Eastern Thailand: A report in Files of Economic Geology Division. Department of Mineral Resources: 23p

Taiyaqupt, M., Charusiri, P., Pongsapich, W. 1986. Geology and stratigraphy of the Sri racha area, Chonburi Province, Eastern Thailand, GEOSEA V Proceedings vol. 11, Geological Society of Malaysia: 59-71.

Teyssier, C., and Whitney, D. L. 2002, Gneiss domes and orogeny, Geology 30, 12: 1139-1142

Tullis, J., Christie, J. M., and Griggs, D. T. 1973. Microstructures and preferred orientations of experimentally deformed quartzites. Bulletin Geological Society of America 84: 297-314.

Urai, J. L. 1983. Water assisted dynamic recrystallization and weakening in polycrystalline bischofite. Tectonophysics 96: 125-157.

Van der Pluijm, B. A., and Marshak, S. 1997. Earth structure: an introduction to Structural geology and tectonic. United of America: WCB/McGraw-Hill.

Winkler, H. G. F., 1979. Petrogenesis of Metamorphic Rocks. Springer, New York 348p.

Workman, D. R. 1972. Geology of Laos, Cambodia, South Vietnam and the Eastern part of Thailand – a review. Institute of Geological Sciences, London, v. 19, 49p.

Yardley, B. W. D., 1989. An Introduction to Metamorphic Petrology. Earth Sciences Series: Longman, 248p.

Yardley, B. W. D., MacKenzie, W. S., and Guilford, C. 1990. Atlas of metamorphic rocks and their textures. 1st ed. New York: Longman Group UK Limited, 120p.

APPENDICES

APPENDIX A

MESUREMENT OF C- AXES OF QUARTZ

Measurement of quartz c-axes is possible in aggregates with a grain size exceeding 20 μm. strong internal deformation such as undulose extinction inhibits accurate measurement. The sequence of measurement given below must be carried out exactly in the given order to obtain correct measurements (Figure A)

a) Turn the U-stage table and the thin section parallel to the microscope table by turning A2 and A4 axes to their zero position. Make sure that the A5 axis is at its standard position.

b) Choose a quartz grain and shift its centre to the centre of the cross hairs in the image. Use crossed polars. If the grain is in extinction, rotate around A1 until its goes out of extinction; if it still remains dark, rotate A2 slightly till it goes out of extinction.

c) Insert the gypsum plate and check the position of the indicatrix of the grain – take the gypsum plate out again.

d) Rotate around A1 such that the long axis of the indicatrix is exactly EW. The rotation angle around A1 rotating direction depends on the orientation of the quartz indicatrix as indicated by the blue or yellow color of the grain (blue – long axis of the indicatrices of the quartz grain and the gypsum plate are in the same quadrant; yellow – in opposite quadrants). Rotate A2 back to its zero position in case it was tilted.

e) Tilt the u-stage table over at least $30°$ by rotation of the A4 axis. The grain usually becomes lighter; leave the A4 axis in this position.

f) Tilt the U-stage table around the A2 axis, with A4 inclined, until the grain goes into a maximum extinction position. The indicatrix is now either steep or horizontal; this will be determined in the next steps.
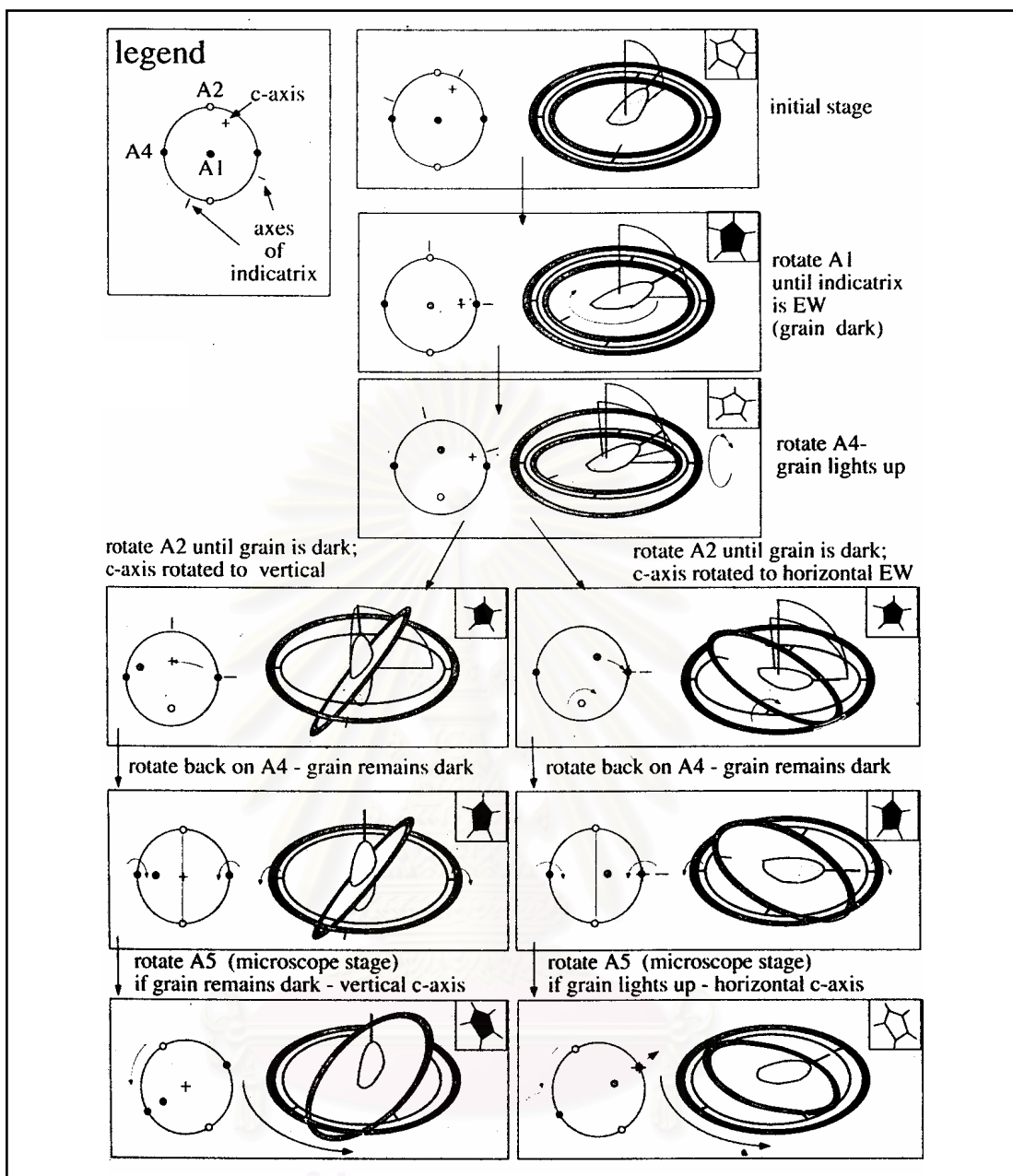
Figure A Procedure for measuring c-axes of quartz with a U-stage, illustrated by a sequence of windows. At left in each window, stereograms with the position and rotation angles of a c-axis and of U-stage axes are indicated. Lines on the outside of the sterogram indicate the extinction position of the indicatrix for each case. At the centre of each window the U-stage and an indicatrix are shown; arcs indicate the indicatrix orientation in each case. Black bold line is the c-axis; bold grey line is the projection of the c-axis in the horizontal plane. The aspect of the grain to be measured as seen through the microscope is shown at top right in each window. Further explanation in text

g) Rotate A4: the grain should now remain dark; if it goes out of its extinction position, one of the following possibilities applies: there is an error in the measurement sequence; the steps (e) and (g) were insufficiently accurate; the grain has strong undulose extinction; or it is not quartz. In any case, the sequence has to be started again.

h) Ring the A4 axis into its zero position and rotate around A5. there are two possibilities (Figure);

1. The grain lights up; the c-axis is E-W horizontal

2. The grain remains dark; the c-axis is vertical parallel to the microscope tube.

i) Return the A5 axis to its standard position and fix it.

j) Read the measurement. If the U-stage has automatic data storage facilities, this may be a push of the button; if not, a procedure for reading and notation of measurements is described below. After some exercise, the measurement procedure given above should take less than a minute per grain.

k) Find the next grain and continue measuring. Follow a distinct path through the section in order to avoid measuring the same grain twice. It may also be useful to measure recrystallized and old grains separately. A photograph of the thin section with numbered grains may be useful in such a case.

APPENDIX B

ATTITUDE OF STRUCTURAL DATA

1. Locations and attitude of bedding planes

No.	Map Sheet	Grid Reference		Attitude of Bedding Strike-Dip (RH rule)	
		Longitude (E)	Lattitude (N)	Strike	Dip Angle
1	5134 II	0709535	1403353	356	12
2	5134 II	0711969	1402236	280	10
3	5134 II	0709043	1403176	3	45
4	5134 II	0709262	1407238	50	38
5	5134 II	0713935	1404803	18	50
6	5134 II	0713680	1406995	346	50
7	5134 II	0713236	1407776	260	28
8	5134 II	0713565	1398878	9	24
9	5134 II	0713055	1409002	103	33
10	5134 II	0713236	1407776	102	32
11	5134 II	0713085	1394088	150	73
12	5134 II	0713425	1393321	178	54
13	5134 II	0712201	1393446	149	60
14	5134 II	0708974	1395837	356	50
15	5134 II	0709746	1397749	150	50
16	5134 II	0710647	1396097	180	40
17	5134 II	0701785	1411151	338	32
18	5134 II	0700108	1405379	28	22
19	5134 II	0699569	1408120	258	40
20	5134 II	0700644	1407278	20	10
21	5134 II	0701601	1405459	217	10
22	5134 II	0701898	1406183	14	35
23	5134 II	0702606	1406335	268	10

1. Locations and attitude of bedding planes (continued)

No.	Map Sheet	Grid Reference		Attitude of Bedding Strike-Dip (RH rule)	
		Longitude (E)	Lattitude (N)	Strike	Dip Angle
24	5134 II	0700942	1401640	352	10
25	5134 II	0700860	1401436	266	14
26	5134 II	0701603	1401639	351	9
27	5134 II	0703371	1400865	253	40
28	5134 II	0702553	1400277	256	47
29	5134 II	0703653	1399613	277	23
30	5134 II	0703960	1399608	358	26
31	5134 II	0704103	1399585	343	26
32	5135 II	0704193	1448324	232	75
33	5135 II	0708866	1451782	236	43
34	5135 II	0703565	1446204	200	45
35	5135 II	0708288	1452622	264	54
36	5135 II	0706164	1452192	230	32

2. Attitude of fractures in Sattahip area

2.1 Sattahip Area

No.	Strike	Dip	No.	Strike	Dip	No.	Strike	Dip
1	338	64	48	286	50	95	175	90
2	123	82	49	206	65	96	164	82
3	124	60	50	136	85	97	105	80
4	180	79	51	258	40	98	342	50
5	4	75	52	52	55	99	277	84
6	95	34	53	154	65	100	79	84
7	292	60	54	6	60	101	9	24
8	290	70	55	102	84	102	194	54
9	356	74	56	229	25	103	280	10
10	288	70	57	34	84	104	255	87
11	282	50	58	210	53	105	137	20
12	250	40	59	355	63	106	315	72
13	92	64	60	275	75	107	325	70
14	86	40	61	129	70	108	122	65
15	49	47	62	35	70	109	116	75
16	312	72	63	294	70	110	137	57
17	50	85	64	165	50	111	137	70
18	305	80	65	302	59	112	30	74
19	234	66	66	47	40	113	287	14
20	306	60	67	205	67	114	242	40
21	202	32	68	293	63	115	110	76
22	314	60	69	100	22	116	76	48
23	252	82	70	274	56	117	147	86
24	118	65	71	260	38	118	155	85
25	113	50	72	230	50	119	145	60
26	120	31	73	256	75	120	6	72
27	58	57	74	145	83	121	28	75
28	296	70	75	51	15	122	357	87
29	144	84	76	290	39	123	22	58
30	167	44	77	282	72	124	105	62
31	90	80	78	306	75	125	47	40
32	172	70	79	95	33	126	260	28
33	92	35	80	117	23	127	102	70
34	78	55	81	22	75	128	15	87
35	45	65	82	245	80	129	225	22
36	75	57	83	319	85	130	85	28
37	130	74	84	274	70	131	269	70
38	332	40	85	223	62	132	105	88
39	291	64	86	287	54	133	347	73
40	103	75	87	56	19	134	68	60
41	307	57	88	325	87	135	227	80
42	276	83	89	66	86	136	55	60
43	25	73	90	110	90	137	292	84
44	282	70	91	302	88	138	140	90
45	57	63	92	39	49	139	182	82
46	314	64	93	357	18	140	170	90
47	24	28	94	232	54	141	80	77

No.	Strike	Dip	No.	Strike	Dip	No.	Strike	Dip
142	87	89	155	122	65	168	41	90
143	56	32	156	215	70	169	325	60
144	119	89	157	143	56	170	340	70
145	272	72	158	220	88	171	107	62
146	22	62	159	293	76	172	17	65
147	142	85	160	72	30	173	47	65
148	123	74	161	258	50	174	200	57
149	133	79	162	300	65	175	230	65
150	195	84	163	305	81	176	317	15
151	315	24	164	112	59	177	80	15
152	160	50	165	230	80	178	213	80
153	104	63	166	334	52	179	212	85
154	350	40	167	94	42			

2.2 Sri Racha Area

No.	Strike	Dip	No.	Strike	Dip	No.	Strike	Dip
1	10	30	31	110	45	61	130	60
2	180	45	32	305	80	62	100	70
3	330	50	33	230	90	63	200	70
4	10	30	34	30	75	64	245	50
5	180	45	35	320	85	65	210	80
6	340	45	36	80	60	66	280	70
7	0	65	37	50	60	67	340	45
8	30	55	38	280	50	68	140	50
9	0	45	39	340	50	69	160	85
10	150	40	40	230	60	70	290	90
11	0	45	41	30	75	71	230	65
12	150	45	42	320	85	72	250	65
13	350	70	43	230	60	73	285	35
14	270	65	44	140	50	74	45	60
15	175	25	45	345	65	75	345	80
16	345	75	46	40	40	76	340	50
17	270	60	47	55	80	77	90	50
18	170	25	48	230	70	78	70	65
19	355	40	49	300	80	79	350	45
20	160	45	50	90	50	80	270	80
21	255	80	51	210	80	81	10	65
22	135	55	52	285	90	82	330	50
23	255	80	53	200	60	83	105	80
24	135	50	54	290	55	84	160	80
25	255	80	55	200	40	85	5	65
26	135	50	56	0	50	86	325	15
27	0	50	57	30	50	87	155	80
28	20	50	58	50	75	88	75	65
29	210	80	59	140	70			
30	15	70	60	60	65			

APPENDIX C

ATTITUDE OF QUARTZ C AXES IN QUARTZ TECTONITES

1. Attitude of quartz c axes in SM1

No.	Plunge	Trend	No.	Plunge	Trend	No.	Plunge	Trend
1	55	143	34	10	60	67	6	74
2	24	118	35	33	45	68	40	44
3	33	103	36	37	104	69	51	71
4	44	51	37	36	27	70	7	109
5	56	46	38	12	118	71	24	125
6	48	112	39	11	100	72	25	43
7	19	44	40	46	40	73	21	110
8	51	72	41	21	109	74	78	94
9	23	82	42	24	95	75	27	116
10	16	95	43	2	102	76	15	70
11	60	24	44	2	253	77	24	48
12	76	107	45	18	70	78	3	127
13	3	254	46	55	136	79	5	290
14	28	78	47	27	63	80	30	83
15	28	48	48	13	88	81	20	117
16	37	64	49	17	104	82	16	106
17	62	108	50	45	40	83	8	110
18	8	267	51	54	112	84	26	113
19	9	71	52	4	107	85	29	44
20	9	125	53	28	33	86	27	126
21	68	93	54	0	250	87	38	46
22	14	88	55	47	70	88	43	47
23	42	49	56	47	52	89	15	71
24	6	123	57	31	39	90	51	127
25	21	72	58	3	100	91	44	115
26	59	159	59	5	76	92	9	97
27	0	77	60	19	130	93	61	68
28	56	80	61	74	35	94	49	104
29	62	76	62	4	90	95	21	132
30	28	98	63	27	41	96	21	53
31	31	70	64	54	110	97	22	100
32	69	61	65	54	64	98	18	45
33	28	124	66	5	52	99	69	132

2. Attitude of quartz c axes in SM2

No.	Plunge	Trend	No.	Plunge	Trend	No.	Plunge	Trend
1	42	59	32	44	78	63	5	228
2	13	162	33	61	56	64	39	51
3	48	22	34	43	56	65	67	53
4	63	77	35	54	62	66	54	55
5	34	27	36	47	54	67	56	88
6	18	71	37	32	60	68	24	48
7	55	28	38	52	24	69	51	350
8	33	45	39	77	50	70	19	222
9	38	25	40	43	41	71	10	146
10	37	69	41	30	327	72	53	37
11	57	45	42	48	46	73	43	34
12	79	42	43	10	60	74	25	55
13	80	40	44	10	198	75	31	59
14	35	74	45	53	70	76	56	26
15	33	54	46	43	44	77	58	57
16	31	52	47	69	22	78	66	22
17	33	59	48	58	334	79	47	39
18	7	200	49	28	199	80	4	36
19	43	35	50	39	51	81	32	66
20	59	72	51	34	67	82	62	82
21	68	40	52	48	27	83	59	26
22	42	59	53	48	51	84	43	42
23	34	66	54	43	73	85	36	69
24	47	69	55	63	53	86	50	44
25	43	69	56	26	51	87	64	76
26	46	343	57	51	42	88	51	35
27	33	63	58	19	352	89	32	44
28	5	68	59	61	19	90	55	28
29	48	72	60	62	30	91	53	84
30	54	89	61	47	359	92	46	44
31	25	60	62	61	40			

3. Attitude of quartz c axes in SM3

No.	Plunge	Trend	No.	Plunge	Trend	No.	Plunge	Trend
1	23	343	24	40	66	47	17	61
2	36	55	25	34	76	48	86	250
3	21	55	26	36	82	49	35	68
4	21	55	27	69	251	50	34	64
5	46	118	28	70	201	51	5	35
6	49	307	29	9	53	52	5	35
7	10	359	30	30	83	53	11	52
8	13	10	31	48	73	54	26	67
9	19	33	32	48	73	55	39	104
10	31	71	33	67	86	56	14	64
11	68	61	34	58	77	57	3	48
12	41	93	35	85	45	58	67	33
13	37	65	36	33	66	59	71	38
14	36	75	37	46	76	60	50	55
15	33	66	38	38	10	61	52	56
16	48	61	39	25	358	62	41	51
17	48	61	40	31	85	63	32	66
18	31	67	41	30	69	64	60	111
19	27	58	42	-4	187	65	29	71
20	45	57	43	25	57	66	63	46
21	43	344	44	64	274	67	44	72
22	18	69	45	25	46	68	61	119
23	39	90	46	78	104			

4. Attitude of quartz c axes in SM4

No.	Plunge	Trend	No.	Plunge	Trend	No.	Plunge	Trend
1	3	230	18	55	338	35	50	197
2	10	78	19	60	185	36	13	71
3	56	179	20	50	184	37	67	350
4	4	67	21	26	291	38	60	168
5	61	147	22	68	152	39	33	197
6	6	217	23	58	231	40	0	289
7	51	335	24	76	87	41	52	323
8	19	200	25	54	123	42	18	70
9	65	157	26	58	236	43	11	53
10	75	188	27	26	291	44	64	198
11	14	207	28	53	196	45	2	247
12	60	189	29	41	185	46	51	196
13	31	310	30	2	68	47	25	190
14	40	196	31	50	105	48	5	50
15	46	184	32	62	148	49	2	68
16	1	291	33	79	110			
17	51	230	34	53	196			

BIOGRAPHY

Miss Chuthathip Bussai was born on October 24, 1980 in Changwat Ratchaburi, western Thailand. She accomplished her undergraduate study and received the Bachelor of Science degree in Geology from the Department of Geology, Faculty of Science, Chulalongkorn University in 2001. After that she entered the Master's degree program at the same department. In addition she was funded her study in Master's program for two years by supporting of Chulalongkorn University scholarship. During her study in Master's degree, she was a teaching assistant in structural geology which is a field interest of her postgraduate study.